GEOCHEMICAL CHARACTERISATION OF THE WITBANK COALFIELDS, SOUTH AFRICA.

KEDIBONE THWALA

Submitted in fulfilment of the requirements for the degree

Magister Scientiae in Geohydrology

in the

Faculty of Natural and Agricultural Sciences

(Institute for Groundwater Studies)

at the

University of the Free State

Supervisor: Prof. K.T Witthueser

Co-supervisor: Dr R.N Hansen

30 November 2020

DECLARATION

I, KEDIBONE THWALA, hereby declare that the dissertation hereby submitted by me to the Institute for Groundwater Studies in the Faculty of Natural and Agricultural Sciences at the University of the Free State, in fulfilment of the degree of Magister Scientiae, is my own independent work. It has not previously been submitted by me to any other institution of higher education. In addition, I declare that all sources cited have been acknowledged by means of a list of references.

I furthermore cede copyright of the dissertation and its contents in favour of the University of the Free State.

_____

KEDIBONE THWALA

30 November 2020

ACKNOWLEDGEMENTS

I would hereby like to express my sincere gratitude to my academic supervisor Prof. Kai Witthueser for his support, motivation and guidance in the completion of this study. Special thanks to Dr. Robert Hansen for his input and guidance.

I would also like to send special thanks to my mother, Lizzie Thwala who supported me emotionally whenever I called her to complain that I am quitting, she told me to persevere. This goes without forgetting my siblings, Victor, Tumelo and Silvia Thwala who played a major role in encouraging, supporting me and providing humour when I needed it. Many thanks are also extended to Rinae Makhadi for her support, motivation and encouragement, as well as shedding light on aspects that did not make sense.

Lastly, I would like to give thanks to God the Almighty for giving me the strength, wisdom and understanding throughout the course of this research.

ABSTRACT

The Witbank Coalfield is one of the 19 coalfields found in South Africa and has been exploited for coal for more than a century. The coalfield is located in the Mpumalanga Province, roughly 100 km east of Johannesburg. The dissertation focuses on the Witbank Coalfield wherein Arnot, Goedehoop, Mafube, Zibulo, Landau and Greenside collieries, as well as Blaauwkrans and Greenside Discard Facilities were investigated. Coal mining in this area has proven to be problematic, has caused contamination of surface and groundwater resources, and changed the quality of the water over the years. The purpose of this study was to investigate the acid generating potential of the Witbank coalfield by examining the groundwater chemistry, acid-base-accounting predictions as well as sulphur contents of the coal seams and host rocks. The data obtained from the mines were processed using tools such as WISH, ABACUS and PHREEQC to create descriptive diagrams that aided in further understanding the acid generating properties of the study area. Arnot, Goedehoop, Greenside colliery and its discard dump are the most problematic due to their high sulphate concentrations. Sulphur contents of coal seams were compared to the groundwater sulphate concentrations. Although this was instrumental in understanding the relationship between sulphur and sulphate concentrations, sulphur is not evenly distributed amongst and within the different seams, leading to certain hotspots. Geochemical speciation showed hydrated metals and carbonates are likely to precipitate as secondary mineral phases. Overall, the results demonstrated that the groundwater of the investigated study sites was sulphate contaminated and that the majority of samples collected from the sites were potentially acid generating. ABA data was compared with the groundwater chemistry to evaluate whether the ABA predictions were reflected in the groundwater quality. Results of this study confirmed that ABA is a useful tool to predict potential constituents of concern in groundwater.

Keywords: Acid Base Accounting, Groundwater chemistry, Water types, Sulphate concentrations, Sulphur contents.

TABLE OF CONTENTS

LIST OF FIGURES

LIST OF TABLES

ABBREVIATIONS

ABA: Acid Base Accounting

ARD: Acid Rock Drainage

SACE: South African Coal Estates

PAG: Potential Acid Generating

NAG: Non-Acid Generating

AP: Acid Potential

NP: Neutralising Potential

NNP: Net Neutralising Potential

NPR: Neutralising Potential Ratio

XRD: X-ray Powder Diffraction

CHAPTER 1:
INTRODUCTION

1.1 GENERAL INTRODUCTION

Coal is currently South Africa's main primary source of energy and the coal-fired power stations generate about 95% of electricity in the country (Jeffrey, 2005). South Africa has 19 coalfields that are found primarily in KwaZulu-Natal, Mpumalanga, Limpopo and Free State Provinces; however, small amounts also occur in Gauteng, North West and Eastern Cape Provinces (Jeffrey, 2005). These coalfields are hosted in the Karoo Supergroup rocks of about 300 to 180 million years in age (McCarthy & Rubidge, 2005). The Witbank coalfield has been exploited for coal for more than a century. The mining operations cover larger areas and have longer periods of operation, resulting in the mining activities changing the geological and geohydrological environments.

One of the most important impacts caused by coal mining is the pollution of surface water and groundwater by acid mine drainage (Buzzi *et al.*, 2013). The environmental impact does not end when mining stops, but continues for years after mining has halted. The mining activity exposes more sulphide bearing rocks to the oxygen and moisture rich atmosphere, which accelerates the generation of acid mine drainage (Ochieng *et al.*, 2010).

Although, mining houses have remediation plans for the duration of life of mine and post-closure, somehow acid mine drainage still causes a great deal of pollution in both surface water and groundwater resources.

1.1.1 Uses of Coal

Historically coal was mined to produce gas that was utilised in gaslights in many cities around the world. However, it is currently used to generate electricity in which it provides approximately 39% of the world's electricity. Coal is of utmost importance in the iron and steel production wherein the coal is employed in blast furnaces; also serves as a source of energy in the production of cement. Coal is converted to refined liquid fuel in some countries to produce transport fuels, as well as other oil products, such as plastics and solvents. Furthermore, it is essential for usage in water filters and air purification; construction material reinforcement and machines for kidney dialysis (World Coal Association, 2009).

1.1.2 Environmental impacts of coal

1.1.2.1 Coal combustion

Coal contains carbon, sulphur, oxygen, hydrogen and trace amounts of nitrogen as well as heavy metals as its main components. Combustion of coal leads to the emission of gases such as, CO_2, CO, SO_2, SO_3, NO_2 and NO; and these gases are known to be poisonous to human beings and animals (Longwell *et al*., 1995; Munawer, 2018). The emission of these gases can be associated with changes in the air quality, as they are known to be greenhouse gases. An increase in concentrations of gases such as carbon dioxide cause global warming, which has led to significant climatic changes.

The emission of SO_2 into the atmosphere leads to the formation of acid rain. When this gas reacts with rainwater, it subsequently produces rainwater that has a slightly lower pH. This acidic rainwater damages crops on the ground surface, buildings and statues. The accumulation of these gases in the atmosphere may be detrimental to the health of human beings and animals. Inhalation of such gases by human beings may for instance cause lung damage and heart diseases.

Coal-fired power stations produce large amounts of fly-ash, which is disposed in ash heaps. However, these ash heaps are unaesthetic and take up a lot of space on the ground surface (Bullock & Bell, 1997). Furthermore, the fly-ash has known beneficial uses in the management of acid mine drainage.

1.1.2.2 Coal mining

Mining involves the excavation of open pits or subsurface hollows, and these activities may cause disturbances to the water table. Mining may decrease the water quantity as well as change the flow direction of the groundwater in severe cases. The most essential impact that arises from coal mining is acid mine drainage, which may find its way into the groundwater system and pollute the water. Additionally, during decanting, especially from abandoned mines, acid mine drainage may find its way to the surface water bodies where it causes a decrease in the water pH as well as elevated sulphate and heavy metal concentrations (Bell & Bullock, 2001; Hobbs *et al*., 2008; Udayabhanu & Prasad, 2010; Favas *et al*., 2016).

Subsurface coal mining is also known to be associated with the subsidence of the land, which in severe cases may lead to complete collapse of the mined areas. This renders the land wherein the mining took place useless (McCarthy & Pretorious, 2009). It also changes the degree to which the rocks of the surrounding areas will support large surficial structures, such as infrastructure. The noise and dust from the blasting and excavation during open pit mining may be detrimental to both human beings and animals, wherein the dust may cause respiratory diseases.

1.2 AIMS AND OBJECTIVES

The main aim of this dissertation is to investigate the acid generating potential of the Witbank coalfield with the use of ABA data of the coal seams and host rocks, as well as the groundwater chemistry data collected over time going back as far as 1990 for some study sites.

The objectives of this study include:

- Investigation of the quality of the groundwater from the Witbank coalfield;
- Compare the groundwater chemistry to the ABA predictions;
- Compare the sulphate output of the different study sites in the Witbank area;
- Investigate the relationship between sulphate output and time; and
- Relate sulphur contents of the coal seams and host rocks to sulphate concentrations in the groundwater

1.3 APPROACH TO THE RESEARCH

The first step towards achieving the above-mentioned aim and objectives was to collect and evaluate the available data on ABA predictions and groundwater chemistry. This involved large quantities of data from different mining houses in the Witbank area and reviewing the available literature related to the study area. The groundwater chemistry data were sorted and converted into the correct format to be compatible with the WISH software package for generation of descriptive diagrams that aid in the classification of the groundwater.

Hydro-geochemical modelling tools such as Phreeqc was used to further characterise and analyse the water chemistry. The groundwater chemistry was be compared to the ABA predictions to see if there are deviations. Maps were used to further investigate the relationship between sulphur contents of the seams and host rocks and groundwater sulphate concentrations.

1.4 STRUCTURE OF THE THESIS

This paper consists of five chapters.

- Chapter 1 it serves as an introduction. It also gives an overview of the background information on coal, its uses and impacts of coal mining.
- Chapter 2 focuses on the literature reviewed with topics that are related to this study.

- Chapter 3 discusses all the methods that were employed during the course of this study; which include data collection and processing.
- Chapter 4 is a discussion on the analysis, comparisons and interpretation of the results.
- Chapter 5 comprises conclusions and recommendations relevant to the study area.
- Reference list, this provides a list of all the sources that were cited and used in the completion of this paper.
- Appendices, these provide all the data that was used in the completion of this paper; these appendices were put on a disc due to large quantities of data. Please note that coordinates that were used for the generation of maps presented in this paper were deliberately omitted.

CHAPTER 2:
THEORETICAL FRAMEWORK

2.1 INTRODUCTION

The Witbank coalfield has been mined for more than a century and the mining operations cover large areas of land, and have altered the surrounding and underlying environments. This chapter gives an overview of the site descriptions of the collieries and discard facilities by focusing on the distance from the nearest towns; names of roads passing by; names of the farms the collieries occur on; year of establishment; area covered; method of mining; seams mined; geology and geohydrology; and depth to weathering.

The chapter also provides background information on the study area such as topography and climate. This paper focuses on the groundwater qualities of the collieries and discard facilities. Therefore, it is important to first understand the main causes of groundwater quality deterioration associated with coal mining, which is acid mine drainage (AMD). Furthermore, it is essential to understand the formation of coal and pyrite to be able to fully understand the formation of AMD. Previous work done on AMD and groundwater quality deterioration of the Witbank coalfield is also given towards the end of this chapter.

2.1.1 Locality

The Witbank coalfield is one of the 19 coalfields found in South Africa and one with the longest history of mining. This coalfield is situated in the north-eastern part of the country, in the Mpumalanga Province (refer to Figure 2.2) approximately 100 km east of Johannesburg (Cairncross *et al*., 1990). It extends from roughly $25^{0}30^{|}$ S, $28^{0}30^{|}$ E to $26^{0}30^{|}$ S, $30^{0}00^{|}$ E and covers an areal extent of 568 000 ha (Hancox & Gotz, 2014). This coalfield hosts about a fifth of South Africa's total coal resources and therefore can be considered a major contributor to the country's energy and export reserves (Cairncross *et al*., 1990).

This paper focuses on the following mines and discard facilities from the Witbank coalfield:

- Arnot Colliery
- Goedehoop Colliery
- Mafube Colliery
- Zibulo Colliery

- SACE Complex (Landau and Greenside collieries; Greenside and Blaauwkrans discard facilities)

Figure 2.1 below is a map of the Mpumalanga province, showing the exact locations of the above mentioned study sites and their distances in relation to one another; whilst these sites are further described in the next section.

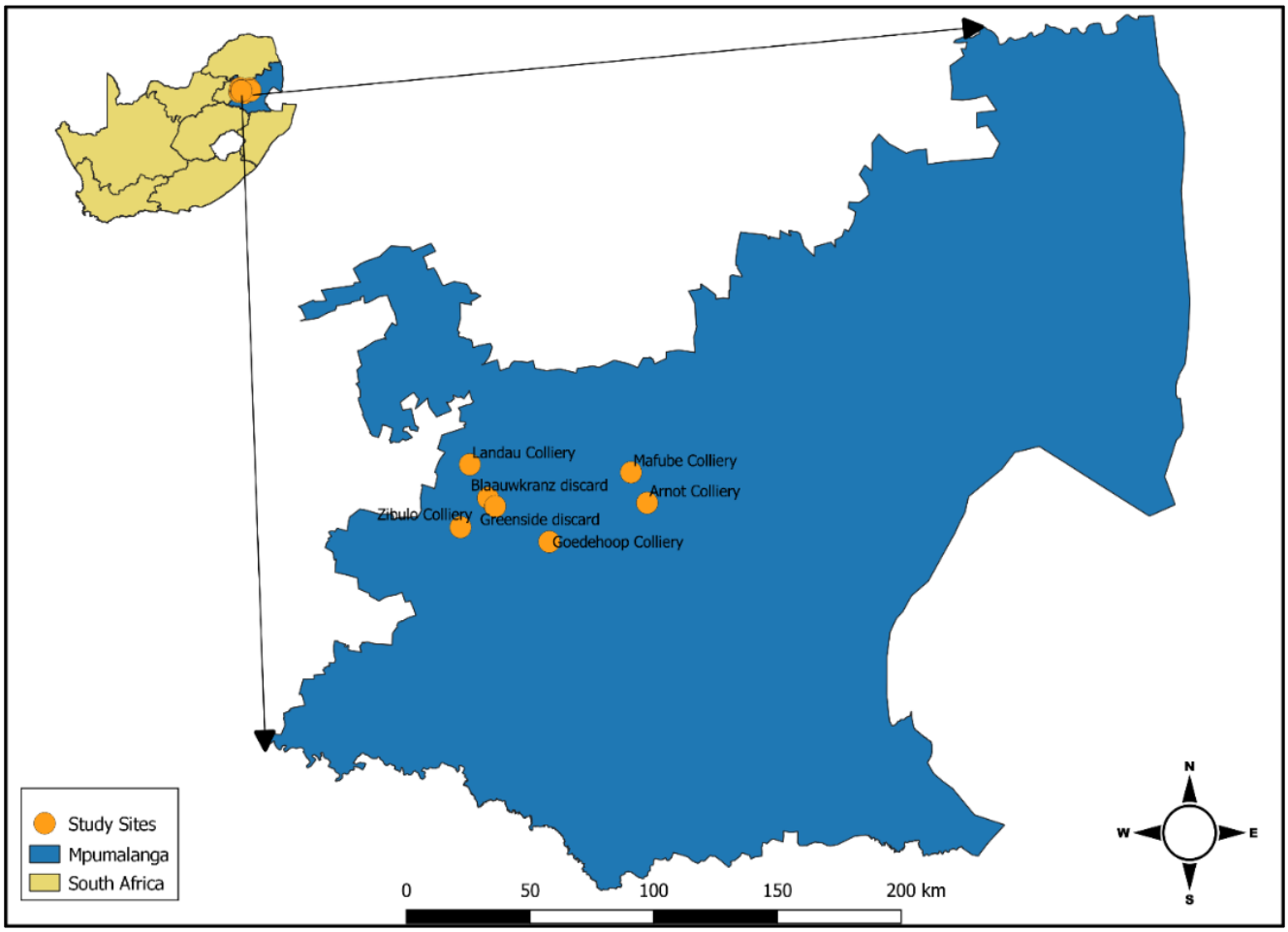

Figure 2.1: Map showing the locations of the specific sites in relation to one another.

Figure 2.2 shows the location of all the coalfields in the Mpumalanga Province with the Witbank coalfield highlighted in the orange colour.

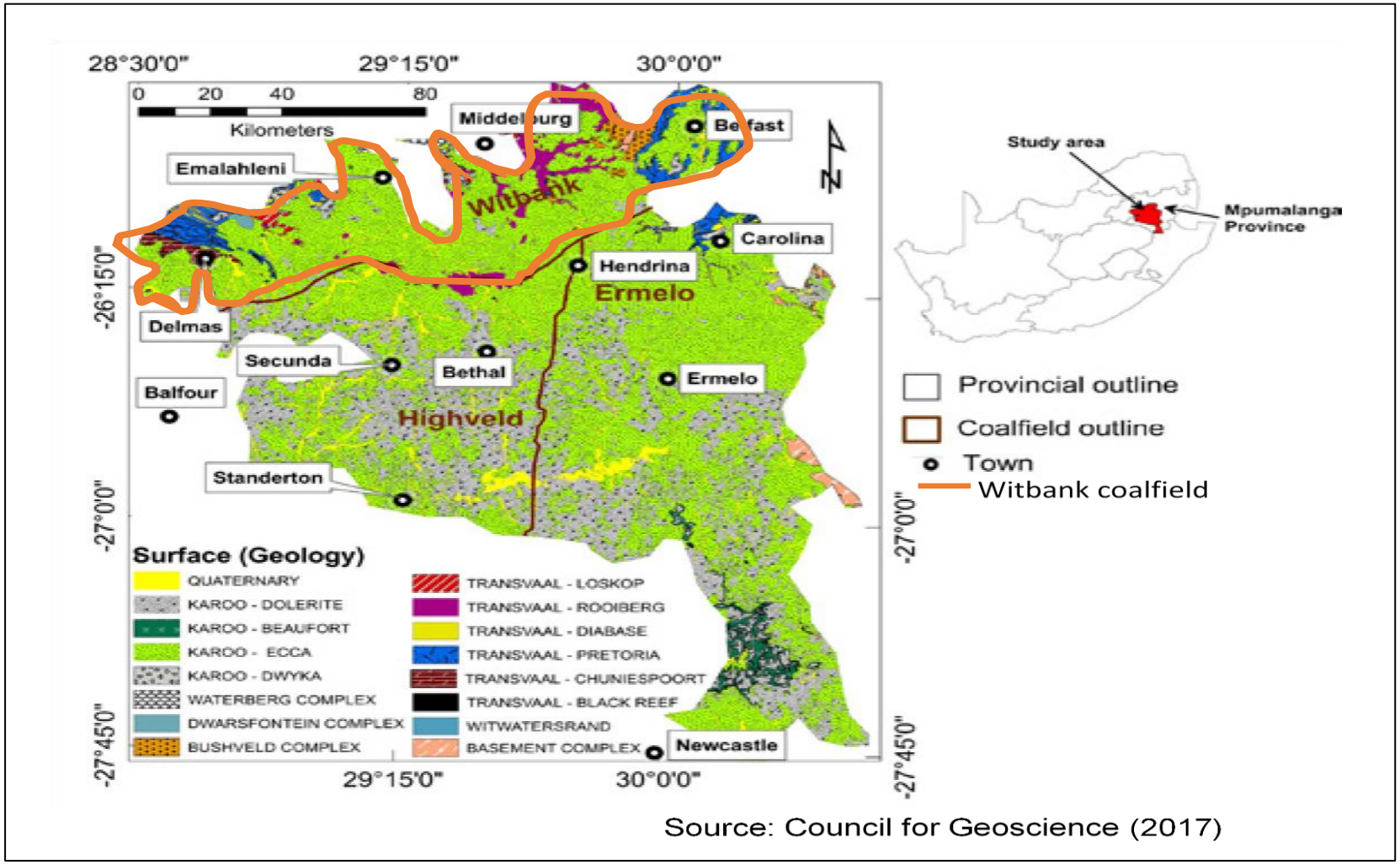

Figure 2.2: Map showing the location and outline of the Witbank coalfield as shown by the orange coloured line.

2.1.1.1 Site descriptions

2.1.1.1.1 Arnot Colliery

This colliery is situated approximately 40 km south-east of the Middelburg town and approximately 12 km to the south of the N4 highway that goes to Mbombela. It occurs on the Rietkuil 491JS and Nooitgedacht 493JS farms (XMP Consulting CC, n.d). This colliery uses both underground and opencast operations to extract coal, and produces 5 Mtpa of coal (XMP Consulting CC, n.d). It was closed in 2015 but operations commenced again in 2020.

2.1.1.1.2 Goedehoop Colliery

This colliery is situated approximately 40 km south-east of Emalahleni, between the R554 road to Belfast and the R35 from Middelburg going to Bethal; and about 6 km west of the Komati Power Station. It occurs on the farms Goedehoop 46IS, Haasfontein 28IS and Enkeldebosch 201S. It was established in April 1983 and later underwent a merger with the Banks colliery in 2005. This colliery produces coal in excess of 11 Mt from the No. 2 and No. 4 coal seams from four underground operations (XMP Consulting CC, n.d).

These operations include the Hope, Vlaklaagte, Simunye and South Shafts. It is divided into the South and North operations, in which the South operation covers an area of approximately 13 614 ha and consists of numerous underground workings and two opencast pits. However, opencast mining in the South operation ceased in 2013.

The extraction of coal in this colliery is with the use of bord-and-pillar methods, stooping and opencast; the No. 5 coal seam is also exploited for coal. The Goedehoop colliery covers an area of 28 000 ha and operations are estimated to run until 2035.

The groundwater in this area largely occurs within the weathered zone, joints and fractures of the competent rocks such as Sandstones of the Ecca Group (JMA Consulting Pty Ltd, 2012a).

a. Goedehoop North Operation

The Vryheid Formation that overlies the Dwyka Group underlies this operation and the rocks observed from monitoring boreholes include Shales, Siltstones, clayey to gritty Sandstones and thin Coal layers. Borehole logs show that the type of aquifer in this site is a laterally extensive shallow weathered zone aquifer (JMA Consulting Pty Ltd, 2012a).

This aquifer stretches across this entire site and its thickness varies between 6 and 18 m with an average of 12.19 m (Hodgson, 2011). The weathered zone is encountered at a depth that varies between 13 and 19 m, with an average of 16. 25 m.

b. Goedehoop South Operation

The Vryheid Formation underlies this site and the rocks observed from monitoring boreholes are Shales, Siltstones, Sandstones and Coal layers. The aquifer in this area is formed in the weathered zone and is also perched on fresh bedrock. This aquifer stretches across the entire site, varies in thickness, extends down to about 10 m, and the depth to weathering is also 10 m (Hodgson, 2011). This uppermost section consists of transported colluvium and weathered sediments, which overlie the unconsolidated sedimentary rocks (JMA Consulting Pty Ltd, 2012b).

2.1.1.1.3 Mafube Colliery

Mafube colliery is located approximately 30 km east of Middelburg between the R104 road going to Belfast and N4 highway, and about 14 km north of the Arnot Power Station. It is located on the farms Elandsfontein 433JS, Kleinfontein 432JS and Springboklaagte 416JS. This colliery is a 50:50 joint venture partnership between Anglo Coal and Exxaro (XMP Consulting CC, n.d). It began as a small pit operation in June 2004 and reached full production in January 2008. It comprises of the Nooitgedacht and Springboklaagte operations; in which No. 1, 2 and 4 coal seams are preserved at Nooitgedacht and No. 1 and 2 seams at Springboklaagte. This colliery extracts coal predominantly from the No. 2 coal seam and subordinately from the No. 1 seam by making use of the opencast mining method.

The thickness of the weathered zone varies for the Nooitgedacht area between 3.6 and 25.5 m, with an average thickness of 10.6 m (Delta-H Water Systems Modelling Pty Ltd, 2017). The Vryheid Formation rocks such as, Shale, Siltstone, Sandstone and Coal, which dominate the geology at this colliery. The colliery consists of shallow primary aquifers that are weathered and the fractured Karoo aquifers. However, perched aquifers may also occur localised on clay layers and lenses. Groundwater flow in this area is governed by secondary porosities such as faults, fractures, joints, bedding planes or other geological contacts (including coal seams); (Delta-H Water Systems Modelling Pty Ltd, 2016a). The rock matrix is considered impermeable. Water levels are often shallow, a few meters below ground level in the unconfined aquifer in the weathered sediments.

2.1.1.1.4 Zibulo Colliery

It is situated approximately 25 km south-east of Ogies, opposite the Klipspruit colliery and it is the first of several coal mines owned by Anglo Inyosi. It occurs on the farm Oogiesfontein 4IS and it is 73% owned by Anglo Coal, and 27% by Inyosi (XMP Consulting CC, n.d). This is a new multi-

product mine that was formerly recognised as the Zondagsfontein project, as well as the Greenfields projects of Elders, New Largo and Heidelberg (XMP Consulting CC, n.d). It comprises both underground and opencast operations; and has been operational since 2009. This colliery exploits the No. 2, 4, 5 coal seams and produces 7 Mtpa and 1 Mtpa from the underground and opencast operations respectively (XMP Consulting CC, n.d).

The rocks as observed from the exploration borehole logs are Sandstones, Gritstones, Siltstones, Coal, Shales, Mudstones, Limestones, Conglomerates, Diamictite and Dolerites. The thickness of the weathered material is 13 km and this includes both slightly and severely weathered material. The average depth to the weathered material is 13 km (Delta-H Water Systems Modelling Pty Ltd, 2018).

2.1.1.1.5 South African Coal Estates Complex (SACE)

This complex is situated within the Witbank coalfield and consists of the Greenside, Kleinkopje and Landau-Navigation operations near Emalahleni. All these operations fall within the upper Olifants Catchment. In this complex, the weathered zone of the Karoo sediments hosts the unconfined or semi-confined shallow weathered Karoo aquifer or hydro-stratigraphic zone (Delta-H Water Systems Modelling Pty Ltd, 2016b). This weathered zone is up to 15 km in thickness and water levels are often shallow to a few meters below ground level (Hodgson, 2013; Hodgson, 2014).

a. Landau Colliery

This colliery is situated about 17 km north west of Witbank between the R544 road going to Verena and N4 highway on the right hand side of the road going to Bronkhorstspruit. It occurs on the farms Kromdraai 279JS, Merwede 272JS and Coronation 280JS (XMP Consulting CC, n.d). It consists of four sections: the Kromdraai opencast mine, Excelsior, the Schoongezicht small-pit and the Umlazi small-pit. The Kromdraai operation mines the No. 1 and No. 2 coal seams (XMP Consulting CC, n.d). Furthermore, opencast mining methods are used to extract coal from the above-mentioned coal seams. This colliery covers an area of approximately 4 622 ha.

Sandstones of the Vryheid formation dominate the geology as observed from the exploration borehole logs; and a small area in the south is underlain by Dolerite. The weathering of the underlying sandstone results in the formation of sandy soils that allow easy infiltration of rainwater. Therefore, the aquifers of this colliery are weathered and shallow perched water aquifers.

b. Blaauwkrans Discard Facility

This discard facility is situated west of eMalahleni and covers an area of approximately 197 ha. Material from the Landau Colliery is dumped in this facility and it was reported to have 25.5 Mt of waste in 2010 (Scholtz, 2017). It is further estimated that 27.9 Mt of discard will be added to this

facility by 2025 (Scholtz, 2017). It is underlain by Shales, Siltstones and Sandstones of the Vryheid Formation. Three aquifers have been identified in the area in which this discard facility occurs; shallow perched unconfined aquifer, weathered unconfined aquifer and fractured confined or semi-confined aquifer (Datamine Africa Pty Ltd, 2017). The depth to the weathering zone in this area ranges between 3 and 20 m.

c. Greenside Colliery

This colliery is situated approximately 15 km south-west of eMalahleni and is near the N12 highway going to Johannesburg. It is located on the farms, Groenfontein 331JS and Klipfomtein 332JS seams (Golder Associates Africa Pty Ltd, 2018). It is bounded to the north by the Landau Colliery, and to the south by the Kleinkopje Colliery. The No. 4 coal seam is principally extracted using bord-and-pillar methods and production is estimated to continue until 2027 seams (Golder Associates Africa Pty Ltd, 2010).

Three types of aquifers have been identified in the area covered by this colliery; the shallow perched water aquifer, a deeper fractured rock aquifer system formed by fractures in the underlying Vryheid formation, and the coal seam aquifers within the sedimentary succession (Boshoff & Steenekamp, 2015).

d. Greenside Discard Facility

This discard facility is underlain by a Vryheid sequence of rocks, which is host to three main aquifer units. The first aquifer occurs in the weathered bedrock and the second one in deeper fracture-flow dominated by Sandstone and Shale (Marais, 2014). Waste material from the Greenside colliery is discarded at this facility.

2.1.2 Topography and Climate

South Africa is known to be a semi-arid region, experiencing low rainfall and extremely high summer temperatures; the country's climate is largely influenced by the cold Benguela and warm Mozambique and Agulhas currents. The area over which the coalfield occurs typically has moderate and dry climate, with summer rainfall. The warm summer season continues for 6.2 months; starting on September 19, lasting until March 25. During the summer period, daily temperatures reach an average above 24^{o}C. Model reconstructions and statistical analyses of past hourly reports from January 1, 1980 to December 2016 were used to determine the weather typical of Stations contributing to these model reconstructions are Springs, Pretoria Irene, Standerton and Nelspruit (Weather Spark, 2019).

This area experiences moderate summers and cold winters, with July being the coldest month (Banks *et al.*, 2011) as can be seen in Figure 2.3 below. The winter season lasts for 1.9 months, starting on June 1 and lasting until July 31 (Weather Spark, 2019). During this cool period, average daily temperatures reach below 19°C.

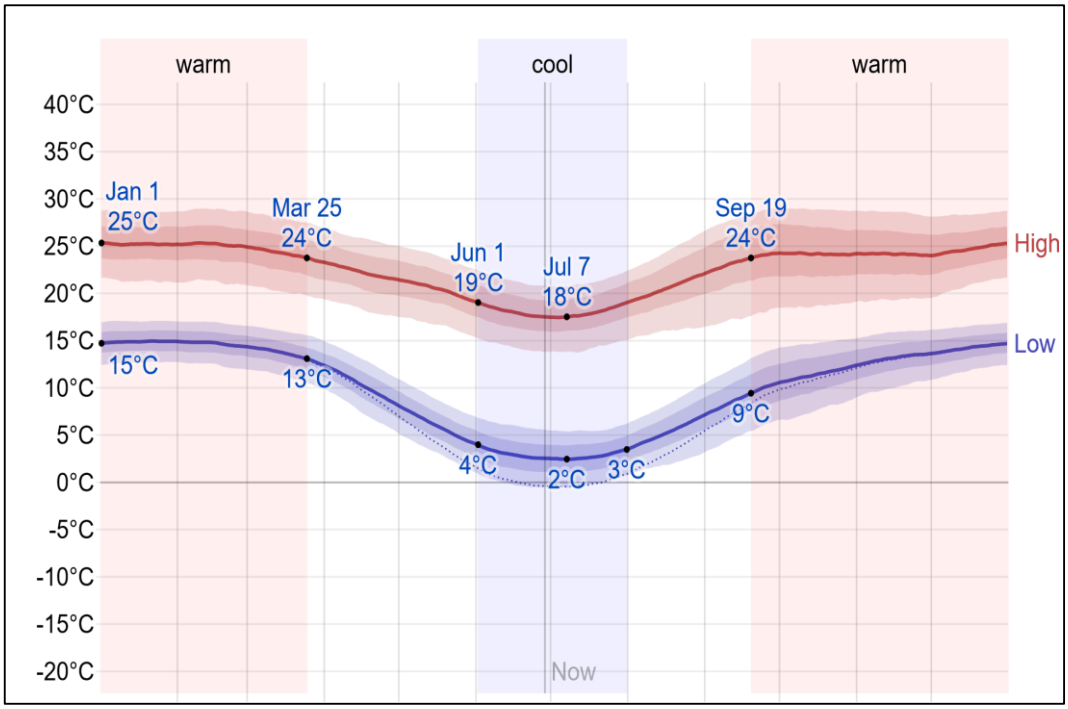

Source: Weather Spark (2019)

Figure 2.3: Average monthly temperatures for Witbank, expressed in Degrees Celsius.

The Witbank coalfield falls within the Olifants River Catchment, and this catchment area is known to receive an annual rainfall of between 500 and 800 mm (van Zyl *et al.*, 2001), and has an evapotranspiration rate of 1450 mm (Banks *et al.*, 2011). The rainy period for this area lasts for eight months, starting in September 7 and lasting until May 9. December is when the Witbank receives most of its rainfall, with a total average accumulation of 99 mm (Weather Spark, 2019).

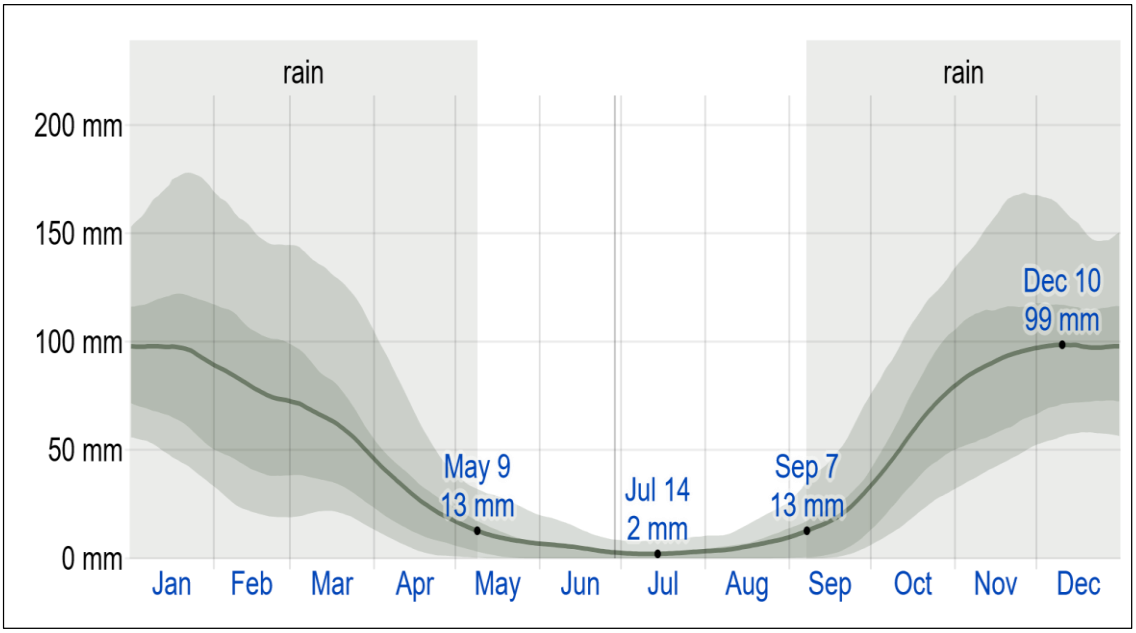

Source: Weather Spark (2019)

Figure 2.4: Average monthly rainfall recorded in Witbank, expressed in millimetres.

Furthermore, the dry period of this area lasts for four months, from May 9 to September 7, with less rain in July (refer to Figure 2.4). The topography of the study area is characterised by a fairly flat rolling landscape, that consists of valleys and small hills/ridges with the maximum elevation being 1635 m and minimum of 1406 m. Figure 2.5 shows the rolling landscape of the Witbank area, as well as how the topography is influenced by the different geological units.

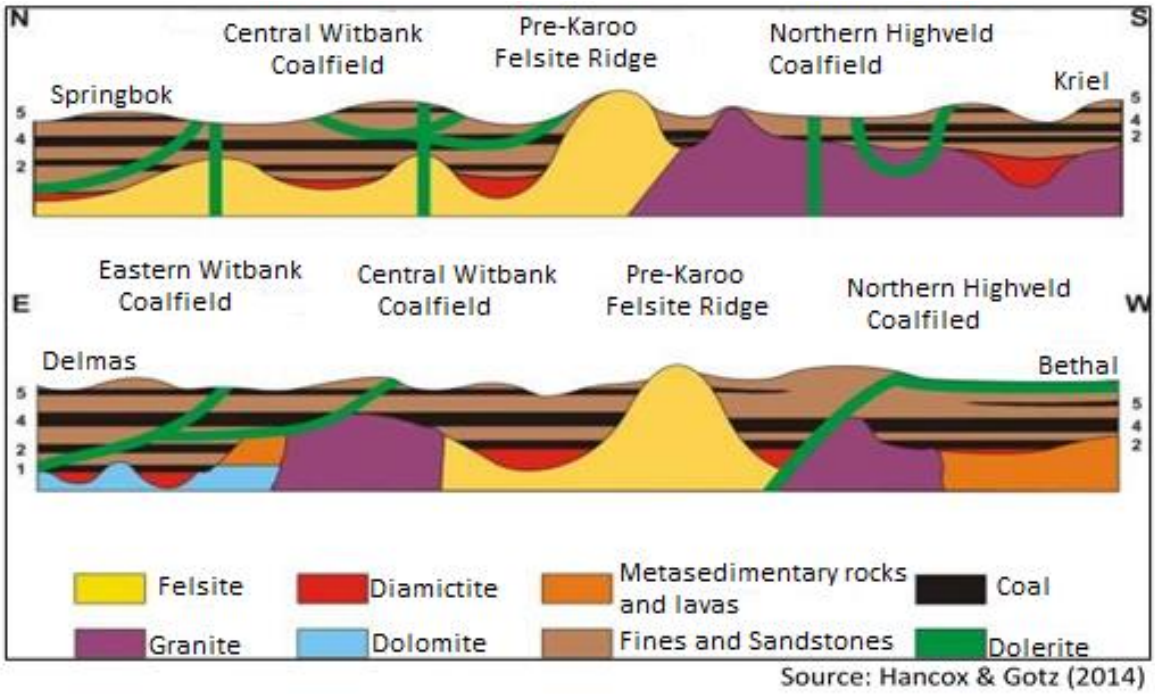

Source: Hancox & Gotz (2014)

Figure 2.5: Schematic sketches of profiles across the Witbank, showing the rolling landscape.

2.2 LITERATURE REVIEW

2.2.1 Geology

2.2.1.1 The formation of the Karoo Basin

During the northward drift of the Gondwana landmass, a subduction zone developed to the south of the Kaapvaal Craton about 330 Ma (McCarthy & Rubidge, 2005). The compressional forces that were active at the time led to the formation of a mountain range known as the Cape Fold Belt by causing folding and faulting of the Cape Supergroup sediments (McCarthy & Rubidge, 2005). The formation of this mountain range caused the sagging of the crust in the interior of the Kaapvaal Craton, forming an asymmetrical foreland basin (McCarthy & Rubidge, 2005).

This basin was deep along the southern margin and shallow to the north of the Kaapvaal Craton as seen in Figure 2.6 below; therefore, the sedimentary succession deposited in this basin becomes thin towards the north (Cadle *et al*., 1993; McCarthy & Rubidge, 2005).

The Karoo Supergroup was deposited between 330 and 180 Ma and is characterised by five distinct groups: Dwyka, Ecca, Beaufort, Stomberg and Drakensberg Groups.

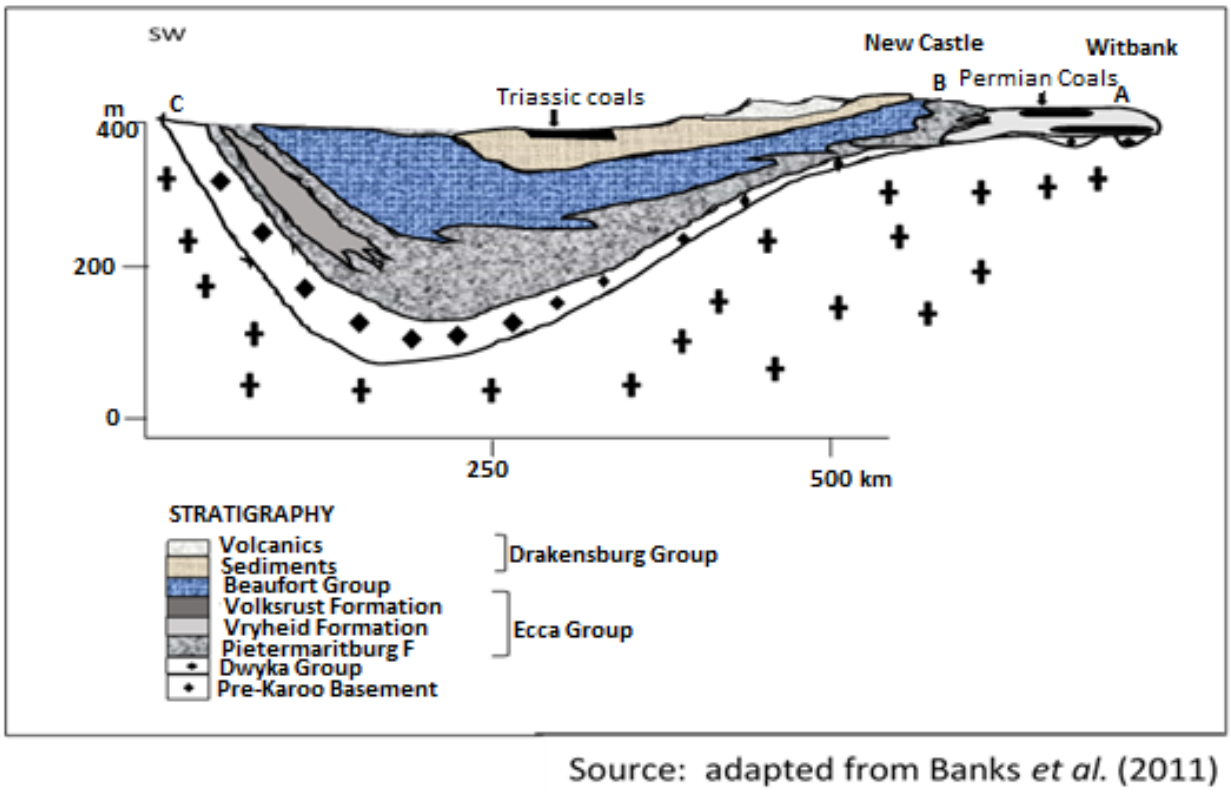

Source: adapted from Banks *et al.* (2011)

Figure 2.6: A SW-NE cross-section through the Karoo basin showing the varying thickness of the strata due to the shape of the basin.

2.2.1.2 The deposition of the Karoo Supergroup rocks

Sedimentation in the Karoo Basin began in the late Carboniferous period during which the Dwyka group sediments were deposited. During the Cape Fold Belt times, South Africa was situated over the South Pole and the northward drift of Gondwana resulted in glaciation. The Dwyka Group formed as a result of the glaciation that took place, and this group comprises subglacial till, glacio-lacustrine shale, terrestrial moraine and fluvio-glacial outwash (Cadle *et al*., 1993). The deposition of these sediments was due to advancing and retreating of ice sheets, which surrounded the basin.

As Gondwana continued to drift in a northward direction, moving out of the South Pole, the glaciers melted and this left a large inland body of water (inland sea) inside the Karoo Basin (Cadle *et al*., 1993; McCarthy & Rubidge, 2005). The existence of this inland water body was followed by a sediment infill from the south and north of the basin, wherein rivers formed deltas along the shoreline of the Karoo Sea. During the early Permian, there was deposition of deep marine Shales, submarine-fan Sandstones and Shales along the southern margin of the basin; these rocks make up the Ecca Group (Holland *et al*., 1989; Cadle *et al*., 1993).

The Ecca Group is divided into 3 formations:

- Pietermaritzburg and Volksrust Formations:

These two Formations are represented by Shelf-shales, which join southwards to wherein the central part of the Ecca Shale facies is formed.

- Vryheid Formation:

This formation is represented by an alternating sequence of Conglomerates, Sandstones and Shales, which host the economically extractable coal seams (Cadle *et al*., 1993; Cairncross, 2001). These sediments are coarse and therefore represent a regressive wedge of deltaic, fluvial and shallow marine sediments (Cadle *et al*., 1993).

The Beaufort and Stomberg Groups of sediments are indicative of a change in the evolution of the basin, depositional environments and climatic conditions during the late Permian and Triassic Periods (Cadle *et al*., 1993; McCarthy & Rubidge, 2005). The Cape Fold Belt mountain range continued to rise and therefore it was the major source of sediment to the Karoo basin. The depositional environment in the basin changed from marine to braided and meandering fluvial, lacustrine and wet-and dry-desert environments (McCarthy & Rubidge, 2005).

The sedimentary rocks of the Beaufort Group were deposited by large northward-flowing meandering rivers that led to the accumulation of sand. Periodic floods led to the deposition of mud on the floodplains of the rivers and silt. Furthermore, these meandering rivers were replaced by braided rivers that deposited sand.

The deposition of the Beaufort Group was terminated by a short period wherein there was uplifting of the Karoo strata; this caused erosion of pre-existing sediments (Cadle *et al*., 1993). These events led to the formation of the Stomberg Group, which is indicative of a gradual change to arid conditions.

The change in climatic conditions during the deposition of the Stomberg Group is recognizable in the following formations as described by (Cadle *et al*., 1993; Johnson *et al*., 1996; McCarthy & Rubidge, 2005):

- Molteno Formation: This sequence of rocks was deposited by braided rivers
- Elliot Formation: The Karoo Basin became arid and this change in climatic conditions is considered to have occurred when the floodplain sediments were beginning to form. This aridification of the Karoo depression is seen in rocks that have a distinct red colouration.
- Clarens Formation: This formation is considered to have been deposited during desert conditions as temperature and aridity increased.

Sedimentation in the Karoo Basin was terminated by the extensive eruption of the Drakensberg lavas. These lavas solidified as dikes and sills. This volcanic eruption marked the rifting that led to the separation of Gondwana (Smith, 1980). The stratigraphy of the Karoo Supergroup, from the oldest to the youngest group is showed in Figure 2.7 (adapted from Hancox & Gotz, 2014).

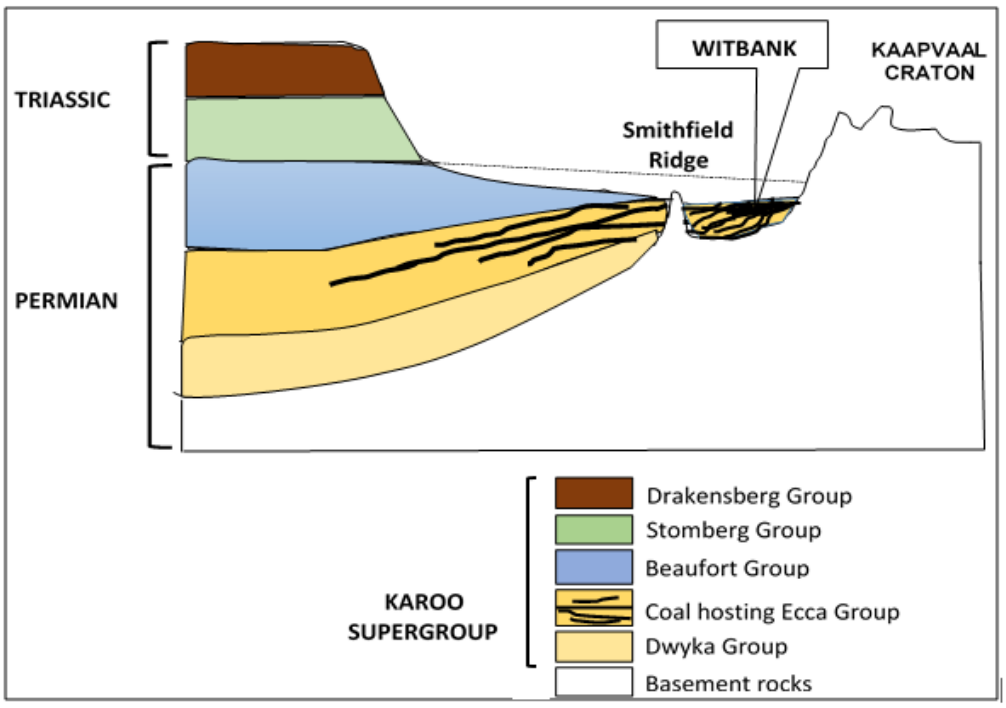

Source: adapted from Hancox & Gotz (2014)

Figure 2.7: Schematic illustration of the stratigraphy of the Karoo Supergroup.

2.2.1.3 Coal seams

The coal seams are hosted in the rocks of the Ecca Group. The rocks were deposited by the southward flowing deltaic rivers that were draining the highlands that formed to the north of the Karoo Basin during the continued northward drifting of Gondwana (Cadle *et al*., 1993; McCarthy & Rubidge, 2005).

Tree-like plants such as, Glossopteris dominated the deltas in the northern margin of the Karoo basin; these plants grew in swamps (McCarthy & Rubidge, 2005).

The dead plant matter accumulated more rapidly than it could decay forming thick strata of peat, which were covered by the sediment carried by the deltaic rivers to later form coal (McCarthy & Rubidge, 2005).

Therefore, the northward colonization of the delta plains by the tree-like plants is responsible for the coal presence in the north and not the south of the Karoo Basin (refer to Figure 2.8). The coal seams occur in the Early Permian Vryheid Formation and the Triassic Molteno Formation (Teichmüller, 1989; Cadle *et al*., 1993).

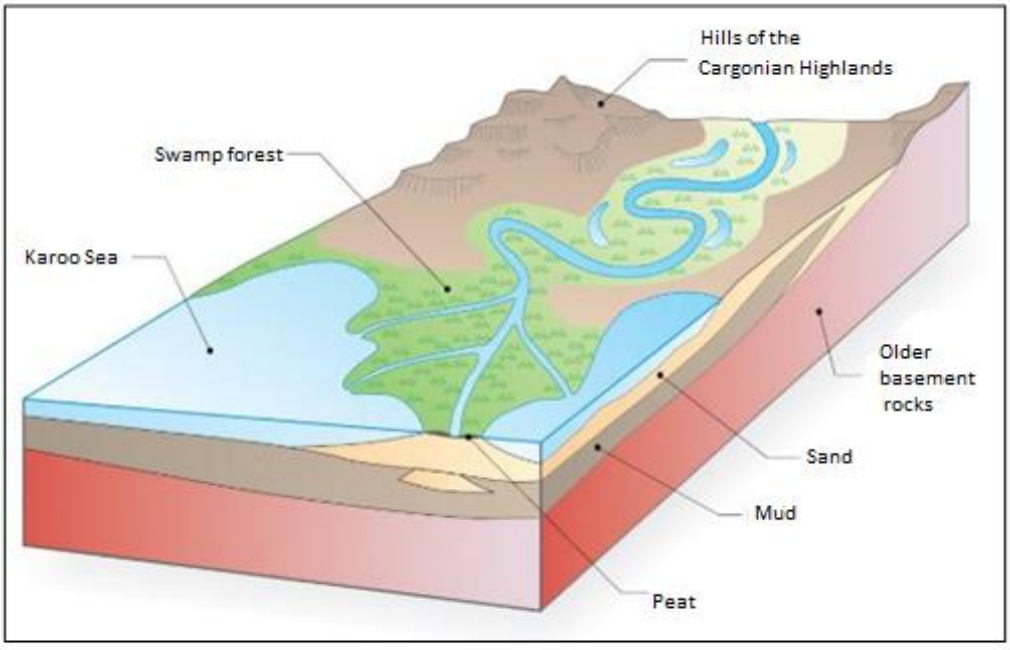

Source: McCarthy & Rubidge (2005)

Figure 2.8: A diagram showing the formation of coal by the invasion of the floodplains of deltaic rivers by plants.

The Witbank coalfield is characterised by five coal seams (No. 1 to No. 5) of varying thickness and quality. The seams are numbered No. 1 at the bottom of the sequence and No. 5 at the top (refer to Figure 2.9). The coal seams can described as follows:

- No. 1 seam is approximately 0-3 m thick and is patchily developed due to the Pre-Karoo stratigraphy; and contains local sandstone and siltstone partings. This seam comprises of lustrous to dull coal of high quality and is a source of A-grade steam coal and metallurgical coal with low phosphorus (Telfer *et al*., 2017). Average total ash percentages of about 25% are characteristic of this seam and the trend has been noted to increase from west to east across the Witbank coalfield. According to Pinetown (2003), SiO_2, Al_2O_3, K_2O and TiO_2 concentrations decrease from east to west; Fe_2O_3 and S show a similar distribution but are more concentrated in the south eastern region since they are associated with pyrite.
- No. 2 seam is approximately 4.5-20 m thick and is the most economically important for export. This seam displays well-defined zoning, with about six zones that have different coal qualities (Telfer *et al*., 2017). SiO_2, TiO_2, Al_2O_3, Na_2O and K_2O concentrations show a northeast-southwest distribution (Pinetown, 2003). This seam was found to have high concentrations of Fe_2O_3 and S north-west of the seam.
- No. 3 seam is an approximately 0.5 m thick poorly developed seam; of high quality and low economic importance. As a result it is less studied in comparison to the other seams.
- No. 4 seam is about 2.5-6.5 m thick, split into No. 4A, Upper 4 and lower 4 seams by mudstone/siltstone partings. It is of low quality but is economically important as compared to No. 2 seam. It consists of dull to dull lustrous coal and mining is mostly limited to the No. 4 lower seam (Telfer *et al*., 2017). This seam has SiO_2, TiO_2, Al_2O_3, Fe_2O_3 and S concentrations that are similar to concentrations of No. 1 and No. 2 seams; and SiO_2 and Al_2O_3 concentrations are highest in the north eastern region of the seam (Pinetown, 2003). Fe_2O_3 and S concentrations show a decreasing trend from west to east.
- No. 5 seam is about 0-2 m thick and is an erosional remnant; it comprises bright-banded coal mixed with thin partings of a clastic nature. This seam is of high quality coal with low phosphorus content (Telfer *et al*., 2017). This seam has Fe_2O_3 and S concentrations that are evenly distributed across the seam. This seam is enriched in vitrinite and sulphur compared to the underlying seams (Roberts, 1988).

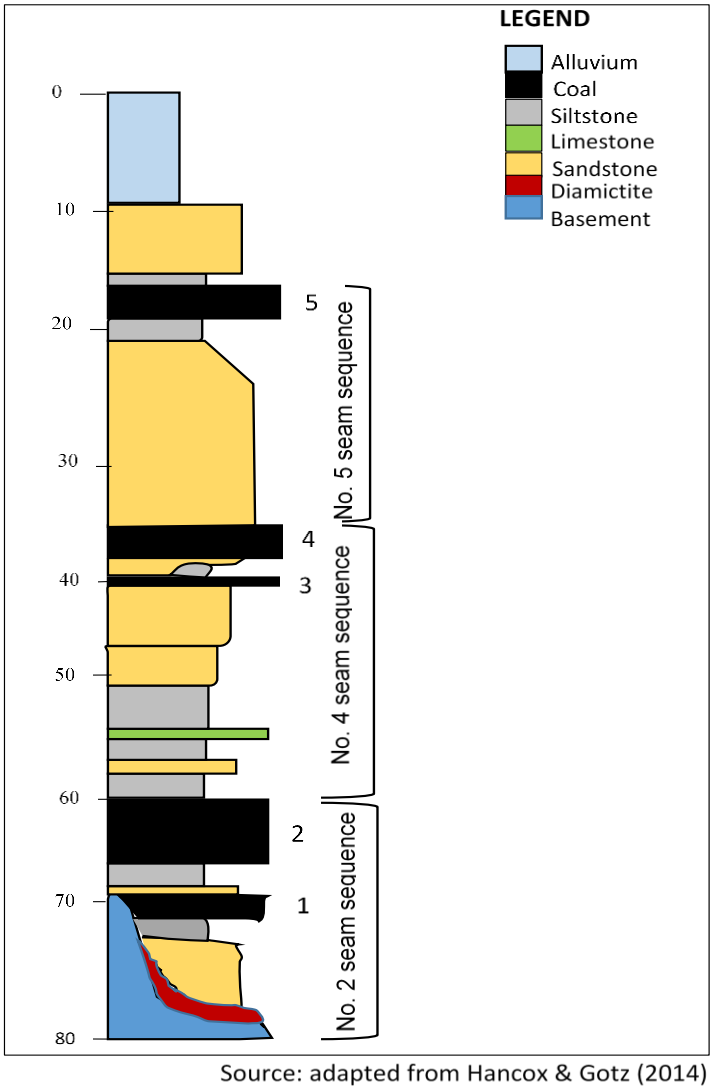

Source: adapted from Hancox & Gotz (2014)

Figure 2.9: A stratigraphic column showing the positions of the different coal seams.

Figure 2.9 is an illustration of a stratigraphic column showing the coal seams in sequence and the type of rocks occurring between seams and thereby separating the coal seams.

The lowermost No. 1 and 2 coal seams are associated with sediments that accumulated during the northward retreat of glaciers (Cairncross *et al*., 1990). This is indicated by the glacio-lacustrine shales and dropstones that were derived from floating ice-bergs. Furthermore, No. 3, 4, 5 seams are associated with sediments that were deposited in deltaic and fluvial environments. The vegetation that formed these seams appears to differ from the one that formed the No. 1 and 2 seams (Cairncross *et al*., 1990).

2.2.2 Geohydrology

The Witbank coalfield has a geohydrological system that is made-up of three aquifers namely: an upper weathered aquifer, a fractured aquifer and a pre-Karoo aquifer (Digby Wells & Associates, 2011; Gomo & Vermeulen, 2014). These three aquifers are described below.

- The Ecca weathered aquifer

Throughout the Olifants Catchment, Ecca Group sediments are weathered to depths of 5-12 m below the surface and the water level is between 5 and 10 meters below ground level (mbgl), (Hodgson & Krantz, 1995; Digby Wells & Associates, 2011; Erasmus, 2018). According to Digby Wells & Associated (2011), these sediments were weathered in situ and underwent transportation as part of the erosion process.

This weathered aquifer is recharged by rainfall and it is estimated that the percentage recharge received is 1-3% of the annual rainfall. This weathering allows the rocks to store and transmit water. This aquifer type is generally low yielding, ranging between 100 and 200 L/hourr (Hodgson & Krantz, 1995).

According to Digby Wells & Associates (2011), the weathered aquifer has a porous flow. Furthermore, it should be noted that recharge values vary from one region to the next in such weathered systems. This is considered to be due to the weathered sedimentary rocks having compositions that range from coarse-grained sand to fine-grained clays.

The water found in this weathered aquifer is known to be of great quality and this is due to soluble salts being leached with the flow the groundwater through the weathered sediments, these sediments act as a sieve (Hodgson & Krantz, 1995; Vermeulen & Usher, 2006a; Digby Wells & Associates, 2011). The flow of groundwater follows the surface topography and forms natural springs where it intersects the surface; and this is a low yielding aquifer due to its insignificant thickness (Erasmus, 2018).

- The Fractured Ecca aquifer

This aquifer consists of the various lithologies of the Ecca Group, such as, siltstone, shale, sandstone and the coal seams (Digby Wells & Associates, 2011). The rifting brought by the eruption of the Drakensberg lavas in the form of dykes and sills that further led to the separation of Gondwana caused fracturing of these pre-existing rocks; the fractures are commonly noticed in competent rocks such as sandstone. The pores of the Ecca sedimentary rocks are cemented and this hinders the free movement of groundwater in these sedimentary rocks. Therefore, the principal flow mechanism occurs along secondary structures including faults, cracks, joints, and bedding plane fractures (Hodgson & Krantz, 1995; Vermeulen & Usher, 2006a; Digby Wells & Associates, 2011; Erasmus, 2018).

However, the fractures, cracks and joints in the Karoo rocks allow groundwater to move along these secondary structures. It should be noted that not all of these secondary structures are water-bearing (Hodgson & Krantz, 1995). Vermeulen & Usher (2006a) suggest that this fractured aquifer contains

water enriched in salts as compared to the upper weathered aquifer; and these higher salt concentrations are the result of longer contact time between the host rocks and the water.

- Pre-Karoo aquifers

Few farmers in the study area obtain water from the aquifers underneath the Dwyka group rocks, as only limited drilling has intersected the basement below the Karoo Supergroup (Hodgson & Krantz, 1995). The Dwyka tillites, which act as an aquiclude, separate this aquifer from the overlying fractured Karoo aquifer.

Furthermore, the crystalline nature of the basement granitic rocks causes the flow mechanism in this aquifer to be fracture flow (Digby Wells & Associates, 2011). This aquifer is characterised by water enriched in fluoride. This coupled with low yields, deep expensive drilling and the low recharge rates limits the exploitation of this aquifer for usable water (Digby Wells & Associates, 2011; Erasmus, 2018).

2.2.3 Mining methods and flow hydraulics

The Mpumalanga Coalfields have been exploited for coal for more than 100 years. Mining firstly took place to the west of the town of Witbank. However, over the years, many of these mines have been closed down. Mechanisation of mines occurred in 1970 and since then, different mining methods have been used. The choice of the mining methods is dependent on the thickness of the coal seams and the depth of mining. The major methods used for coal extraction in South Africa include opencast, underground and bord-and-pillar mining:

a) Opencast mining:

This method of mining involves the excavation of a large hole in the surface of the Earth to expose coal. The hole evolves in the direction that is necessary to expose more coal. The hole is dug in the form of benches to remove the overburden and ensure the stability of the sides of the pit. This method involves the use of open pit and strip mining and it is known to have the greatest impact on the quality of groundwater (van Niekerk, 1997; Usher *et al*., 2003).

b) Underground mining:

- Shallow underground mining: This method of mining involves mining into the weathered aquifer, and it is usually conducted by bord-and-pillar methods in the Witbank area.
- Deep underground mining: This method is defined as mining that does not mine into or interfere with the weathered aquifer.

- High extraction underground mining involves several mining methods:
    - Longwall mining: This method is the predominant method; the Longwall panels are 200 m wide on average with lengths ranging between 1000 and 3000 m (Hodgson & Krantz, 1995). This method causes the overlying strata to collapse in a circular fashion and extension of major fractures all the way to the surface. This method is usually carried out in areas that do not have a lot of structural disruptions
    - Shortwall mining: This method involves much smaller widths than in the case of longwall mining, panel widths of about 100 m; it also causes the overlying strata to collapse.
    - Stooping mining: This mining method involves the extraction of coal pillars after bord-and-pillar mining has been completed; it results in limited collapse.

c) Bord-and- Pillar extraction:

This method involves leaving coal pillars behind for support of the overlying geological strata and it may require a certain amount of blasting. However, these pillars may be extracted at a later stage. Bord-and-pillar and opencast mining are the most dominant methods used in the Witbank coalfield.

Mine drainage is a problem of utmost importance in areas involved in coal mining. It starts during active operations when the mines fill up with water from groundwater and/or surface water systems. The different mining methods play a role in the movement and accumulations of water into the mine workings, which in-turn cause acid-mine drainage problems.

The influx of water into bord-and-pillar mine workings is generally slow and the quantification of these water influxes is difficult, if not impossible (Grobbelaar, 2011). This is due to many depressions that serve as areas of accumulation of water before it is pumped out to central pumping facilities.

Furthermore, water that occurs on the coal seam is pumped out only if it interferes with the mining process. The many current excess water and water quality problems mostly come from operations that use secondary mining through stooping (Grobbelaar, 2011).

Longwall mining operations experience water influx problems in which the water that comes from the collapsed overlying strata and rainfall enters into the cracks in the rocks in the mine workings. Approximately 0.2 ML/d of water is derived from each km^2 of area mined (Grobbelaar, 2011). In opencast mines, the pits are said to be recharged by an average of 20% of rainfall during the operational stage and after mine closure (refer to Table 2.1).

Table 2.1: Recharge rates of the different mining methods

Mining method	Recharge as per percentage of the average annual rainfall
Bord-and-pillar	1-3%
Stooping	6-13%
Longwall and shortwall	15-20%
Opencast	10-30%

Source: Steenekamp (2011)

The water that accumulates in the mine workings is pumped out; however, in some cases it drains out from the mines to the surrounding areas. During active operations, water is pumped out from the mines; however, water fills these mine workings once the mines have been closed and eventually discharges into the surface water bodies (Havenga, 2011).

The flow of water in coal mines in governed by the following factors (Havenga, 2011):

- Geometry of the mine
- Discharge elevation
- Extent of collapse and subsidence
- Coal unmined boundaries
- The extent of fracturing
- The general nature of overburden
- Condition at the outcrop

The geometry of the mine controls the nature of flow; whether the flow will follow a downward direction toward a low discharge elevation, or exit the flooded mined at the lowest surface elevation (Havenga, 2011). The discharge elevation determines the static water level in a flooded mine. The direction and velocity of flow of water in the subsurface is influenced by the location of unmined coal boundaries and the extent of collapse and subsidence (Havenga, 2011). Furthermore, in opencast mine workings, the flow of groundwater will be directed toward the pit due to the presence of an artificial gradient change.

The normal groundwater flow and direct recharge into the spoils, is known to create a groundwater level in the spoil heap that will eventually decant when a decant level is reached (Havenga, 2011). The decanting water from the spoils and surface run-off of the spoils will follow the natural gradient and flow into the nearest river or stream if not managed accordingly or seep into the subsurface water resources. Decanting points of mine water in underground mine workings are likely to coincide with the collapsed strata in low-lying topographic areas (Grobbelaar, 2011).

2.2.4 Chemical and biological activity associated with South African coals

The chemical and microbial activities that take place during the deposition of peat and formation of coal are the important factors influencing the ash and sulphur content of the coals. Clastic depositional processes and the pH of the swamp water are important parameters in determining the ash content of coal. According to Havenga (2011), the pH of the swamp water controls the rate and degree of plant degradation during the formation of peat. The presence of microorganisms is critical during the peat stage and is controlled by the pH. The microbial activity is highly effective at pH of more than 4.5 (Havenga, 2011).

Coals contain more organic matter than mineral matter because they were derived from peat that accumulated under highly acidic conditions of pH < 4.5 (Cairncross & Cadle, 1988; Havenga, 2011). If the peat swamp pH is > 4.5, then the vigorous nature of the microbial activity will prevent organic material from producing coal (Cairncross & Cadle, 1988; Havenga, 2011). Peat accumulation in swamps characterised by pH > 5 would result in the production of black, highly carbonaceous shales or impure bone coal that contains more than 33% ash. If there was a brief period of unfavourable conditions, then the coal will have partings (Cairncross & Cadle, 1988; Fourie, 2007; Havenga, 2011). This would render an explanation to the presence of carbonaceous shale partings that occur in coal seams with little or no change in thickness.

Microbial and bacterial activity are dependent on temperature. Therefore, the pH of the swamp water in which the No. 1 and No.2 coal seams formed may have been greater than 4.5 (Havenga, 2011). The cooler temperatures prevent peat degradation under higher pH-values would therefore have suppressed bacterial activity (Fourie, 2007). Havenga (2011) suggested that when the lower seams were deposited, acidic water conditions were already prevailing in the swamp waters. These pH conditions are very important in understanding the observed minerals that are commonly associated with the coal seams in the Mpumalanga Coalfields.

It is presumed that the peat was preserved under fairly anoxic conditions, otherwise the bacterial metabolism of the organic material would have been intensified (Havenga, 2011). Furthermore, the pH conditions allowed the preservation of peat to occur and pyrite could form in the peat. Pyrite formation during accumulation and preservation of peat is therefore dependent on the presence of organic matter that can easily be metabolised, the diffusion of sulphate in the reacting sediments, the total concentration and reactivity of iron minerals and the production of elemental sulphur (Havenga, 2011).

2.2.4.1 Pyrite formation

The pyrite that forms in the coal seams and the host sedimentary rocks becomes oxidised in the presence of water and forms Acid Rock Drainage (ARD) or Acid Mine Drainage (AMD). The former occurs naturally, whereas the latter is due to the mining process because the rocks will now be more exposed to the oxygenated atmosphere. The formation of pyrite occurs during shallow burial of sediments, in which the detrital iron minerals in the sediment react with H_2S (Berner, 1984). The H_2S is a product of the reaction during which bacteria wherein sedimentary organic matter acts as a reducing agent reduce interstitial dissolved sulphate and a source of energy. Pyrite is not the initial product of this reaction but a sequence of metastable iron mono-sulphides, which readily change to pyrite during early diagenesis during a process that is rather poorly understood (Berner, 1984).

The quantity of pyrite that can be formed in sediment is controlled by the organic matter content; reactive iron minerals that are deposited in sediment and the availability of dissolved sulphate (Berner, 1984). The primary step in the overall process that leads to the formation of sedimentary pyrite is the reduction of sulphate by bacteria, and this process only occurs under anoxic conditions. The anoxic conditions are primarily recognised in most subaqueous sediments because the organic matter deposited in large amounts consumes the oxygen in the system. Furthermore, the dissolved oxygen migrates from the overlying water down into the sediment by molecular diffusion, wave and current stirring, or bioturbational irrigation (Berner, 1984). However, oxic bacteria that lives near the sediment-water interface consumes this dissolved oxygen by converting the organic matter to CO_2 (Berner, 1984).

According to Berner (1984), the rapid consumption of oxygen that occurs near the sediment-water interface prevents the penetration of this oxygen far into the sediment. Consequently, the sediment will be oxygen deprived and these anoxic conditions are essential for the reduction of sulphate by bacteria; the reaction of H_2S with iron minerals can take place both prior and after burial and even sedimentation under anoxic conditions. The overall process is as follows (Berner, 1984):

$$\mathbf{2CH_2O + SO_4^{2-} \rightarrow H_2S + 2HCO^{3-}} \qquad \textbf{Equation 1}$$

More pyrite forms in areas of high rates of sedimentation, especially in nutrient rich waters because there are high levels of H_2S that result from a high production rate of organic matter and sedimentation, rapid burial that permits the availability of reactive compounds and more organic matter for bacterial sulphate reduction at depth (Berner, 1984). The added amount and reactivity of detrital iron minerals to the sediment also limit the formation of pyrite (Berner, 1984).

2.2.4.2 The relationship between macerals and sulphur in South African coals

The presence of sulphur-bearing minerals such as pyrite in coals makes the mining of these coals detrimental to the environment. The sulphur concentration in the coals of the Permian Vryheid Formation has a positive correlation with the content of the vitrinite maceral group, and a negative correlation with the inertinite maceral family (Roberts, 1988). This relationship is observed at intraseam, interseam and intercoalfield levels (Roberts, 1988).

In the peat-forming environments wherein the Eh was low and water table was high, vitrinite precursors were formed (Roberts, 1988). These conditions were favourable for bacterial sulphate reduction that resulted in H_2S reacting with Fe^{2+} and organic components found in the peat. On the other hand, inertinite precursors were formed where the Eh was high and the water table was low, wherein aerobic respiration conditions were dominant and there was little production of H_2S (Roberts, 1988; van Vuuren, 1989). According to Roberts (1988), inertinite-rich coal with low sulphur content is enriched in organic sulphur that was derived from peat-forming plant tissues. Furthermore, high sulphur coals have a high content of pyritic sulphur in comparison with organic sulphur and this is the result of the preferential reaction of H_2S with Fe^{2+} (Roberts, 1988).

Macrinite-rich coal has a low sulphide content and this is due to the sulphur reduction bacteria in low-pH, raised swamps (Roberts, 1988). Vitrinite are the sulphide rich coals and they are thought to record peat accumulation in swamps that are fed by groundwater, where the anaerobic bacterial activity was promoted by high pH in the swamps (Roberts, 1988). The total sulphur in peats is a contribution from the sulphur that is fixed in the original plant tissue and the one dissolved in water that is associated with peat-forming environments (Roberts, 1988). Vitrinite and inertinite maceral groups of the Vryheid Formation coals have similar botanic origins; therefore, differential incorporation of dissolved sulphur is believed to have occurred during the early diagenesis of the peats (Roberts, 1988).

The incorporation of sulphur into the matrix during sedimentation is predominantly due to the respiratory activity of anaerobic bacteria such as Desulfovibrio (Roberts, 1988). Furthermore, there are two paths to introduce the sulphur from H_2S formed by sulphate reduction into peat, namely pyrite formation and reaction with organic peat constituents (Roberts, 1988). Pyrite (FeS_2) is formed by the reaction of H_2S with Fe^{2+} to produce FeS, which will combine with elemental sulphur to form FeS_2 (Roberts, 1988). Moreover, low redox potentials and pH that approaches neutrality promoted these reactions. Peat and coals influenced by marine processes are known to have elevated sulphur contents and this is widely attributed to high pH and SO_4^{2-} concentration in seawater relative to fresh water, which promotes sulphate reducing bacterial activity (Roberts, 1988).

Many of the Vryheid peats were formed in paralic settings, which suggests marine influence (Roberts, 1988). Roberts (1988) suggests that the bright (high sulphur) and dull (low sulphur) coal bands record the relative fluctuations in sea level. The relatively low redox potentials resulted from periods of high water table in the peat-forming environments. The sulphur content of the peat was increased by the reaction of iron and organic peat components with H_2S to form pyrite and organic sulphur (Roberts, 1988).

According to Roberts (1988), coals that are rich in macerals of the vitrinite-group comprise of elevated concentrations of sulphur as compared to the high-inertinite coals in the Permian Vryheid Formation; carbominerite-rich coals contain sulphur in small amounts.

2.2.5 Acid Mine Drainage (AMD)

2.2.5.1 Formation of Acid Mine Drainage

Acid mine drainage is a common problem in mines extracting gold, copper, nickel and coal; therefore, understanding its formation is of utmost importance. AMD is the outflow of acidic waters rich in sulphate and heavy metals/metalloids and is the result of the reaction of sulphide minerals with oxygen in the presence of water. It can be a naturally occurring phenomenon. However, mining activities promote its generation by increasing the amount of exposed sulphide-bearing material. The naturally occurring phenomenon is referred to as Acid Rock Drainage; whereas Acid Mine Drainage refers to the phenomenon promoted by mining activities and there are many sources of AMD associated with mining activities (refer to Table 2.2).

AMD is characterised by low pH, high concentrations of sulphate and heavy metals, as well as other toxic elements; and it can cause severe contamination of groundwater, soils and surface water bodies (Bell & Bullock, 2001; Akcil & Koldas, 2006; Fourie, 2007; McCarthy, 2011; McCarthy & Humphries, 2013). According to Akcil & Koldas (2006), iron sulphides are the most common acid generating minerals; however, other metal sulphide minerals also have acid-generating potential and such acid-generating sulphide minerals include pyrite, pyrrhotite, chalcopyrite, bornite and enargite.

Table 2.2: Sources of Acid Mine Drainage

Primary sources	Secondary sources
Mine rock dumps	Treatment sludge pounds
Tailings impoundment	Rock cuts
Underground and open pit mine working	Concentrated load-out
Pumped/nature discharged groundwater	Stockpiles
Diffuse seeps from replaced overburden in rehabilitated areas	Concentrate spills along roads
Construction rock used in rocks, dams, etc	Emergency ponds

Source: Akcil & Koldas (2006)

The following are the primary ingredients for the formation of AMD according to Akcil & Koldas (2006):

- Sulphide minerals
- Water
- An oxidant(oxygen from the atmosphere or from other chemical sources)

AMD effluents are characterised by low pH, high specific conductivity, high concentrations of iron, aluminium and manganese, as well as low concentrations of toxic metals/metalloids (Akcil & Koldas, 2006).

Akcil & Koldas (2006) indicated that the rate of acid generation is dependent on chemical, biological and physical factors, wherein physical factors such as the permeability of the waste rock dump are of utmost importance. For example, highly permeable waste rock dumps are characterised by high oxygen entry, and this contributes to higher chemical reaction rates. The rate of acid generation can be slow or fast and is dependent on the following factors (Akcil & Koldas, 2006):

- pH
- Temperature
- Oxygen concentration of the gas phase, if saturation is below 100%
- Oxygen content in the water (liquid phase)
- The degree of saturation with water
- The Chemical activity of Fe^{3+}
- The exposed metal sulphide's surface area
- The activation energy needed to start the acid generation process

- Bacterial activity

If the environment is conducive enough, acid generation takes place as illustrated by the following reactions examining pyrite (FeS_2) oxidation, since it is the most common sulphide mineral involved in the formation of AMD (Gray, 1997).

$$\mathbf{FeS_2 + {}^{7}/_{2}O_2 + H_2O \rightarrow Fe^{2+} + 2SO_4^{2-} + 2H^+} \qquad \textbf{Equation 2}$$

This equation involves the oxidation of pyrite (sulphide mineral) into sulphate, dissolved iron and hydrogen. The products (Fe^{2+}, SO_4^{2-} and H^+) are in an aqueous phase, and thereby cause an increase in the acidity and total dissolved solids of the water.

Much of the ferrous iron (Fe^{2+}) will oxidize to ferric iron (Fe^{3+}) if the surrounding environment is sufficiently oxidizing as shown by the following reaction:

$$\mathbf{Fe^{2+} + {}^{1}/_{4}O_2 + H^+ \rightarrow Fe^{3+} + {}^{1}/_{2}H_2O} \qquad \textbf{Equation 3}$$

Ferric iron precipitates as $Fe(OH)_3$ and jarosite at pH values of 2.3 and 3.5, and leaves small amounts of Fe^{3+} in solution while simultaneously decreasing the pH as shown by the following reaction:

$$\mathbf{Fe^{3+} + 3H_2O \rightarrow Fe(OH)_{3(Solid)} + 3H^+} \qquad \textbf{Equation 4}$$

Additional pyrite may be oxidised by any Fe^{3+} that did not precipitate from solution according to Equation 3 and can be described in the following equation:

$$\mathbf{FeS_2 + 14Fe^{3+} + 8H_2O \rightarrow 15Fe^{2+} + 2SO_4^{2-} + 16H^+} \qquad \textbf{Equation 5}$$

Bacterial activity is one of the primary factors that affect the rate of acid generation. Therefore, the environmental conditions have to favour the survival and thriving of the bacteria; and the influence of bacteria on the generation of acid will be minimal if the conditions are not conducive enough. For example, bacteria species such as, Acidithiobacillus ferrooxidans and Leptospirillum are highly active in waters that have a pH of less than 3.2 (Akcil & Koldas, 2006; Dold, 2014).

When the above reactions are simplified, an overall reaction can be created by combining Equations 1-3; wherein acid generation producing iron eventually results in the precipitation of $Fe(OH)_3$, (Akcil & Koldas, 2006).

$$\mathbf{FeS_2 + {}^{15}/_{4}O_2 + {}^{7}/_{2}H_2O \rightarrow Fe(OH)_3 + 2SO_4^{2-} + 4H^+} \qquad \textbf{Equation 6}$$

2.2.5.2 Secondary minerals

Secondary minerals are produced from ferrous and ferric rich mine water that reaches the surface and fully becomes oxidised and hydrolysed. Ferrihydrite, schwertmannite, goethite, jarosite, hematite and lepidocrocite are all secondary minerals that precipitate from the oxidation and hydrolysis of iron rich mine water (Hammarstrom *et al.*, 2005; Jönsson *et al.*, 2006; Dold, 2014).

According to Dold (2014), secondary minerals such as jarosite, schwertmannite and ferrihydrite are known as meta-stable minerals and can easily transform into goethite.

The minerals lepidocrocite precipitates at pH of 7, and a mixture of goethite, ferrihydrite and schwertmannite precipitates at a pH of 5.5. The precipitation of secondary minerals depends on the pH-Eh conditions, presence of metal ions and other complexing ligands (Jönsson *et al*., 2006; Dold, 2014). The metal(loid)s in solution are adsorbed by the Fe^{3+} of secondary minerals that precipitated from the acidic mine water; the adsorption depends on the pH of the water (Jönsson *et al*., 2006).

2.2.5.3 Treatment methods

AMD is an environmental problem that remains even after mining has ceased. Therefore, scientists have had to develop methods that make it possible for this problem to be addressed and dealt with. These ways include source control, migration control and remediation techniques.

2.2.5.3.1 Source control

This method is based on the saying that "prevention is better than cure", and therefore involves controlling the pollution from the source point. Several techniques that are employed with regards to this method are as follows:

- Flooding/sealing underground mines: oxygen and water are the key ingredients in the formation of AMD, therefore excluding either of both of these can possibly prevent or minimise the production of AMD. The underground mine workings can be flooded with water, and the dissolved oxygen present in the water will be consumed by mineral oxidizing organisms and other microorganisms present in the water (Johnson & Hallberg, 2005).
- Underwater storage of mine tailings: the objective of this technique is to prevent minerals from being in contact with dissolved oxygen; and therefore the sulphide bearing mine tailings are buried under water to cut off oxygen, the other essential ingredient of AMD formation.
- Land-based storage in sealed waste: this involves covering the waste heaps with a dry cover constructed from clay material (Peppas *et al*., 2000; Johnson & Hallberg, 2005; Pozo-Antonio *et al*., 2014). However, the cover is easily affected by climatic conditions; for example, in areas experiencing wet and dry seasons drying and cracking of the cover layer makes it ineffective.
- Blending of mineral wastes: this technique involves blending acid-generating and acid consuming materials to produce environmentally friendly composites. For instance, adding solid-phase phosphates (apatite) to pyrite-bearing mine waste results in the precipitation of

ferric iron as ferric phosphate, therefore, decreasing further oxidation of sulphide minerals (Johnson & Hallberg, 2005).

- Application of anionic surfactants: this involves the use of anionic surfactants such as sodium deodecyl sulphate (SDS) to kill iron and sulphur-oxidizing bacteria that have an important role in the generation of AMD (Johnson & Hallberg, 2005).

2.2.5.3.2 Migration control

All the measures aimed at controlling the migration of AMD involve controlling the water flow since water is a transport medium for contamination. Typically, water enters a site in its clean natural state, and leaves contaminated.

Therefore, water ingress into the site of acid formation can be controlled by any of the following ways as outlined by Akcil & Koldas (2006):

- Diverting surface water that flows towards the pollution site
- Preventing infiltration of groundwater into the pollution site
- Preventing the seepage of hydrological water into the affected areas
- Controlling the placement of acid-generating waste

Diversion of surface water commonly involves digging ditches, which may be difficult to maintain. Furthermore, infiltration of hydrological water can be prevented by installing under-drains in locations of dumps (Akcil & Koldas, 2006). Several methods exist for the treatment of AMD in open pit mines; these include flushing, containment, evaporation, and discharge into wetlands, neutralisation, precipitation and desalination (Akcil & Koldas, 2006).

2.2.5.3.3 Remediation techniques

Remediation involves treating the surface water and groundwater that is contaminated with AMD, as well as wastewater from the mines. South Africa is facing serious environmental threats to the limited available fresh water resources due to the polluted water that arises from past and on-going mining operations. Therefore, this polluted water has to be treated. The remediation techniques that are commonly used to treat AMD waters are as follows:

- Acid-Neutralisation: this is the most commonly used and environmentally effective method of remediation and it involves the addition of a neutralising chemical agent. The neutralising chemical agents that are used for this method include lime (calcium oxide), slaked lime, calcium carbonate, sodium carbonate, sodium hydroxide, magnesium oxide, hydroxide, soda ash, caustic soda, ammonia calcium peroxide, kiln dust and fly ash (Sherlock *et al*., 1995;

Johnson & Hallberg, 2005; Akcil & Koldas, 2006; McCarthy & Pretorious, 2009). Furthermore, adding alkaline material to AMD results in an increase in the pH, increased rate of chemical oxidation of ferrous iron and results in the precipitation of the many metals present in solution as hydroxides and carbonates (Maree & du Plessis, 1994; Skousen *et al*., 2019).

- Evaporation dams: Most of the mines that are faced with the problem of disposing severely contaminated excess water have constructed shallow dams wherein water is allowed to evaporate and leave salts behind (McCarthy & Pretorious, 2009).
- Rhodes Biosure process: In 18 January 2005, the first plant in the world that uses the Rhodes Biosure process was launched in South Africa to treat acid mine drainage. This process reduces sulphate in the acid mine water without any addition of chemicals. It is the most cost effective biological treatment method that uses primary sewage sludge, a by-product from the East Rand Water Treatment (ERWT) to ensure water quality; and production of safe and stable biosolids, instead of using expensive carbon and electron donor sources to reduce the sulphate in the acid mine water (Akcil & Koldas, 2006).
- Permeable reactive barriers (PRBs): a wide range of polluted groundwater is treated using this method. The construction of these barriers involves digging a trench or pit in the flow path of the contaminated groundwater and using sufficiently permeable reactive materials to fill the voids to allow the undisturbed flow of the groundwater (Johnson & Hallberg, 2005; Jeen & Mattson, 2016). Metals are removed as sulphides, hydroxides and carbonates through the alkaline-generating reductive microbiological processes that take place within the PRBs.
- Wetlands: Akcil & Koldas (2006) defined wetlands as complex systems that represent an interaction site between terrestrial and aquatic systems. These complex systems are typically characterised by a variety of habitats that represent a range from permanently wet open water areas to temporary wet areas that occur on the margins of the wetland (Akcil & Koldas, 2006). According to Ochieng *et al*. (2010), wetlands are known to make use of naturally available energy sources such as topographical gradient, microbial metabolic energy and photosynthesis to allow the heavy metal ions to precipitate out of solution as well as to decrease the acidity of the water. This method uses microorganisms to generate alkalinity and immobilise metals and therefore reversing the reactions that lead to the formation of AMD (Johnson & Hallberg, 2005; Oyewo *et al*., 2018).

2.3 PREVIOUS WORK DONE

McCarthy & Pretorius (2009) focused on implications of coal mining in the quality of water. They outlined the environmental problems associated with coal mining using the Witbank coalfield as an example. The method of mining in the early mines of the Witbank coalfield was the bord-and-pillar method which subsequently left some of the seams in the ground which caused many of the mines to catch fire after closure; resulting in roof collapse (Falcon, 1986; Bullock & Bell, 1997; McCarthy & Pretorious, 2009).

McCarthy and Pretorious (2009) suggested that the longwall mining method causes more acid generation than the bord-and-pillar mining. The mining process causes disturbance to the structure of the aquifer, subsequently increasing the sensitivity of groundwater to pollution by acid mine drainage. Mining increases the surface area and permeability of the Karoo rocks, thereby allowing free movement of water through the rocks, thus increasing the rate of acid generation than it can be neutralised naturally (McCarthy & Pretorious, 2009).

McCarthy & Pretorius (2009) determined the NNP of the coal seams and their host rocks in the Witbank area; in which positive values indicate sufficient presence of carbonate in the rock to neutralise the acid, and negative values indicate that calcium carbonate needs to be added to neutralise the acid (refer to Figure 2.10).

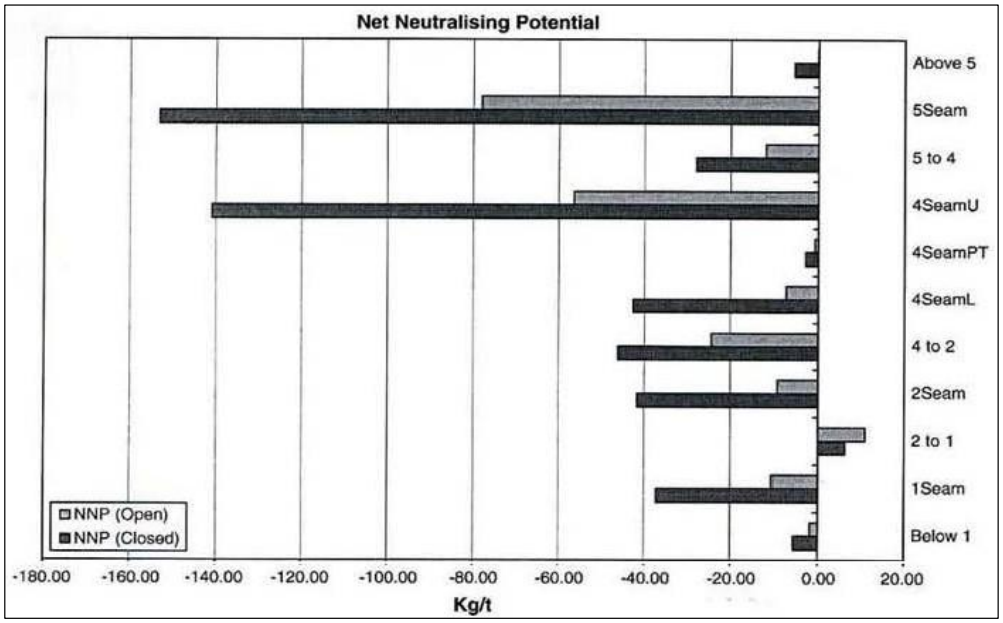

Source: McCarthy & Pretorious (2009)

Figure 2.10: Net Neutralising Potential of the coal seams and their host rocks in the Witbank coalfield.

Figure 2.10 shows that the coal and host rocks from the Witbank area produce acid and therefore need addition of calcium carbonate to neutralise this acid (McCarthy & Pretorious, 2009).

According to McCarthy & Pretorious (2009), the water quality in the Witbank and Middelburg dams show a steady increase in total dissolved solids and sulphate concentrations over the past years (refer to Figure 2.12 and Figure 2.13). These dams fall in the Olifants River catchment area (refer to Figure 2.11).

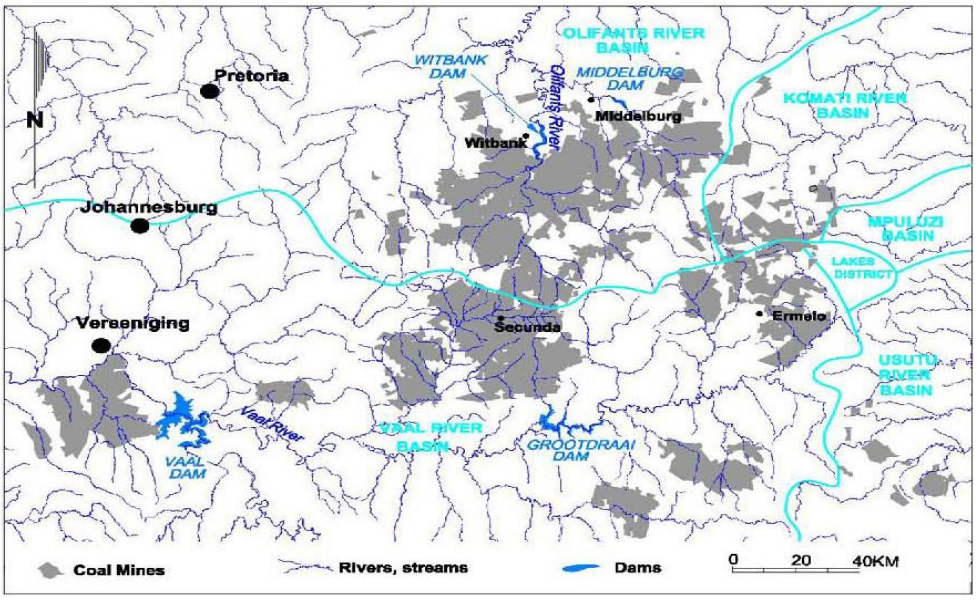

McCarthy & Pretorious (2009)

Figure 2.11: Map showing the positions of the Middelburg and Witbank dams in relation to catchment basins.

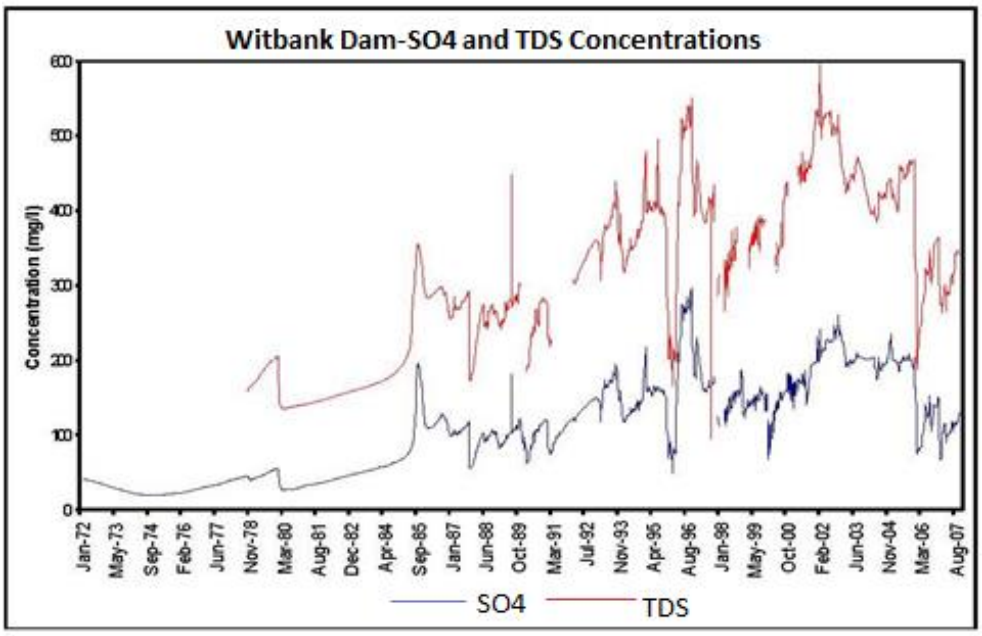

Source: McCarthy & Pretorious (2009)

Figure 2.12: Graph showing the concentrations of sulphate and total dissolved solids in the Witbank dam from 1972-2007.

The sulphate concentration of the water in the Middelburg and Witbank dams exceed the maximum recommended concentration for human consumption and is likely to continue to rise, (McCarthy & Pretorious, 2009).

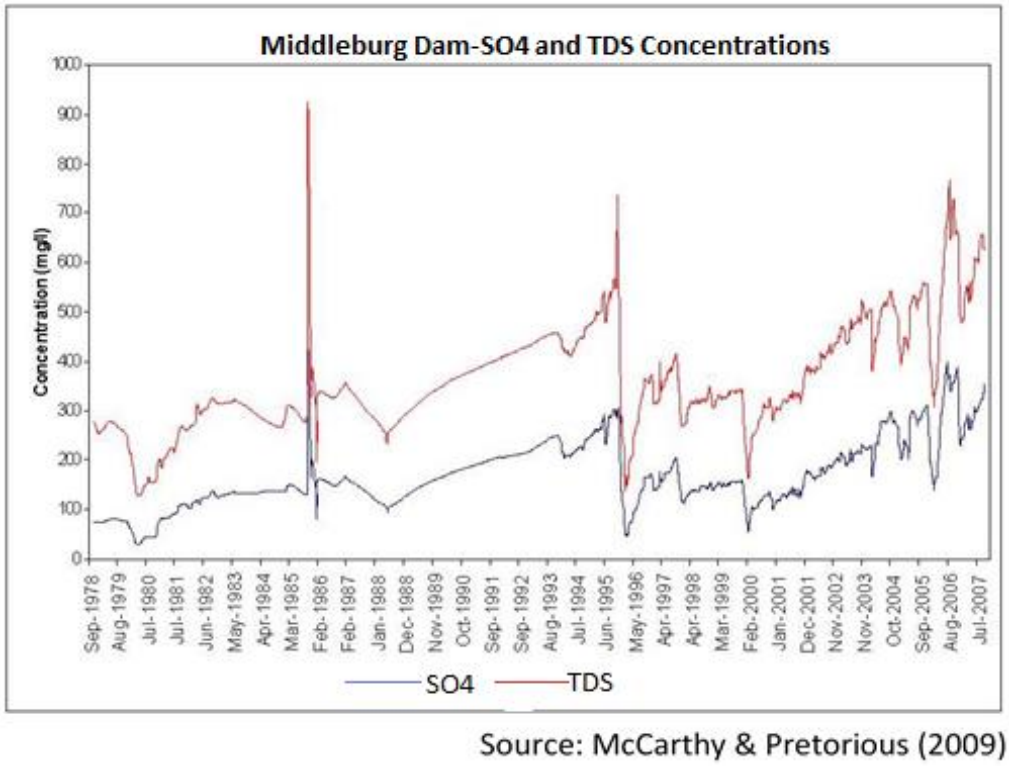

Figure 2.13: Graph showing the concentrations of sulphate and total dissolved solids in the Middelburg dam from 1978-2007.

A study by Sakala *et al*. (2017) focused on the hydrogeological investigation of the Witbank, Ermelo and Highveld coalfields, investigating the movement of acid mine drainage within the soil, unsaturated zone and aquifers.

Sakala *et al.* (2017) divided the 130-groundwater samples collected from the boreholes in the study area into 75% that were used for Artificial Neural Networks (ANN) training and 25% for ANN testing. Sakala *et al.* (2017) defined Artificial Neural Networks as belonging to the *"data-driven branch of artificial intelligence which is inspired by the biological neural system whereby the computer is trained to do the functions which at the moment humans do best like learning"*. The ANNs produced the transport and attenuation factors for the coalfields involved in the study successfully and the results showed positive spatial relationship with high sulphate concentrations found in the groundwater.

The environmental and geohydrological investigation done by Digby Wells and Associates for the Northern Coal (Pty) Ltd on the Weltevred farm, in the Witbank coalfield were done on geological drill core, host rock and overburden to test for acid-base accounting and neutralisation potential

(Digby Wells & Associates, 2011). The results indicated that the No. 2 coal seam and host rock had a possible low acid generating potential (Digby Wells & Associates, 2011).

A study by Sakala *et al.* (2016) on the vulnerability of groundwater to pollution by acid mine drainage in the Witbank coalfields produced ANN results that indicated that the surrounding area to the Olifants River and its tributaries showed high vulnerability of groundwater to acid mine drainage pollution.

The highly vulnerable zones are characterised by shallow water tables, less clay content in the soil and the rocks overlying these zones have poor neutralising potential making the groundwater highly vulnerable to pollution (Sakala *et al*., 2016; Sakala *et al*., 2019). Low pH and high sulphate concentrations in groundwater and surface water are recorded in current and abandoned mining sites (Sakala *et al*., 2016)

They recommended that the sulphide generating activities associated with land use such as coal mining be avoided on the zones that were deemed highly vulnerable to pollution; and continuous rehabilitation of the coal mining areas situated near or within the highly vulnerable areas that are still generating AMD.

Hodgson & Krantz (1995) compiled a report for the Water Research Commission, in which they investigated the deterioration of groundwater quality in the Olifants river catchment, specifically looking at the Witbank area. The acid-base potential predictions of the selected mines in the Witbank coalfield and the NNP determinations led them to make the following observations:

- The weathered rocks were characterised by neutral NNPs; this is because of the leaching of most of their acid-base components
- The sandstones showed a high base potential
- The unweathered rocks had acidic NNP averages for closed carbonate systems; and the open carbonate systems had alkaline NNPs for their sediments

Hodgson & Krantz (1995) did an acid-base potential interpretation for each mine, which led them to conclude that the NNPs for the lithologies of the area are influenced by the environment of deposition and secondary mineralisation.

A group of scientists conducted a study on behalf of the Water Research Commission, wherein in they mapped the un-mitigated threat of mining of resources across South Africa, and published a document called the South African Mine Water Atlas. They focused on all the Water Management Areas that are affected by the mining activities, with focus on surface and groundwater resources.

The study of the surface water profile deduced that the upper Olifants Catchment is in an unacceptable salinity state for the main stem Olifants River and many of its tributaries. However, it improves to an allowable status at Loskop dam (Water Research Commission, n.d). Moreover, the middle Olifants River has a salinity that falls within an allowable range and improves to an acceptable status in the lower Olifants River (Water Research Commission, n.d). They suggest that the impacts related to salinity are due to mining, irrigation return flows and wastewater discharges.

The groundwater vulnerability study that was conducted indicated that the following areas are of concern:

- Fresh water aquifer systems
- Large secondary geological features such as, dykes, faults, foliations and unknown lineaments which increases the vulnerability of aquifers as they pose a high risk for localised fluid migrations (Water Research Commission, n.d).
- The Malmani dolomite karst aquifers that support large dolomite springs
- Intergranular (alluvial) aquifer systems in river channel (Water Research Commission, n.d).

CHAPTER 3:
METHODOLOGY DESCRIPTION

3.1 INTRODUCTION

This chapter gives a description of all the methods and materials that were used during this research. It is important to give a detailed explanation of everything that was carried out during the course of the study, such as, data collection and processing methodologies namely: ABA, WISH, box and whisker graphs; and PhreeqC geochemical modelling.

3.2 DATA COLLECTION

The data used in this study was made available to the student by Professor Kai Witthueser from investigative and monitoring reports from mine sites within the Witbank coalfield and discard facilities in the SACE complex. The data obtained was geochemical data for predicting acid generation (ABA) and groundwater quality monitoring data.

Acid-base-accounting data include sulphur speciation, net acid generation and acid base accounting results; wherein sulphur speciation results include the percentages of total sulphur, sulphate sulphur and sulphide sulphur. The net acid generation results mainly focus on the pH, whilst acid base accounting results focus on paste pH, acid potential, neutralising potential and neutralising potential ratio. The sites from which samples were collected for ABA testing, the year the tests were performed and the number of samples that were collected are summarised in Table 3.1 below.

Table 3.1: Study sites and the number of samples collected for ABA testing, as well as the year the tests were conducted

Study Sites	Year	No. of samples
Arnot	2018	10
Goedehoop	2018	13
Mafube	2018	11
Zibulo	2018	10
Blaauwkrans	2017	1
Landau	2011	4
Greenside	2013	4

The groundwater chemistry data was obtained through the chemical analysis of all the compounds and elements found in the groundwater as well as chemical parameters, such as pH, electrical conductivity (EC) and total dissolved solids (TDS). The chemical compounds and elements include

alkalinity, Ca, Mg, Na, K, F, Cl, NO_3, PO_4, NH_4, Al, Fe, Mn and SO_4. For the purpose of this study, the minor elements such as Si, Ba, B, Co, Cd, Cr and Hg were not used.

The number of boreholes, which were investigated for each study site, and the years sampling was done are shown in Table 3.2 below.

Table 3.2: Study sites and the number of boreholes from which samples were collected, as well as the year of sampling

Study sites	Year	No. of boreholes
Arnot	2002,2004,2006,2011,2012,2018	82
Blaauwkrans	2002-2017	11
Goedehoop North	1990-2015	102
Goedehoop South	2013-2015	57
Greenside colliery	2013-2018	89
Greenside discard dump	1998-2010, 2012	15
Landau	2000-2015	19
Mafube	2014-2015	37
Zibulo	2012-2019	15

3.3 DATA PROCESSING

3.3.1 Acid-Base Accounting (ABA)

Skousen *et al*. (2001) defined ABA as a screening analytical tool used to determine the acid-alkaline producing potential of overburden rocks prior to coal mining. Dr. Richard Smith and associates developed this tool at West Virginia University in the late 1960s. This screening tool has become the preferred method in predicting pre- and post-mining water quality specifically after laws were passed to require an assessment of mining impacts on the water quality.

Therefore, ABA is used to qualitatively assess the site's potential to produce acid mine drainage (Skousen *et al*., 2001; Skousen *et al*., 2014). This is a static procedure and does not provide any information of the rate of acid generation and acid-neutralisation; these reaction rates are determined by kinetic weathering and leaching tests (Foli & Gawu, 2017).

The acid potential (AP) of a sample is calculated during ABA testing as a result of the theoretical oxidation of the sample's total sulphur content to sulphuric acid (Foli & Gawu, 2017). Furthermore, the AP is expressed in kg $CaCO_3$/tonne of rock; and the acid potential is calculated using the following equation (Delta-H Water Systems Modelling Pty Ltd, 2018):

$$AP = \frac{\textbf{Sulphur content } (\%) * \textbf{1000 kg}}{\textbf{100}} * \frac{\textbf{molecular weight of CaCO3}}{\textbf{atomic weight of sulphur}} \qquad \textbf{Equation 7}$$

$$AP = \text{sulphur content } (\%) * 31.25 \text{ kg } CaCO_3 \text{ per tonne} \qquad \textbf{Equation 8}$$

Carbonates, hydroxides and silicates provide the sample's neutralisation potential (NP). It is determined by the digestion of hydrochloric acid; and is also expressed in kg $CaCO_3$/tonne of rock.

Two indicators are used in assessing the risk of acid drainage:

1. Net Neutralisation Potential (NNP): this is calculated by the subtraction of the Acid Potential (AP) from the Neutralising Potential (NP)

$$NNP = NP - AP$$

If the NNP value is negative, it indicates the potential to generate acid. If the NNP value is positive, it indicates acid-neutralising potential.

2. Neutralisation Potential Ratio (NPR): this is calculated by dividing the NP by the AP

$$NPR = NP/AP$$

The following criterion is used to assess a sample (Usher *et al*., 2003; Mokoena, 2012):

- NPR greater than 2 indicates non-acid generation (NAG), the leachate is neutral or alkaline. However, preferential exposure or reactivity of sulphides an NPR larger 4 is needed for complete acid neutralisation.
- NPR between 1 and 2 is possibly acid generating if the neutralising agent is depleted faster than the sulphide material. This NPR is sometimes considered inconclusive and therefore, more static and kinetic tests have to be done on samples falling in this criterion.
- NPR below 1 indicates potential acid generation (PAG).

The acid generating potential of sulphide minerals in a rock sample is determined using net acid generation tests (NAG) by oxidation with hydrogen peroxide (H_2O_2) (Brough *et al*., 2013). After the sample has been completely oxidised, the final NAG pH is used as a criterion for the acid generation potential (Usher *et al*., 2003; Mokoena, 2012):

- NAG pH below 3.5 indicates a high risk acid generation
- NAG pH larger than 5.5 indicates no risk of acid generation
- NAG pH between 3.5 and 5.5 indicates a low risk of acid generation

The ABA data reported in this paper is from static tests and the data was used to create descriptive graphs using ABACUS.

Acid-Base Accounting Cumulative Screening (ABACUS) is a tool that calculates acid neutralising potential; acid generating potential; and the difference. Brent Usher developed this screening tool in

2000 as part of the Water Research Commission project (Usher, 2000) and it was used to process ABA data to create presentable graphs.

This Excel based menu driven tool uses prescribed classification criteria and allows for interpretation of each sample and for entire spoil area. This tool was used to process the ABA data for the following sites: Arnot, Goedehoop, Mafube, Zibulo and Blaauwkrans. Screening and classification criteria for the graphs generated using ABACUS are a combination of NPR and NAG criteria that are explained above.

Furthermore, Neutralising Potential Ratio (NPR) graphs in ABACUS classify the samples using open and closed systems. An open system refers to a system that exchanges matter with its surroundings; whilst a closed system refers to a system that is isolated from its surroundings and no exchange of matter in taking place.

However, the ABA data for Landau and Greenside collieries did not contain the final pH, which is needed in order to use ABACUS. Therefore, Ms-Excel was used to create graphs of NPR versus Total sulphur as XY scatter plots. Bold, brightly-coloured lines were drawn at NPR values of 1 and 4 and total sulphur of 0.3% to indicate positions on the graph where the samples will be non-acid generating, inconclusive and acid generating. The screening criteria and classification used for this method are the NPR screening criteria that are explained above.

3.3.2 Groundwater chemistry

3.3.2.1 WISH (Windows Interpretation System for Hydrogeologists)

Windows Interpretation System for Hydrogeologists (WISH) is a comprehensive graphics user interface for hydrogeologists; Elco Lukas programmed it under Frank Hodgson's guidance at the Institute for Groundwater Studies (IGS), University of the Free State (Lukas, n.d).

The water quality data was sorted and put into a WISH template to be able to create Piper and expanded Durov diagrams. For some sites, average values were used to create the above-mentioned diagrams: namely, Greenside, Landau, Mafube and Zibulo collieries, as well as the Blaauwkrans discard facility.

Specialised chemical plots were used to classify the groundwater of the study areas. Piper diagrams are one of the specialised plots that are instrumental in classifying the groundwater. In a Piper diagram, the major cations (Ca, Mg, Na+K) and anions ($Cl+NO_3$, SO_4 and HCO_3+CO_3) are plotted as points in the two triangular diagrams and these data points are projected onto the diamond shaped diagram to plot as one point. The groundwater is classified depending on the position of this point and the classification criteria are given in Figure 3.1 below.

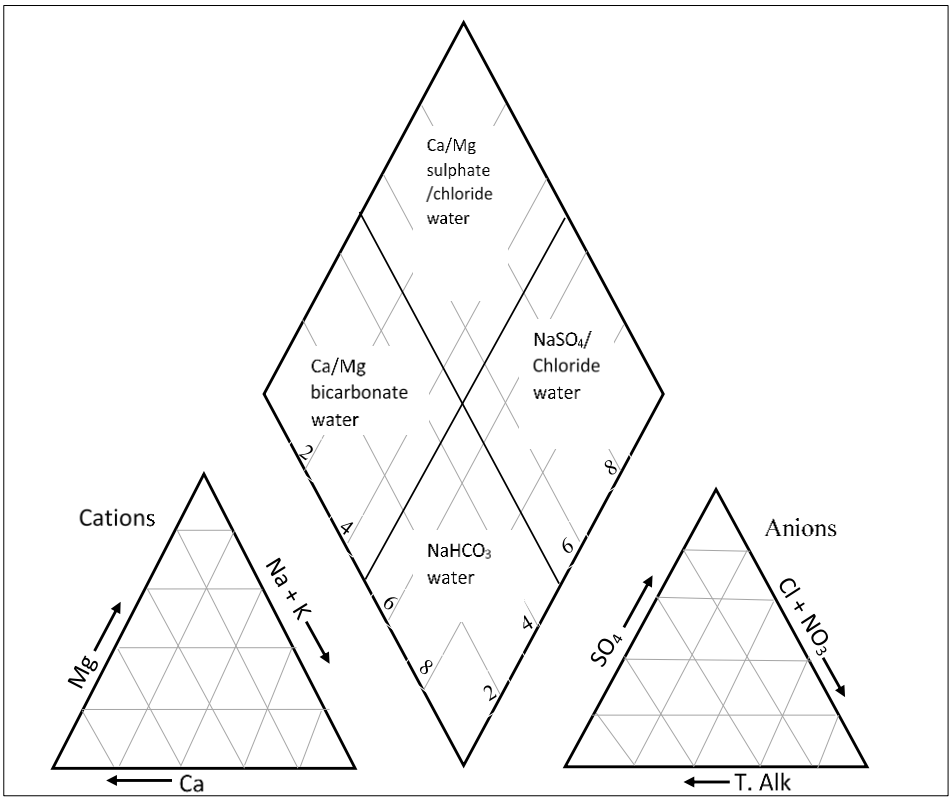

Source: adapted from Hounslow (1995) & Magha *et al*. (2015)

Figure 3.1: An example of a piper diagram plot with the groundwater classification criteria used in this study.

The expanded Durov diagram shows similar ratio techniques to a Piper diagram when plotting the concentrations of the major ions. However, six triangular diagrams are used: three for the anions and three for the cations. On each of the triangles, the sum of the anions adds up to 50% and ions are plotted in different combinations. The result is a plot with nine fields for classification and the concentration is represented in % meq/L (refer to Figure 3.2).

Explanation of the fields (Bosman, 2019):

1. This water type is often a recently recharged water; therefore, it classifies as unpolluted water. This fresh, clean groundwater is dominated by HCO_3^- and CO_3 ions.
2. This water is often associated with dolomite or mafic igneous rocks; classifies as unpolluted water. This young fresh, clean groundwater is undergoing Mg ion exchange.
3. This often indicates ion exchanged water; this classifies as wastewater discharge, irrigation return flow, and high extraction underground coal mines. This clean, fresh groundwater is undergoing Na ion exchange or typically in contact with a Na rich source of contamination or felsic rocks.
4. This represents freshly recharged water in lavas, or water associated with gypsum deposits; this water classifies as acid water that was treated with lime. This essentially is indicative of

groundwater that has been in contact with a SO_4 enriched bedrock or a source of SO_4 contamination.

5. This indicates water resulting from dissolution of mixing, a mixture of clean water from Fields 1 and 2. This mixture of different water types is undergoing SO_4 and NaCl mixing or contamination; this water classifies as opencast coal mine water.
6. This indicates a water type where reverse ion exchange is taking place; wherein groundwater from Field 5 is in contact with a Na rich source; vanadium extraction, gold mine water or power stations.
7. This is not a common water type unless reverse ion exchange is taking place and therefore is seldom found.
8. This suggests that reverse ion exchange is taking place, this water type is seldom found. This groundwater is typically a mixture of water from Fields 1 and 2 that has been contaminated with SO_4 or has undergone Cl mixing/contamination.
9. This indicates an end point water in a water evolution sequence. This is considered very old groundwater that has been stagnant over a long period. Furthermore, this groundwater classifies as water from domestic wastewater dumps, natural saline water or deep mine water.

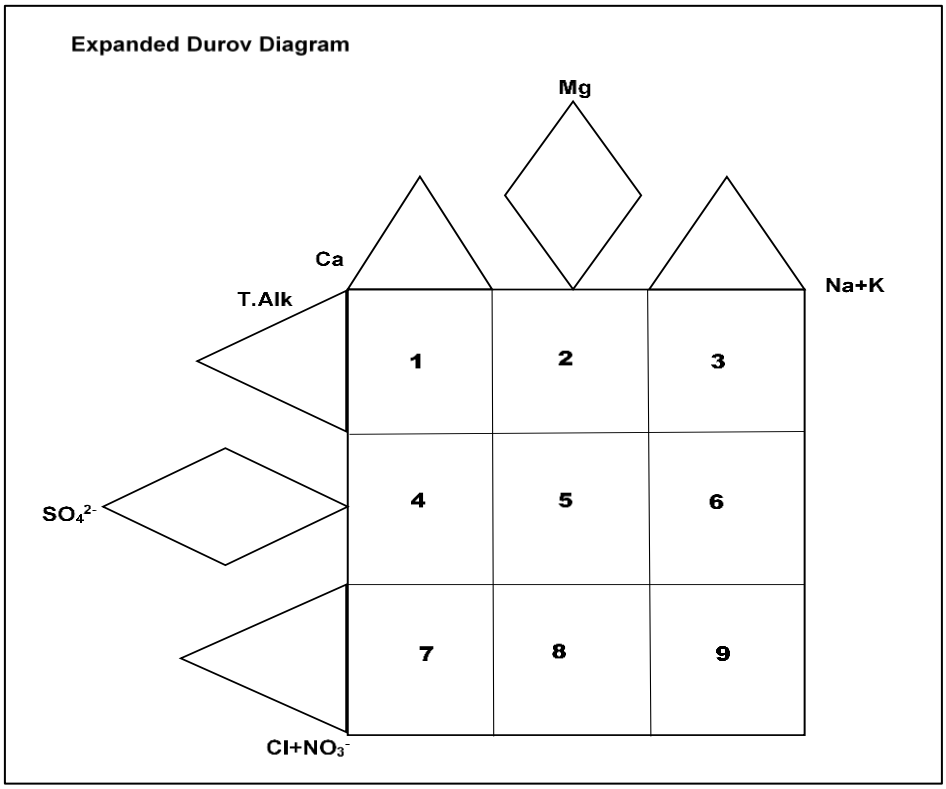

Figure 3.2: Diagram showing the fields found in an Expanded Durov diagram used for groundwater classification.

For the purpose of this paper, both Piper and expanded Durov diagrams will be used to provide a better classification of the groundwater.

3.3.3 Statistical description

Box and whisker plots were created to investigate whether there are potential unusual observations in the data set to understand the change in concentration of SO_4^{2-} for each site over time in years and in other cases, in months. A box and whisker plot is a graph that presents information from a five number summary (refer to Figure 3.3).

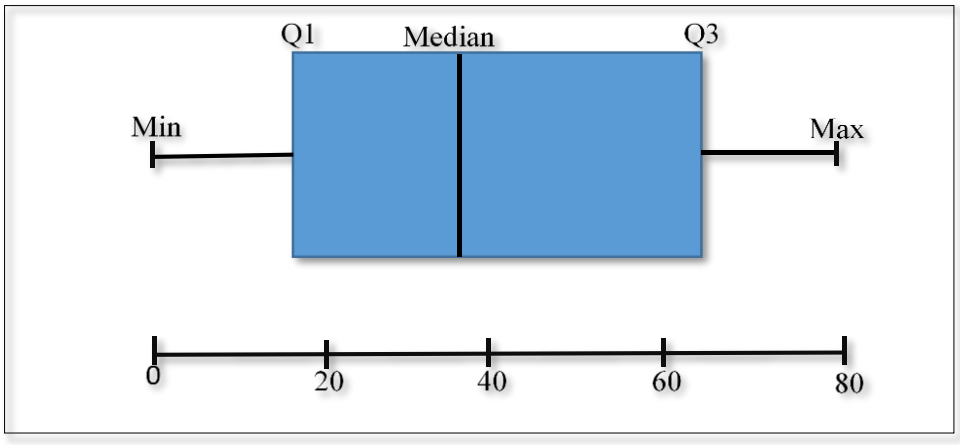

Figure 3.3: An example of a box and whiskers diagram showing all the five numbers.

Wherein:

- Min- is the lowest number in the set
- Q1- first quartile, which is the 25th percentile
- Median- this is the middle most number
- Q3- third quartile, which is the 75th percentile
- Max- is the highest number in the set

Box plots are virtual five number summary of statistical data. The criteria used to interpret the box plots are as follows:

- Median line: if the box plot median line lies outside of a comparison box plot, then there is a difference between the two groups.
- IQR (interquartile range) and whiskers of box plots: this is to study how the data is dispersed between each sample. If the box is long, then the data is more dispersed. If the box is smaller, then the data is less dispersed.

- Range: this interpretation method includes looking at the general spread shown by extreme values at the end of the two whiskers, minimum and maximum values; this indicates the range of scores. The larger the range, the wider the distribution, indicating more scattered data.
- Comparison of sulphate concentration (using IQR) to SANS 241:2015 limit for acute health risk, this excludes outliers.

Time series graphs were created in using average and median values of sulphate concentrations to show how these concentrations change with time for each site.

Scatter plots were created with the sole purpose of checking if the ABA predictions worked, wherein:

- Total sulphur contents from the ABA results were plotted against total sulphate concentrations from the groundwater chemistry results sites.
- NPR was plotted against groundwater pH.
- NNP was plotted against total sulphate of the study.
- Groundwater pH was plotted against sulphide sulphur contents.
- Groundwater pH was plotted against total sulphur contents.
- Groundwater sulphate concentrations were plotted against coal seam sulphur contents SACE Complex study sites.

Average and median values were used to plot these graphs; it is important to note that this method is not the most accurate but provides insight into whether or not what the ABA results predicted is reflected in the groundwater chemistry.

3.3.4 PhreeqC geochemical modelling

According to Parkhurst & Appelo (1999), PhreeqC is a computer program written in C programming language that is designed to perform a wide variety of aqueous geochemistry calculations. This computer program is based on an aqueous model associated with ions and is capable of doing the following (Parkhurst & Appelo, 1999; Parkhurst 1999; Havenga, 2011):

- Speciation and saturation-index calculations.
- Batch-reaction and one-dimensional (1D) transport calculations that involve reversible reactions, which include aqueous, mineral, gas, solid-solution, surface-complexation, and

ion-exchange equilibria, and irreversible reactions, which include specified transfers of reactants, kinetically controlled reactions, mixing of solutions, and temperature changes; and

- Inverse modelling, which finds sets of mineral and gas mole transfers that account for differences in composition between waters, within specified compositional uncertainty limits.

According to Parkhurst & Appelo (1999), PhreeqC is capable of simulating a wide range of geochemical reactions, which include mixing of waters, addition of net irreversible reactions to solution, dissolving and precipitating phases to achieve equilibrium with the aqueous phase as well as effects of changing temperature. Concentrations of elements, molalities and activities of aqueous species, pH, pe, saturation induces, and more transfers of phases to achieve equilibrium can be calculated as a function of specified reversible geochemical reactions, provided sufficient thermodynamic data are available (Parkhurst & Appelo, 1999; Havenga, 2011).

PhreeqC Interactive Version 3.4.0.12927 was used, wherein calculations were done by making use of water quality data available for the studied boreholes. Speciation calculations were performed on each solution and the following calculations were done on the groundwater samples:

- Selection and input of the solutions (Basic simulations)

The solutions were compiled by making use of the borehole groundwater chemistry data. The initial solutions used in the calculations represent the chemical composition of these real samples. The following points describe which parameters were used in the input files:

  - General parameters, such as temperature, pe, redox and density were set to default values; except for pH wherein the values were adjusted for each borehole sample according to pH values observed in the groundwater chemistry data.
  - Units were changed to mg/L and charge balance set to “none”.
  - All major ion concentrations were used for these calculations.

For each of the borehole samples, the saturation indices of the solutions were calculated. These saturation indices were then used to assess which mineral phases are likely to precipitate from the solutions. The saturation index is defined by the following equation (Anderson, 2005):

$$SI = \log\left(\frac{IAP}{Ksp}\right) \qquad \textbf{Equation 9}$$

Where:

IAP = Ion Activity Product $[A]^a$ X $[B]^b$ calculated from the measured concentrations.

Ksp = the solubility product of the solid species [Ax By] obtained from theoretical values.

As a general rule the SI can be used as follows (Anderson, 2005): If:

SI<0, the groundwater is undersaturated in [Ax By] and dissolution will occur

SI=0, the water is in equilibrium with the solid

SI>0, the water is supersaturated with the solid components and precipitation should result.

- Equilibrium simulations

Equilibrium phase is used to define the amount of an assemblage of a pure phase that can react reversibly with the aqueous phase. Pure phases used include mineral phases that had saturation indices greater zero (oversaturated phases) in the basic simulation stage, mineral content and sulphur content as determined by XRD analyses. The following is a summary of steps that were taken during equilibrium calculations:

- Pure rainwater was first equilibrated with atmospheric carbon dioxide (CO_2) and oxygen (O_2) gases. The above mentioned gases were equilibrated using the log of partial pressures of the gases, i.e saturation indices as follows:

$$CO_2\ (g) = -3.5$$

$$O_2\ (g) = -0.7$$

- Convert the mineral composition of the material as determined by XRD analysis from weight percentage to mol/L pore water (refer to the Equations 10 to 13 below)
- The mineral compositions were equilibrated to the infiltrating rainwater
- Secondary minerals, i.e those with positive saturation indices from basic simulations (refer to Table 3.4) were allowed to precipitate as required to reach equilibrium.
- The resulting pore water qualities were recorded

Table 3.3: The parameters that were used to convert weighted mineral phases as well as in input files of equilibrium calculations

Parameter	Value	Unit	Comment
Porosity	0.25	L/L	based on literature values
Density	2.7	g/cm^3	
Bulk density	2.025	g/cm^3	Calculated
Mineral phases	Variable	mol	as determined by XRD analysis
Gas phases	log pO2 = -0.7 log pCO2 = -3.5		
Secondary minerals	variable	mol	as determined by initial

If pure phases are brought into contact with an aqueous solution, each phase will dissolve or precipitate to achieve equilibrium or will dissolve completely. Furthermore, not all mineral phases with positive saturation indices in the basic simulation stage will precipitate from solution. Therefore, www.webmineral.com and mindat.org websites were used to understand the formation environments of each of the mineral phases with positive saturation indices. The minerals that are likely to form as secondary minerals were the ones that were used in the equilibrium simulations (refer to Table 3.4). The Arnot colliery was the only site for which equilibrium simulations were done; as it was the only site with the same boreholes being used for ABA testing and groundwater monitoring.

Table 3.4: Names and chemical formulas of secondary minerals that were used for equilibrium simulations for the Arnot Colliery

Name	Formula	Borehole
Cristobalite	SiO_2	BF2E1
Aragonite	$CaCO_3$	BF2P1
Dolomite	$CaMg(CO_3)_2$	BF2P1 & BF3P1
Magnesite	$MgCO_3$	BF2P1
Rhodochrosite	$MnCO_3$	BF2P1 & BF3P1
Calcite	$CaCO_3$	BF3P1

These secondary minerals together with the mineral content and total sulphur content in the XRD reports were used in the equilibrium simulations to understand which minerals will precipitate and the amount of each mineral that will precipitate. The mineral content and total sulphur content were expressed in weight percentages (wt%) in the XRD reports; these values were converted to mol/L of pore water, the converted values were used in equilibrium simulations. The following formulae were used:

Weight percentage (Wt%) → mol/kg

$$\text{Mol/kg} = 1000 \times \left(\frac{\textit{Weight percentage}}{100 \times \textit{Molar mass}}\right) \qquad \textbf{Equation 10}$$

Mol/kg → mol/L pore water

$$\text{Mol/L} = \text{mol/kg} \times \left(\frac{1}{\textit{Porosity}}\right) \times \text{bulk density} \qquad \textbf{Equation 11}$$

E.g Converting the concentration Quartz from borehole BF2E1 (Arnot Colliery)

- Weight percentage= 67.59%
- Porosity= 0.25 (sediments)
- Bulk density= 0.25 g/cm3

- Molar mass= 60.0843 g/mol

Weight percentage → mol/kg

$$1000 \text{ X } (\frac{67.59}{100 \times 60.0843}) = 11.249 \text{ mol/kg} \qquad \textbf{Equation 12}$$

Mol/L pore water

$$11.249 \text{ X } (\frac{1}{0.25}) \text{ X } 2.025 = 91.118 \text{ mol/L} \qquad \textbf{Equation 13}$$

This is the amount of moles per litre that is added on the PhreeqC input file.

The values for sulphate (SO_4^{2-}) and pH of the basic simulations were compared to the equilibrium simulations to see if there are any differences and improvements. Moreover, molalities calculated by PhreeqC given in the distribution of species are expressed as mol/kg. Therefore, these molalities were converted to the simpler unit (for purposes of the above-mentioned comparisons), mg/L using the following formula:

Mol/kg = mol/L

$$\text{Mg/L} = \text{mol/L X molar mass X } 1000 \qquad \textbf{Equation 14}$$

CHAPTER 4:
RESULTS AND DISCUSSIONS

4.1 INTRODUCTION

This chapter involves the description of the results from all the methods carried out during the course of this project and the interpretations thereof. The results are described in the following sequence: ABA, groundwater chemistry using Piper and expanded Durov diagrams; statistical analysis using box and whisker plots as well as scatter plots; geochemical modelling using PhreeqC and sulphate concentration versus sulphur content of the study sites.

4.2 ACID-BASE ACCOUNTING

4.2.1 Arnot Colliery

Eight samples were collected from both the saturated and unsaturated zones of this study site for ABA testing, excluding duplicates. The sulphur speciation, net acid generation and acid-base accounting values for the Arnot colliery are given in Table 4.1 below (duplicate samples for quality control are highlighted in grey).

Table 4.1: Sulphur speciation, NAG and ABA results for the Arnot Colliery

Sample ID	Lab ID	SULPHUR SPECIATION			NET ACID GENERATION				ACID BASE ACCOUNTING							
		Total Sulphur (%)	Sulphate Sulphur as S (%)	Sulphide Sulphur (%)	pH 4.5 NAG (pH)	pH 4.5 NAG (kg H_2SO_4/t)	pH 7 NAG (pH)	pH 7 NAG (kg H2SO4/t)	Paste pH	Acid Potential (AP) (kg/t)	Sulphide Acid Potential SAP (calc) (kg/t)	Neut Potential (NP) (kg/t)	Net Neut Potential (NNP)	Neut Potential Ratio (NPR)	NNP_S2	NPR_S2
BF4P1 Saturated Zone	48050	0.109	0.11	0.01	7.3	<0.01	7.3	<0.01	7.3	3.41	<0.3	12.00	8.6	3.5	>11.7	40.00
BF4P1 Unsaturated Zone	48051	0.205	0.13	0.08	6.7	<0.01	6.7	<0.01	7.5	6.41	2.5	10.00	3.9	1.6	7.50	4.00
BF3P1 Saturated Zone	50549	0.23	0.22	0.01	7.6	<0.01	7.6	<0.01	7.1	7.26	0.3	19.00	12.0	2.7	18.69	60.80
BF3P1 Unsaturated Zone	50550	0.63	0.08	0.56	2.7	11	4.5	17.00	5.5	20.00	17.5	1.75	-18.0	0.1	-15.75	0.10
BF2P1 Saturated Zone	50548	0.08	0.08	0.01	6.6	<0.01	6.6	0.20	6.5	2.61	<0.31	6.00	3.4	2.3	>5.69	19.36
BF2P1 Unsaturated Zone	50551	0.35	0.19	0.16	3.2	2.94	4.5	12.00	5.9	11.00	5.0	0.50	-10.0	0.0	-4.50	0.10
BF2P1 Unsaturated Zone	50551 D	0.34	0.19	0.15	3.3	2.74	4.5	12.00	5.9	11.00	4.7	1.25	-9.5	0.1	-3.44	0.27
BF2W1 Unsaturated Zone	48052	0.254	0.15	0.1	5.9	<0.01	5.9	0.59	7.0	7.95	3.1	5.05	-2.9	0.6	1.93	1.62
BF2W1 Unsaturated Zone	48052 D	0.251	0.15	0.1	5.9	<0.01	5.9	0.59	7.1	7.85	3.1	4.56	-3.3	0.6	1.44	1.46
BF2E1 Saturated Zone	50547	0.15	0.11	0.04	5.6	<0.01	5.6	0.59	5.3	4.66	1.3	2.00	-2.7	0.4	0.75	1.60

4.2.1.1 Paste pH results

The paste pH values of the tested backfill samples ranged from pH 5.3 (BF2E1 saturated zone) to pH 7.5 (BF4P1 unsaturated zone). The neutral paste pH values (5< pH< 10) suggest the presence of sufficient neutralising agent when the samples were analysed (Delta-H Water Systems Modelling Pty Ltd, 2019).

4.2.1.2 ABA results considering sulphur speciation

All tested Arnot colliery samples showed measurable (>0.01%) total sulphur contents with the derived AP values ranging from 2.6 kg (H_2SO_4)/t to 20 kg (H_2SO_4)/t for BF2P1 saturated zone and BF3P1 unsaturated zone respectively. Three samples plotted in the zone of very high probability of acid generation (refer to Figure 4.1). While six samples plotted in the zone for medium probability of acid generation; three of these are in the 1<NPR<4, these are possibly acid generating if preferentially exposed or inconclusive.

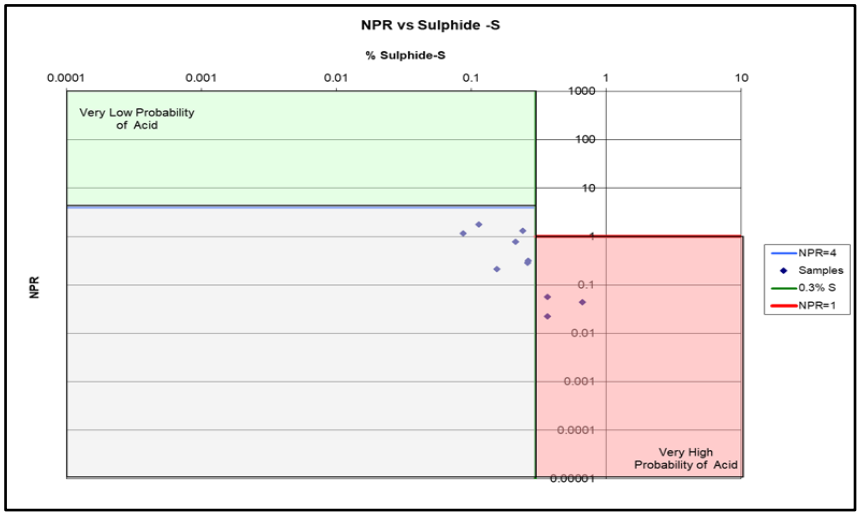

Figure 4.1: Graph showing the relationship between NPR and Sulphide sulphur for the Arnot Colliery.

4.2.1.3 AP versus NP (NPR)

Majority of the samples plotted above the NPR=1:1 line, in the acid generating zone in both open and closed systems. Furthermore, four samples in an open system and three in a closed system plotted in the possibly acid generating or inconclusive zone of 1<NPR<4 (refer to Figure 4.2).

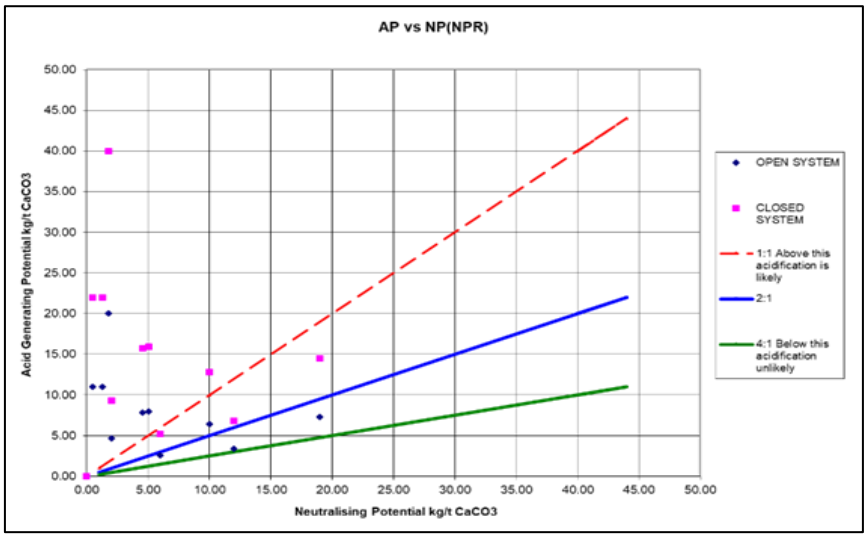

Figure 4.2: Graph showing the relationship between AP and NP for the Arnot Colliery.

4.2.1.4 Initial and final pH versus closed NNP

Four samples plotted in the acid generating zone of negative NNP, while the rest plotted in the grey area around the Y-axis, which means they are inconclusive and can only be acid generating if they are preferentially exposed (refer to Figure 4.3). This plot is valid because the final pH values plotted below the initial pH.

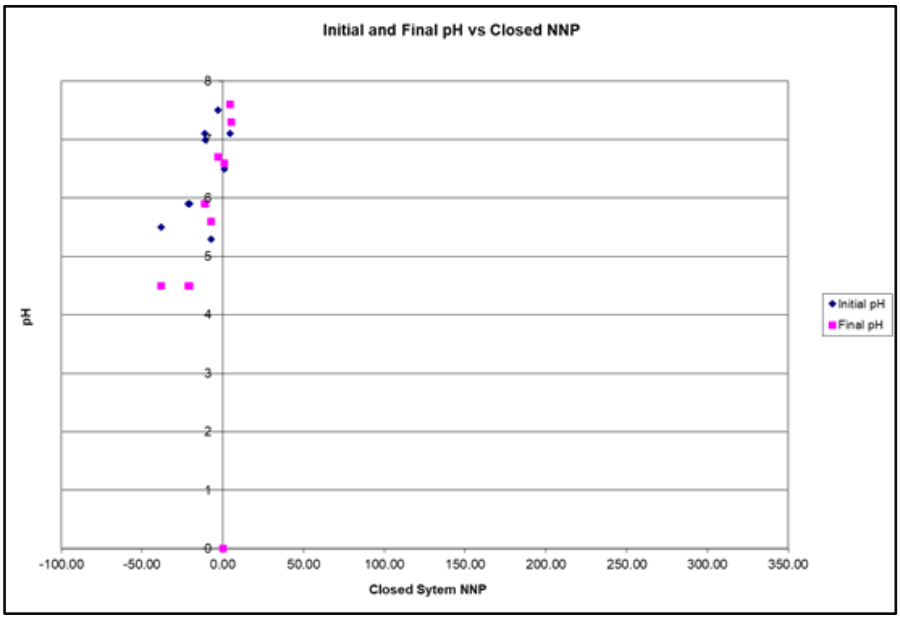

Figure 4.3: Graph showing the initial and final pH versus closed NNP for the Arnot Colliery.

Summary of ABA results

- BF2P1 saturated zone, BF3P1 saturated zone as well as samples BF4P1 unsaturated and saturated zone had positive NNP indicating the presence of a neutralising agent, therefore, are not acid generating.

- BF2P1 unsaturated zone (10 kg/t H_2SO_4) including its duplicate (9.5 kg/t H_2SO_4) as well as BF3P1 (18 kg/t H_2SO_4) had the most negative NNP values, and can be regarded as acid generating.
- BF2E1 saturated zone and BF2W1 unsaturated zone (including its duplicate) had low negative NNP values and are therefore, regarded as uncertain and potentially acid generating if preferentially exposed. Therefore, more tests are needed to verify the results.
- Samples that were classified as possibly acid generating if preferentially exposed or inconclusive require more static and kinetic tests to verify the results.

4.2.2 Goedehoop Colliery

Eleven samples were collected from this site for ABA testing, excluding duplicates. The sulphur speciation, net acid generation and acid-base accounting results are given in Table 4.2 below (duplicate samples for quality control are highlighted in grey).

Table 4.2: Sulphur speciation, NAG and ABA results for the Goedehoop Colliery

Sample ID	Lab ID	SULPHUR SPECIATION				NET ACID GENERATION				ACID BASE ACCOUNTING							
		Total Sulphur (%)	Sulphate Sulphur as S (%)		Sulphide Sulphur (%)	pH 4.5 NAG (pH)	pH 4.5 NAG (kg H2SO4/t)	pH 7 NAG (pH)	pH 7 NAG (kg H2SO4/t)	Paste pH	Acid Potential (AP) (kg/t)	Sulphide Acid Potential SAP (calc) (kg/t)	Neut Potential (NP) (kg/t)	Net Neut Potential (NNP)	Neut Potential Ratio (NPR)	NNP_S2	NPR_S2
Hope Dump	32276	1.31	0.89	0.68	0.42	2.6	17	4.5	24.00	3.8	41.0	13.1	-6.1	-47.0	0.15	-19.24	0.01
Haasfontein BF	32277	0.01	<0.01	0.00	0.01	6.1	<0.01	6.1	0.39	5.7	0.157	<0.3	0.8	0.7	5.30	>0.5	2.67
SBK 1 Dump	32278	5	1.71	0.34	3.29	2.1	79	4.5	29.00	2.6	156.0	102.8	-22.0	-178.0	0.14	-124.81	0.01
SBK 2 Dump	32279	0.86	0.36	0.42	0.5	4.5	<0.01	4.5	15.00	5.2	27.0	15.6	0.3	-27.0	0.01	-15.36	0.02
Vlaklaagte BF	32280	0.58	0.39	0.67	0.2	3.9	1.18	4.5	12.00	3.9	18.0	6.3	-7.1	-25.0	0.39	-13.38	0.01
Kleinshaft Dump	32281	0.32	0.1	0.31	0.22	4.2	0.588	4.5	9.80	4.5	9.91	6.9	-2.3	-12.0	0.23	-9.17	0.01
Co-Disposal	32282	5.52	0.98	0.18	4.55	2.4	81	4.5	30.00	6.9	173.0	142.2	46.0	-127.0	0.26	-96.19	0.32
Bank 5 Dump	32283	5.13	0.75	0.15	4.39	2.2	122	4.5	27.00	2.8	160.0	137.2	-17.0	-177.0	0.11	-154.19	0.01
Bank 2 Coarse	32284	1.13	0.48	0.42	0.65	7.9	<0.01	7.9	<0.01	7.6	35.0	20.3	75.0	40.0	2.14	54.69	3.69
Bank 2 Coarse D	32284 D	1.13	0.42	0.37	0.71	7.9	<0.01	7.9	<0.01	7.7	35.0	22.2	76.0	41.0	2.15	53.81	3.43
Bank 2 Fines	32285	0.79	0.74	0.94	0.05	4.6	<0.01	4.6	7.25	7.4	25.0	1.6	38.0	13.0	1.53	36.44	24.32
Schoonie Dump	32286	0.54	0.52	0.96	0.02	5.8	<0.01	5.8	0.98	7.1	17.0	0.6	24.0	7.4	1.44	23.38	38.40
Schoonie Dump D	32286 D	0.54	0.53	0.98	0.01												

4.2.2.1 Paste pH

The table above shows that the tested samples had a paste pH that ranged from pH 2.6 (SBK 1 Dump) to pH 7.7 (Bank 2 coarse D). Half of the samples (excluding duplicates) showed acidic paste pH values (2.6 <paste pH< 4.5) and the other half showed near neutral paste pH values (5.2 <paste pH< 7.7) (Delta-H Water Systems Modelling Pty Ltd, 2018a).

4.2.2.2 ABA results considering sulphur speciation

The Goedehoop colliery samples showed that the sulphur contents are measurable (>0.01%) with the derived AP values ranging from 9.9 kg/t (H_2SO_4) for the Kleinshaft Dump to 173 kg/t (H_2SO_4) for the Co-disposal in exception of the Haasfontein backfill sample. The backfill samples indicate a heterogeneous nature of the different backfilled areas since the Haasfontein backfill sample had no measurable total sulphur content (<0.01%) and thus the derived AP is <0.157 kg/t H_2SO_4; whereas the Vlaklaagte backfill sample had a total sulphur content of 0.58% and an AP value of 18 kg/t H_2SO_4.

The total sulphur contents of discard dump samples were higher than that of the other samples, the derived AP values ranged from 17 kg/t H_2SO_4 for the Schoonie Dump sample, to a maximum of 150 kg/t H_2SO_4 for the discard dumps. The majority of samples plotted in the zone for very high probability of acid generation whereas two plotted in the zone of 1<NPR< 4. One of these two samples plotted in the field of medium probability of acid generation and are possibly acid generating if preferentially exposed or inconclusive (refer to Figure 4.4).

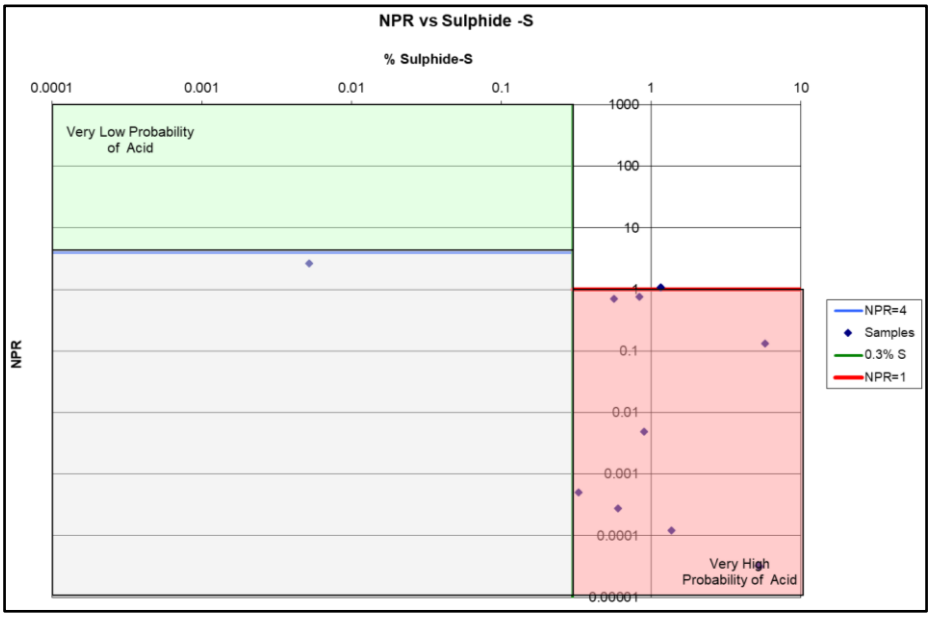

Figure 4.4: Graph showing the relationship between NPR and Sulphur sulphur for the Goedehoop study site.

4.2.2.3 AP versus NP (NPR)

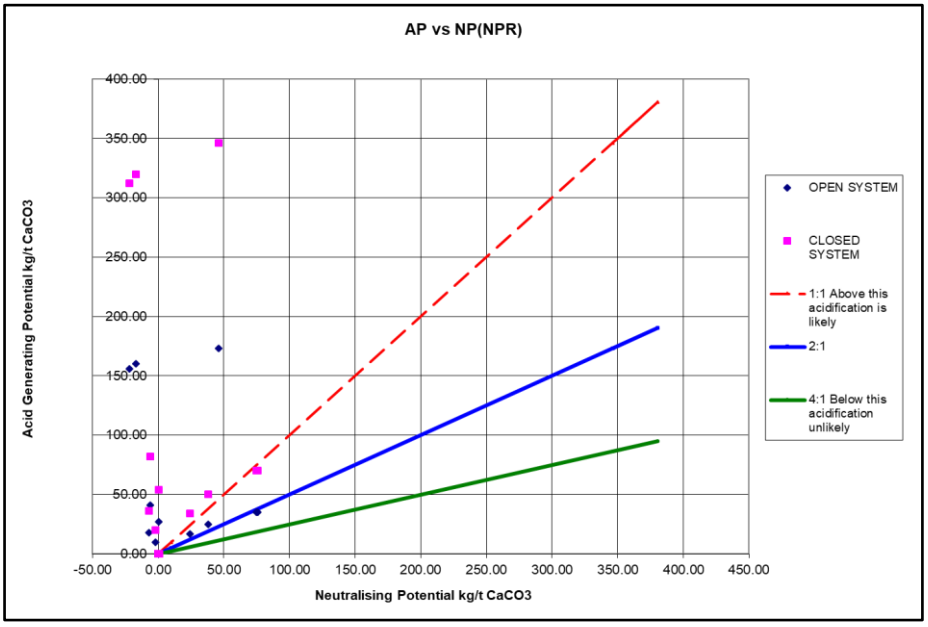

Figure 4.5: Graph showing the relationship between AP and NP for the Goedehoop Colliery.

The NP of the samples partially balanced their AP values, wherein the NP values ranged from absent (negative values for Hope Dump, SBK 1 Dump, Vlaklaagte backfill, Kleinshaft Dump and Bank 5 Dump) to 75 and 76 kg/t H_2SO_4 for the Bank 2 coarse sample and its duplicate analysis.

Figure 4.5 below shows that the majority of samples in both open and closed systems plotted above the NPR= 1:1 line indicating the likelihood of acid generation. In an open system, three samples plotted in the 1<NPR<2 zone and one in a closed system; and therefore, the results of these samples are considered possibly acid generating if preferentially exposed or inconclusive.

4.2.2.4 Initial and final pH versus closed NNP

The majority of the samples plotted in the zone of potential acid generation of negative NNP (refer to Figure 4.6); and the few that plotted in the area near the pH Y-axis are possibly acid generating of preferentially exposed or inconclusive. However, for this graph to be valid the final pH of each sample has to be below its initial pH because the former is generally lower than the initial (paste) pH.

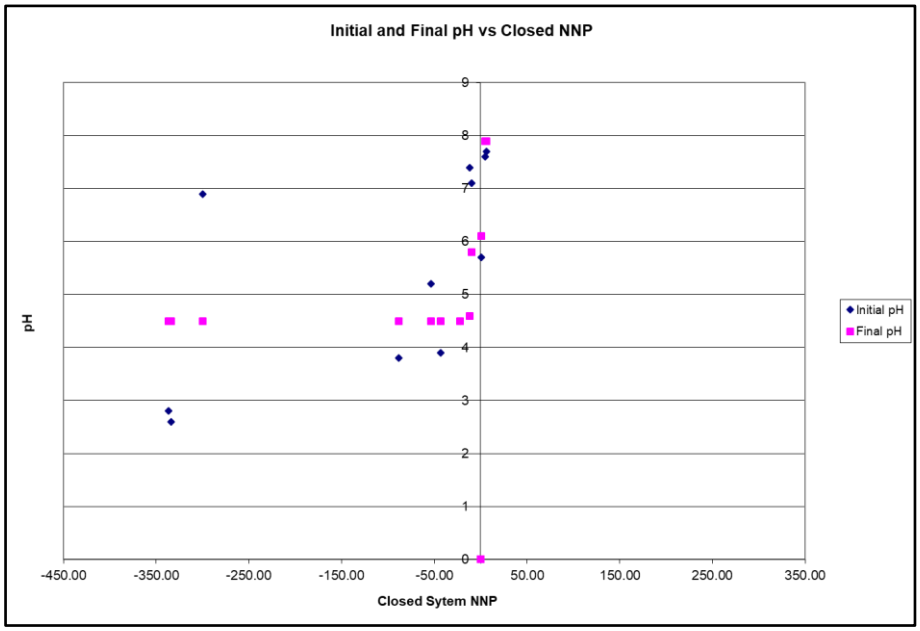

Figure 4.6: Graph showing the initial and final pH versus closed NNP for the Goedehoop Colliery.

Summary of ABA results

- The Haasfontein backfill sample is classified as non-acid generating due to its NNP value of 0.7 kg/t H_2SO_4
- The Vlaklaagte backfill is potentially acid generating due to its NNP value of -25 kg/t H_2SO_4
- Bank 2 coarse, Bank 2 fines, Schoonie dump can be classified as uncertain and can only be acid generating if preferentially exposed.
- The negative values are potentially acid generating, and samples with the most high negative NNP values are the most high risk of acid generation and these samples are:
    - SBK 1 dump=178 kg/t H_2SO_4
    - Bank 5 dump= 177 kg/t H_2SO_4
    - Co-disposal= 127 kg/t H_2SO_4
- Samples that were classified as possibly acid generating if preferentially exposed or inconclusive require more static and kinetic tests to verify the results

4.2.3 Mafube Colliery

Ten samples were collected for ABA testing, excluding one duplicate. The sulphur speciation, net acid generation and acid-base accounting values for the Mafube colliery are given in Table 4.3 below (duplicate samples for quality control are highlighted in grey).

Table 4.3: Sulphur speciation, NAG and ABA results for the Mafube Colliery

Sample ID	Lab ID	SULPHUR SPECIATION			NET ACID GENERATION				ACID BASE ACCOUNTING							
		Total Sulphur (%)	Sulphate Sulphur as S (%)	Sulphide Sulphur (%)	pH 4.5 NAG (pH)	pH 4.5 NAG (kg H2SO4/t)	pH 7 NAG (pH)	pH 7 NAG (kg H2SO4/t)	Paste pH	Acid Potential (AP) (kg/t)	Sulphide Acid Potential SAP (calc) (kg/t)	Neut Potential (NP) (kg/t)	Net Neut Potential (NNP)	Neut Potential Ratio (NPR)	NNP_S2	NPR_S2
Discard 1	28870	2.74	0.447	2.29	2.7	20	4.5	34	7.1	86	71.6	29	-57	0.34	-42.56	0.41
Discard 2	28871	1.18	0.642	0.54	7.5	<0.01	7.5	<0.01	7.2	37	16.9	41	4.02	1.11	24.13	2.43
Fines 1	28872	1.05	0.508	0.55	2.9	43	4.5	43	7.1	33	17.2	37	3.90	1.12	19.81	2.15
Fines 2	28873	0.75	0.696	0.06	6.8	<0.01	6.8	0.39	7.2	24	1.9	67	44	2.86	65.13	35.73
Wes Box Cut_Floor	28874	0.12	0.087	0.03	6.2	<0.01	6.2	0.20	6.9	3.72	0.9	2.91	-0.81	0.78	1.97	3.10
Nooitgedacht Cut_Roof	28877	0.06	0.051	0.01	7.9	<0.01	7.9	<0.01	6	1.84	0.3	0.06	-1.78	0.03	-0.25	0.20
Eastern Spoil 1	28875	0.08	UTD*	UTD*	6.7	<0.01	6.7	0.20	6.7	2.58	-	0.3	-2.28	0.12	-	-
Eastern Spoil 2	28876	0.1	0.096	<0.01	6.3	<0.01	6.3	0.20	6.6	3.01	<0.3	1.96	-1.04	0.65	>1.66	>6.53
Road raw material	28878	0.05	0.044	<0.01	5.6	<0.01	5.6	0.39	5.7	1.48	<0.3	-0.89	-2.37	0.60	> -1.19	>2.96
Road raw material	28878 D	0.05	0.047	<0.01	5.7	<0.01	5.7	0.39	5.7	1.48	<0.3	-0.65	-2.13	0.44	> -0.95	>2.17
Road 1	28879	0.22	0.193	0.03	6.4	<0.01	6.4	4.12	4.6	6.76	0.9	-11	-17	1.57	-11.94	-11.73

4.2.3.1 Paste pH results

The paste pH values of the tested samples ranged from 4.6 (Road 1) to pH 7.2 (Fines 2) indicating that almost all samples were near neutral at the time of analysis. Sample Road 1 showed an acidic paste pH indicating that no neutralisation potential was available at the time of analysis to buffer the already generated short-term acidity in the sample.

4.2.3.2 ABA results considering sulphur speciation

All tested Mafube colliery samples showed measurable (>0.01%) total sulphur contents with the derived AP values ranging from 1.4 (Road raw material) to 86 kg/t H_2SO_4 (Discard 1). The discard coal and coal fines samples showed high total sulphur contents (2.74, 1.18 and 1.05, 0.75% respectively) and the derived AP values were higher than that of the spoil (0.08 and 0.1%), road (0.05 and 0.22%) or box cut (0.12 and 0.065%) samples.

Three samples plotted within the field of very high probability of acid generation; one sample plotted in the possibly acid generating if preferentially exposed or inconclusive field (1<NPR<4). The remaining six plotted in the field of medium probability of acid generation (refer to Figure 4.7).

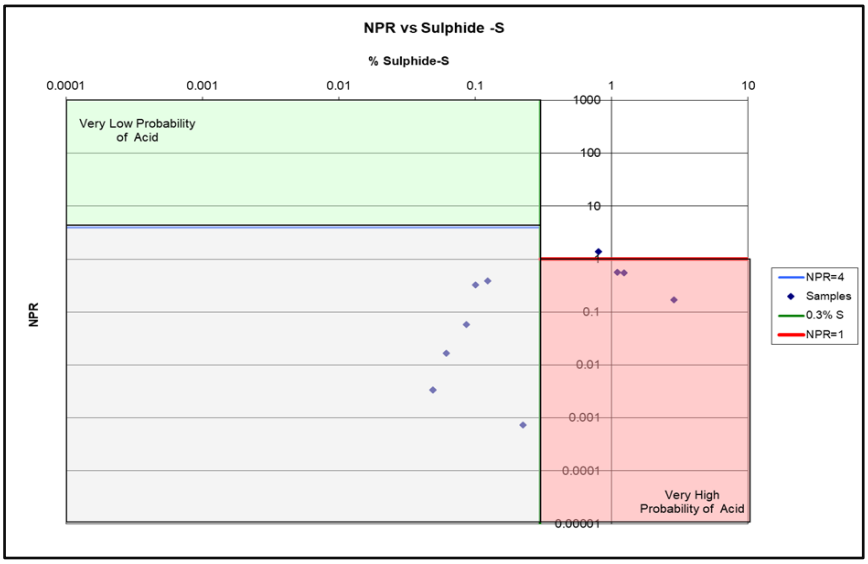

Figure 4.7: Graph showing the relationship between NPR and Sulphide sulphur for the Mafube Colliery.

4.2.3.3 AP versus NP

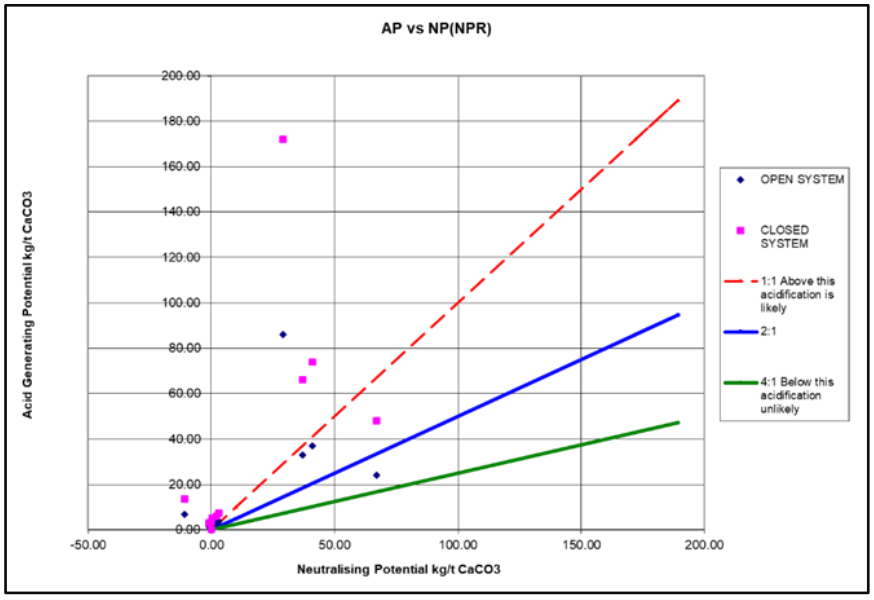

Figure 4.8: Graph showing the relationship between AP and NP for the Mafube Colliery.

The AP values were not completely balanced by the NP, resulting in negative NNP values for the majority of samples. This means that the majority of samples are acid generating. The majority of samples plotted above NPR= 1:1, i.e in the acid generating zone in both open and closed systems (refer to Figure 4.8). Four samples plotted in the open system and one sample in the closed system plotted within the 1<NPR<4 possibly acid generating or inconclusive zone.

4.2.3.4 Initial and final pH versus closed NNP

Figure 4.9 shows that four samples plotted in the acid generating zone, while one plotted in the non-acid generating zone. The remaining three samples plotted in the grey area near the Y-axis, which means they are possibly acid generating if preferentially exposed or inconclusive.

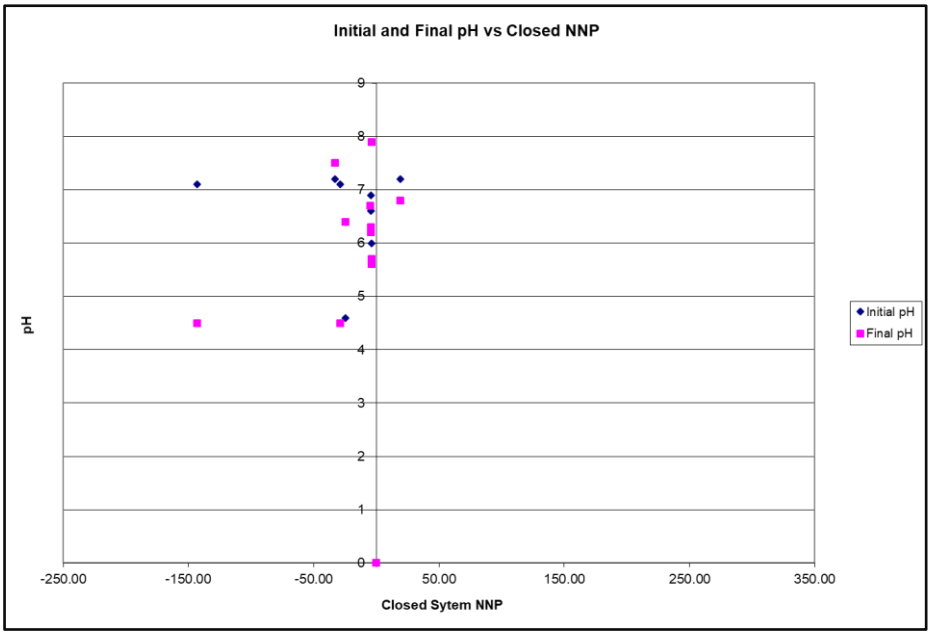

Figure 4.9: Graph showing initial and final pH versus closed NNP for the Mafube Colliery.

Summary of ABA results

- Road material sample (including its duplicate) are potentially acid generating.
- The eastern samples can be classified as uncertain, and only acid generating if preferentially exposed.
- Discard 1 sample is potentially acid generating; discard 2 can be classified as uncertain and only acid generating if preferentially exposed.
- The discard fines are non-acid generating.
- The rest of the samples are uncertain and only acid generating if preferentially exposed.
- Samples that were classified as possibly acid generating if preferentially exposed or inconclusive require more static and kinetic tests to verify the results.

4.2.4 Zibulo Colliery

From the Zibulo colliery, seven samples were collected for ABA testing, excluding duplicates. The sulphur speciation, net acid generation and acid-base accounting values for this study site are given in Table 4.4 below (duplicate samples for quality control are highlighted in grey).

Table 4.4: Sulphur speciation, NAG and ABA results for the Zibulo Colliery

Sample ID	Lab ID	SULPHUR SPECIATION			NET ACID GENERATION				ACID BASE ACCOUNTING							
		Total Sulphur (%)	Sulphate Sulphur as S (%)	Sulphide Sulphur (%)	pH 4.5 NAG (pH)	pH 4.5 NAG (kg H2SO4/t)	pH 7 NAG (pH)	pH 7 NAG (kg H2SO4/t)	Paste pH	Acid Potential (AP) (kg/t)	Sulphide Acid Potential SAP (calc) (kg/t)	Neut Potential (NP) (kg/t)	Net Neut Potential (NNP)	Neut Potential Ratio (NPR)	NNP_S2	NPR_S2
Siltstone 7 - 20m	39103	0.01	<0.01	0.001	6.8	<0.01	6.8	0.00	6.5	0.3	0.0	2.5	2.2	7.9	2.45	79.36
Sandstone 10 - 15m	39104	0.13	0.07	0.06	5	<0.01	5.0	1.18	6.2	4.1	1.9	-0.2	-4.3	0.1	-2.12	0.13
Carb Shale 35 - 40m	39105	0.37	0.21	0.16	6.2	<0.01	6.2	0.59	5.9	12.0	5.0	12.0	0.9	1.1	7.00	2.40
Carb Shale 70 - 80m	39106	0.62	0.21	0.41	7.8	<0.01	7.8	<0.01	7.7	19.0	12.8	62.0	43.0	3.2	49.19	4.84
Carb. Shale COMP 70-80m	40957	0.34	0.2	0.14	8.6	<0.01	8.6	<0.01	8.5	10.0	4.4	51.0	41.0	4.9	46.63	11.66
Basement 110-120m	40958	0.03	0.03	0.001	7	<0.01	7	<0.01	8.8	0.98	0.0	19.0	18.0	20.0	18.97	608.00
Basement 110-120m	40958 D	0.03	0.03	0.001	7	<0.01	7	<0.01	8.8	0.99	0.0	19.0	18.0	19.0	18.97	608.00
Basement/Dolerite 90 - 100m	39107	0.46	0.22	0.24	4.7	<0.01	4.7	13.00	7.8	14.0	7.5	18.0	4.0	1.3	10.50	2.40
Basement/Dolerite 90 - 100m D	39107 D	0.46	0.22	0.24	4.7	<0.01	4.7	12.00	7.7	14.0	7.5	18.0	3.7	1.3	10.50	2.40

4.2.4.1 Paste pH results

The paste pH values of the tested samples ranged from pH 5.9 (carb shale 35-40 m) to pH 8.8 (basement 110-120 m), indicating near neutral pH conditions. The near-neutral paste pH values suggest that at the time of analysis acid potential was absent or limited (Delta-H Water Systems Modelling Pty Ltd, 2018b).

4.2.4.2 ABA results considering sulphur speciation

The majority of tested samples, apart from the siltstone 7-20 m sample, showed measurable (>0.01%) total sulphur contents, ranging from 0.03% to 0.62% and thus derived AP values ranged from 0.98 kg/t to 62 kg/t. On the NPR versus Sulphide sulphur graph, two of the tested samples plotted in the field of very high probability of acid generation; while one sample plotted in the field of very low probability of acid generation (refer to Figure 4.10). Furthermore, one sample plotted in the zone of medium probability of acid generation and three are in the possibly acid generating or inconclusive zone.

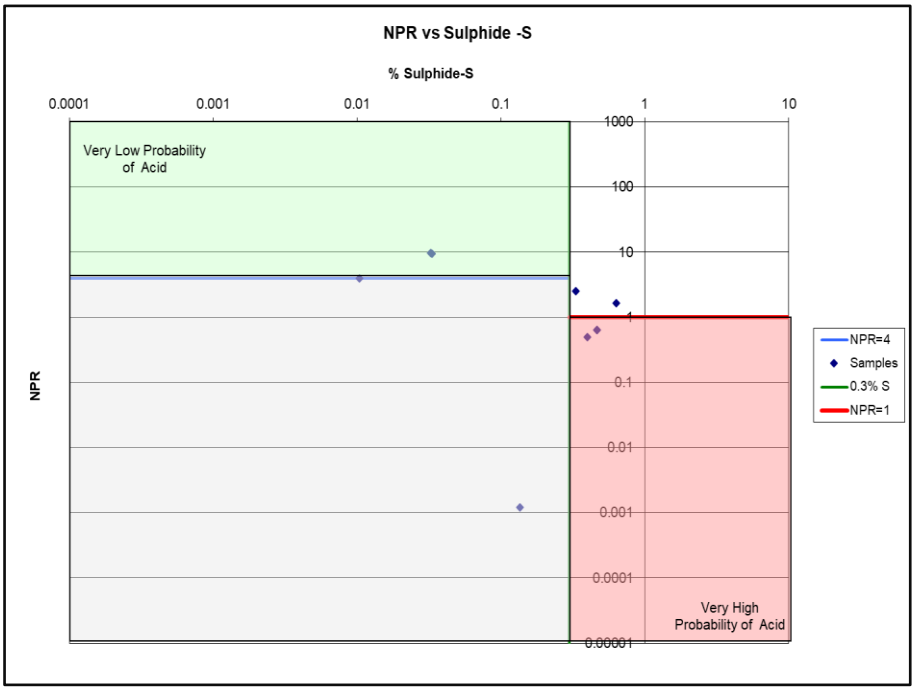

Figure 4.10: Graph showing the relationship between NPR and Sulphide sulphur for the Zibulo Colliery.

4.2.4.3 AP versus NP

Figure 4.11 shows that few of the samples (one in an open system and three in a closed system) plotted in the acid generating field above the NPR= 1:1 line; whereas two in an open system and one in a closed system plotted in the non-acid generating zone below the NPR= 4:1 line. Furthermore, the majority of samples plotted in the possibly acid generating or inconclusive zone (1<NPR<4).

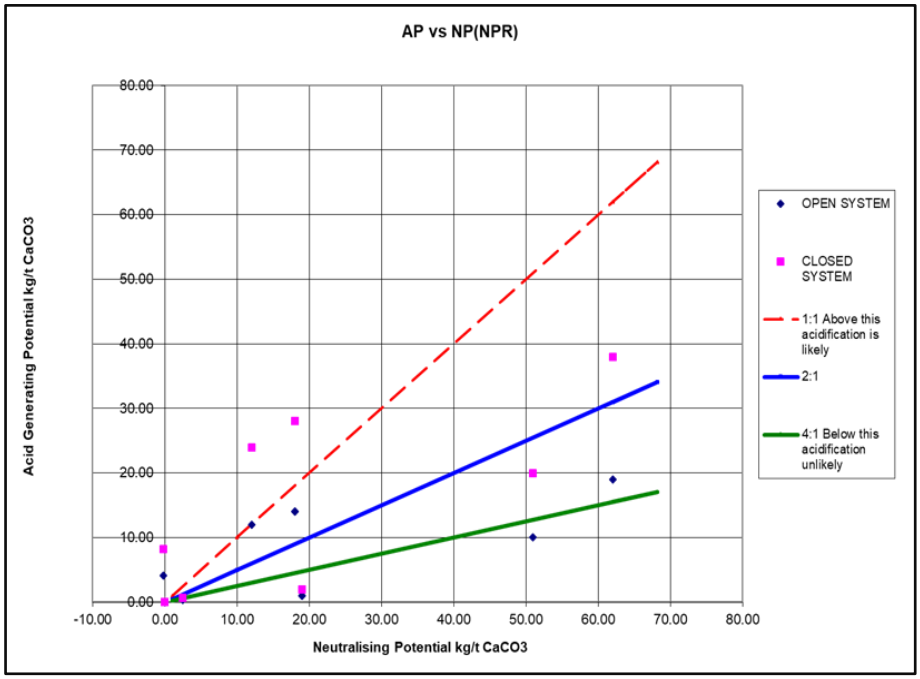

Figure 4.11: Graph showing the relationship between AP and NP for the Zibulo Colliery.

4.2.4.4 Initial and final pH versus closed NNP

Three samples plotted in the neutralising potential zone, whereas the majority of the samples plotted in the grey zone near the Y-axis and are therefore possibly acid generating if referentially exposed or inconclusive (refer to Figure 4.12).

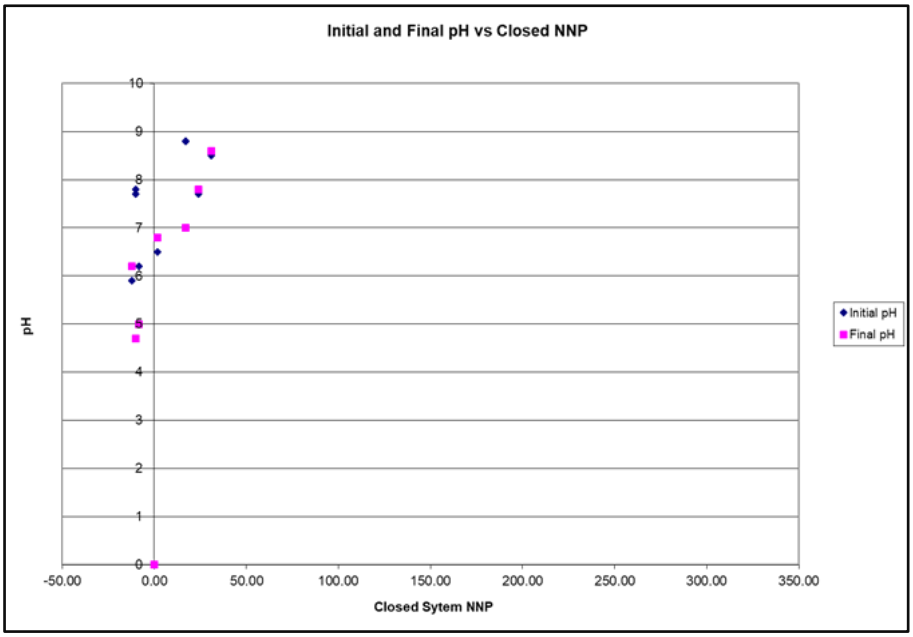

Figure 4.12: Graph showing the initial and final pH versus closed NNP for the Zibulo Colliery.

Summary of ABA results

- The siltstone 10-15 m can be regarded as potentially acid generating
- The card shale 70-80 m and carb shale COMP 70-80 m can be classified as non-acid generating.
- The rest of the samples are uncertain and therefore, more tests need to be done to verify the results.
- The basement dolerite, siltstone 7-20 m, carb shale 35-40 m are uncertain and acid generating if preferentially exposed.
- Samples classified as possibly acid generating if preferentially exposed or inconclusive need more static and kinetic done to be conducted to verify the results.

4.2.5 SACE Complex

4.2.5.1 Landau Colliery

Table 4.5 shows that the total sulphur of the samples was measurable (>0.01%), and ranged from 0.01% (LBH07) to 0.14% (LBH02); and thus the derived AP ranged from 0.313 kg/t (LBH07) to 4.38 kg/t (LBH02).

Table 4.5: Sulphur speciation and ABA results for the Landau Colliery

	SULPHUR SPECIATION			ACID BASE ACCOUNTING					
Sample ID	Total Sulphur (%)	Sulphate Sulphur as S (%)	Sulphide Sulphur (%)	Paste pH	Acid Potential (AP) (kg/t)	Sulphide Acid Potential SAP (calc) (kg/t)	Neut Potential (NP) (kg/t)	Net Neut Potential (NNP)	Neut Potential Ratio (NPR)
LBH 02	0.14			5.5	4.38		4.46	0.082	1.02
LBH 04	0.05			6.1	1.56		2.97	1.41	1.9
LBH 07	0.01			6.2	0.313		-1.48	-1.8	4.74
LBH 08	0.08			5.7	2.5		4.21	1.71	1.68

4.2.5.1.1 NPR versus total sulphur

The graph below (refer to Figure 4.13) shows that sample LBH07 is non-acid generating and the rest plotted in the possibly acid generating or inconclusive zone.

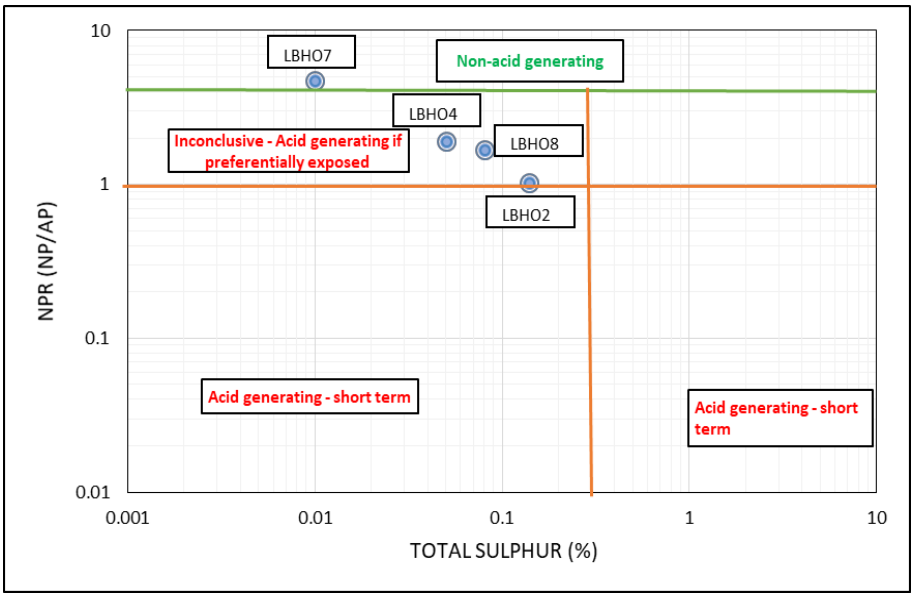

Figure 4.13: Graph showing the relationship between NPR and percentage total sulphur for the Landau Colliery.

Summary of Landau ABA results

- Sample LBH07 is non-acid generating

- The rest of the samples are inconclusive and only acid generating if potentially exposed. Therefore, more static and kinetic tests should be done to verify the results.

4.2.5.2 Blaauwkrans Discard Facility

The sulphur speciation, net acid generation and acid-base accounting values for the Blaauwkrans discard dump are given in Table 4.6 below and only one sample was used for ABA testing.

Table 4.6: Sulphur speciation, NAG and ABA results for the Blaauwkrans Discard sample

Sample ID	Lab ID	SULPHUR SPECIATION			NET ACID GENERATION				ACID BASE ACCOUNTING							
		Total Sulphur (%)	Sulphate Sulphur as S (%)	Sulphide Sulphur (%)	pH 4.5 NAG (pH)	pH 4.5 NAG (kg H_2SO_4/t)	pH 7 NAG (pH)	pH 7 NAG (kg H2SO4/t)	Paste pH	Acid Potential (AP) (kg/t)	Sulphide Acid Potential SAP (calc) (kg/t)	Neut Potential (NP) (kg/t)	Net Neut Potential (NNP)	Neut Potential Ratio (NPR)	NNP_S2	NPR_S2
Old Blaawkrans	5531	0.733	0.2	0.33			2.6		3.92	6.25		0	-6.25	0		

4.2.5.2.1 Paste pH results

The paste pH (pH 2.6) of the old Blaauwkrans discard dump is indicative of potential acid generation.

4.2.5.2.2 ABA results considering sulphur speciation

The total sulphur of the sample was measurable (>0.01%), value of 0.733% and thus the derived acid potential of 6.25 kg/t. The sample plotted in the field of medium probability of acid generation (refer to Figure 4.14).

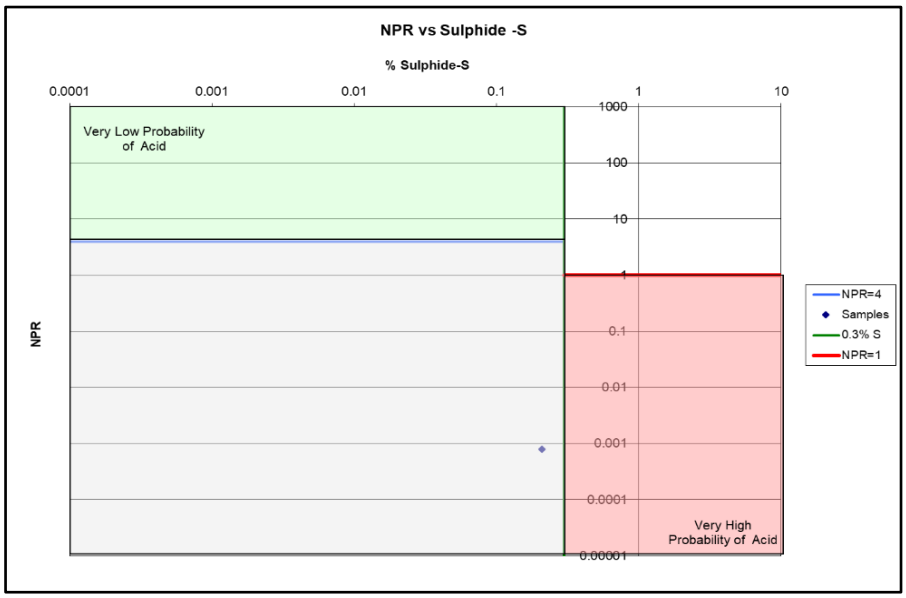

Figure 4.14: Graph showing the relation between NPR and Sulphide sulphur for the Blaauwkrans Discard Facility.

4.2.5.2.3 AP versus NP

This graph shows that the sample plotted above the NPR=1:1 line, indicating potential acid generation; the sample plotted directly on the AP Y-axis due to the absence of neutralising agent (refer to Figure 4.15).

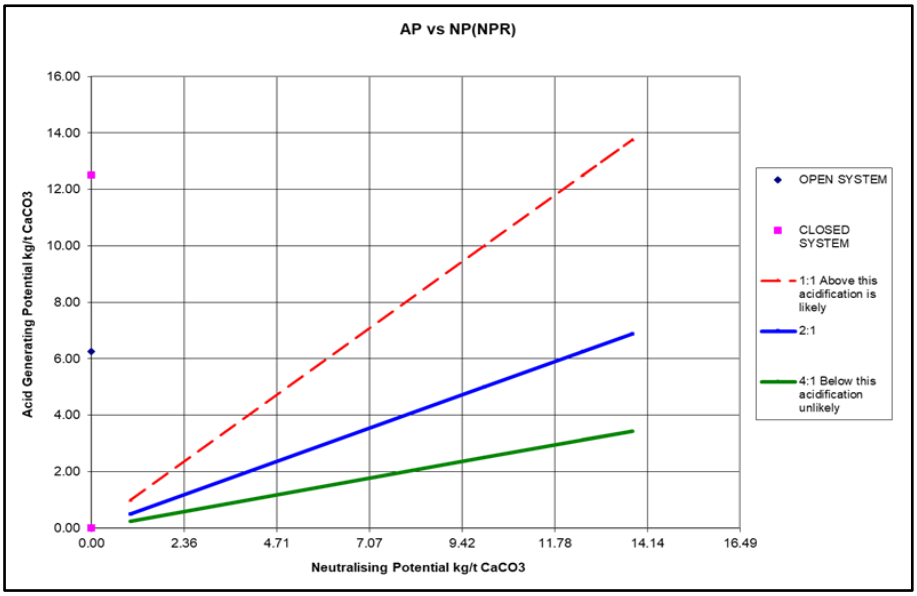

Figure 4.15: Graph showing the relation between NPR and Sulphide sulphur for the Blaauwkrans Discard Facility.

4.2.5.2.4 Initial and final pH versus closed NNP

The old Blaauwkrans sample plotted in the zone for acid generation and this plot is valid because the final pH plots below the initial pH (refer to Figure 4.16).

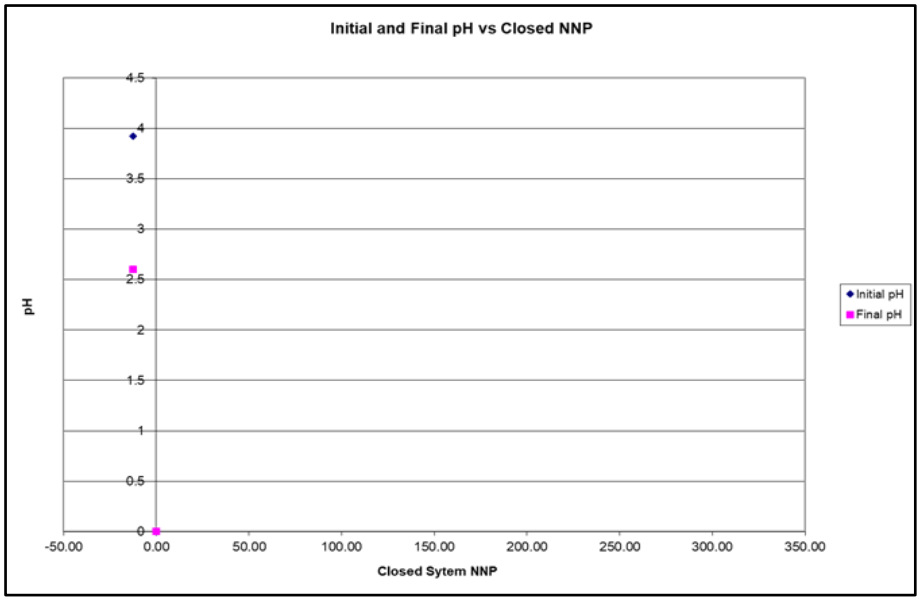

Figure 4.16: Graph showing the initial and final pH versus closed NNP for the Blaauwkrans Discard Facility.

Summary of Blaauwkrans ABA results

- The sample has a high potential to generate acid based on all the above-mentioned analysis and an NNP of -6.25 kg/t (H_2SO_4).

4.2.5.3 Greenside Discard Facility

Table 4.7 below shows that the AP for the Greenside discard samples ranged from 11.25 kg/t (N-Outer) to 126.56 kg/t (SW-Side). The calculated sulphur percentage of the samples ranged from 0.36% (N-Outer) to 4.05% (SW-Side).

Table 4.7: ABA results for the Greenside Discard Facility

		ACID BASE ACCOUNTING			
Sample ID	Calculated S (%) assuming AP calculated as 31.25 x S (%)	Acid Potential (AP) (kg/t)	Neut Potential (NP) (kg/t)	Net Neut Potential (NNP)	Neut Potential Ratio (NPR)
SW-Side	4.05	126.56	37.88	-88.69	0.3
SE-Side	1.7	53.13	7.54	-45.59	0.14
N-side	1.59	49.69	-11.38	-61.06	0.23
N-outer	0.36	11.25	3.42	-7.83	0.3

4.2.5.3.1 NPR versus total sulphur

This graph was created using Ms-Excel because of some missing information needed when using ABACUS. Furthermore, all the samples plotted in the acid generating long-term field (refer to Figure 4.17).

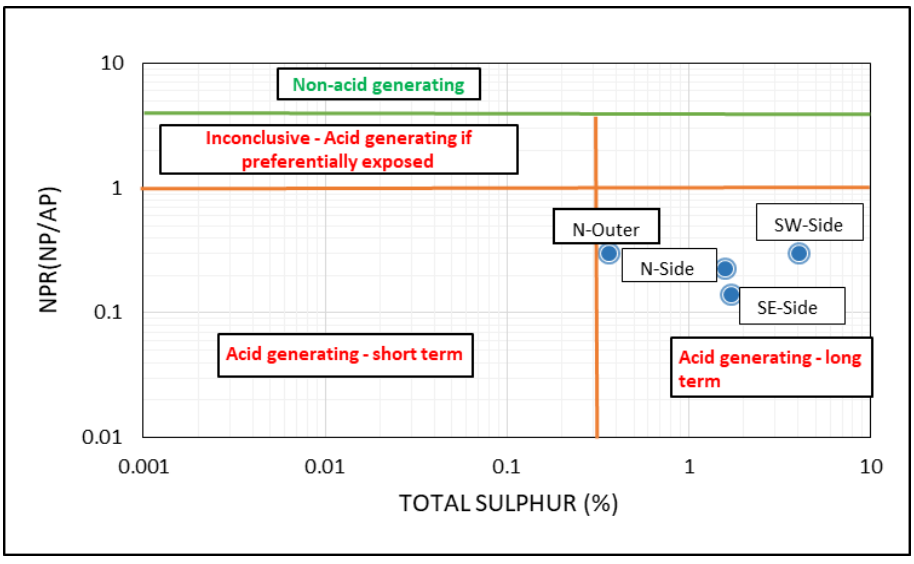

Figure 4.17: Graph showing the relationship between NPR and percentage total sulphur for the Greenside Discard Facility.

Summary of Greenside discard ABA results

- The NNP values indicate that all the samples are potentially acid generating.

4.3 GROUNDWATER CHEMISTRY RESULTS

4.3.1 Graphs: Piper and Expanded Durov Diagrams

4.3.1.1 Arnot Colliery

In Figure 4.18, cation plots show an even distribution across all cations; whereas, anions show high density plot along the SO_4-HCO_3+CO_3 line with a higher density on the SO_4 corner. Groundwater from this site can be classified as $CaMgSO_4$, $CaMgHCO_3$ and $NaHCO_3$ water type, with majority of the samples classifying as $CaMgSO_4$ water type. However, there few samples classifying as $NaSO_4$ or chloride water plotting in field B. Sulphate and bicarbonate are the dominant anions; the sulphate dominance in the groundwater is due to the groundwater being sulphate contaminated as a result of AMD, whilst the bicarbonate is from atmospheric carbon dioxide and the underlying geology.

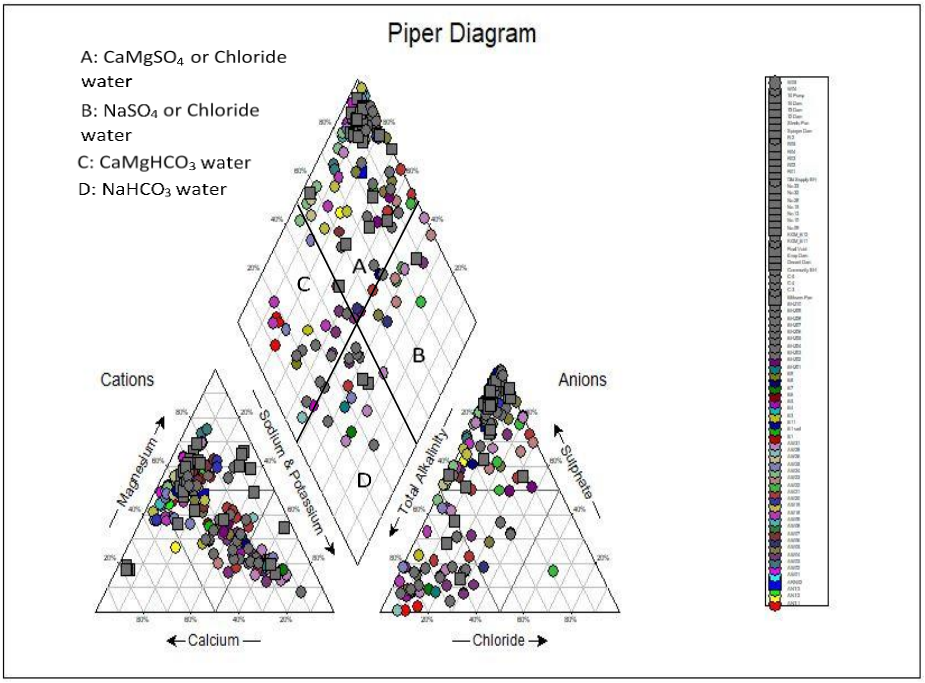

Figure 4.18: Piper diagram plot for the Arnot Colliery.

The expanded Durov diagram presented in Figure 4.19 shows a high density of boreholes that plotted in fields 2 to 6, with the majority of samples in field 5. Samples that plotted in fields 2 and 3 can be classified as fresh water that is undergoing Mg and Na ion exchange. Lastly, the samples in the 6th field can be considered as sulphate contaminated groundwater that has been in contact with a Na rich source.

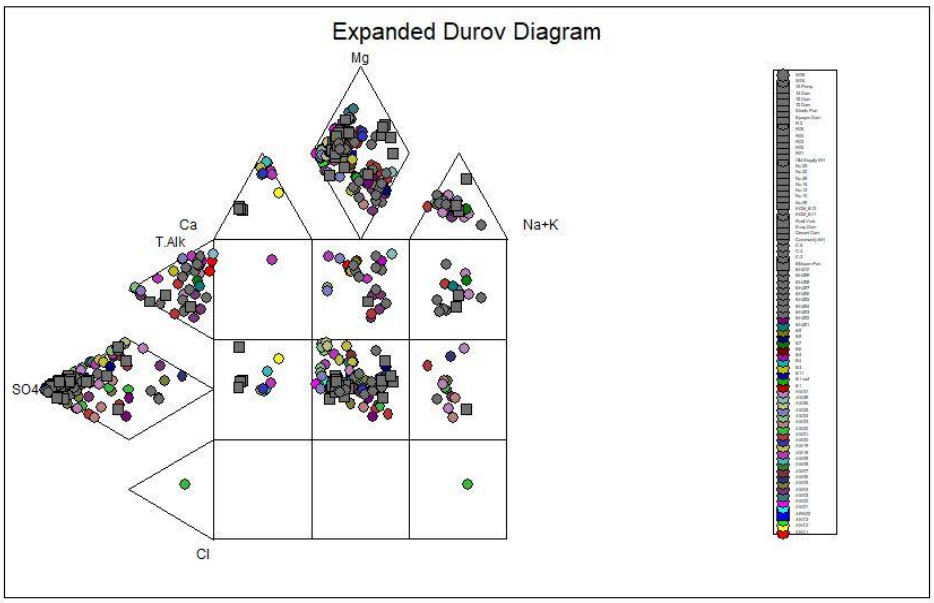

Figure 4.19: Expanded Durov diagram plot for the Arnot Colliery.

4.3.1.2 Goedehoop Colliery

a. Goedehoop North Operation

Figure 4.20 shows that the cations indicate clear trends of dominance from Ca-Mg to Na+K; and anions indicate clear trends of dominance along SO_4-HCO_3+CO_3 with contributions from Cl . Groundwater from this site can be classified as $CaMgSO_4$, $NaSO_4$; few samples classify as $NaHCO_3$, $CaMgHCO_3$ and chloride water types. In addition, sulphate and bicarbonate are the dominant anions.

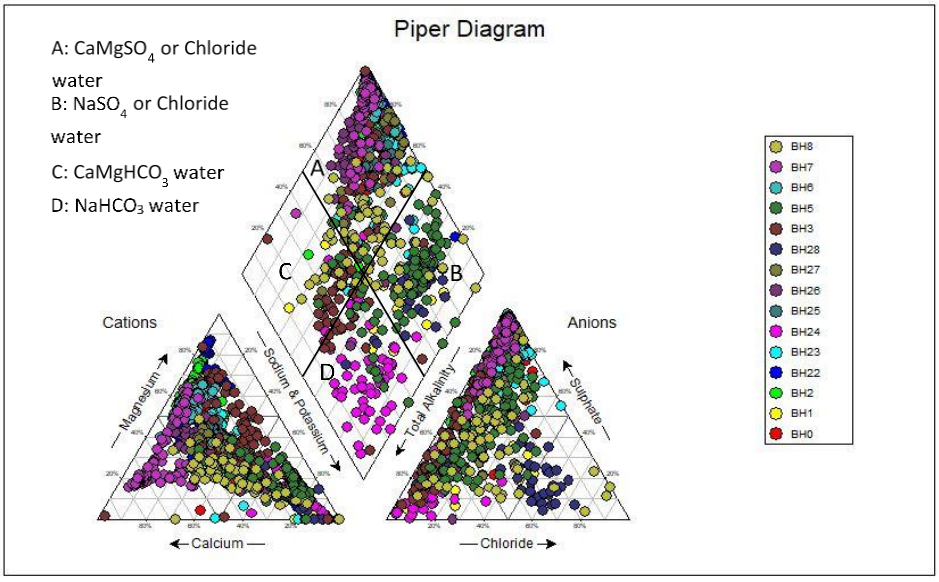

Figure 4.20: Piper diagram plot for the Goedehoop North Operation.

Figure 4.21 shows that the majority of boreholes plotted in fields 2 to 6 and 9. According to the expanded Durov classification given Section 3.3.2.1, fields 2 and 3 represent clean water undergoing Mg and Na ion exchange. Additionally, the samples plotting in field 6 can be classified as sulphate contaminated groundwater from field 5 that has been in contact with a Na rich source. Lastly, high density samples found in field 9 are considered very old groundwater that has not been moving in a long time.

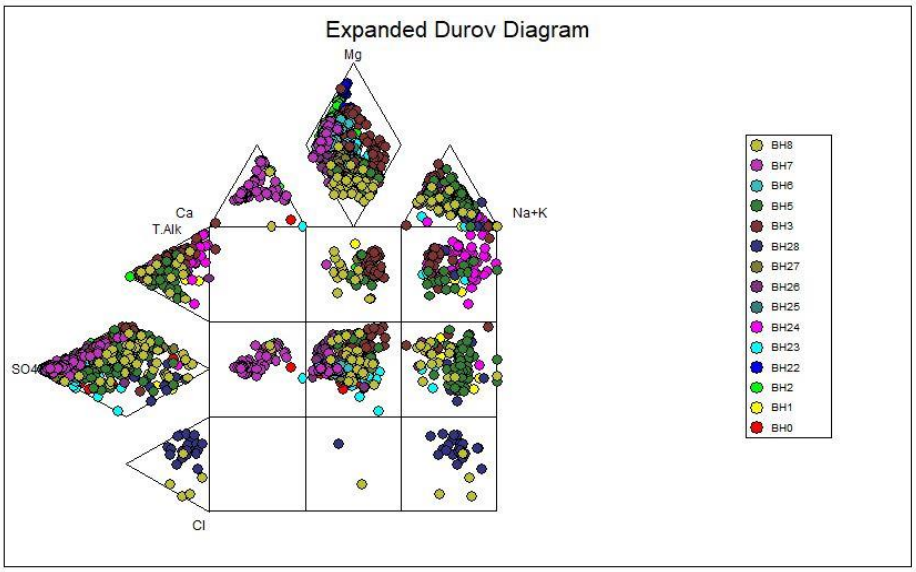

Figure 4.21: Expanded Durov diagram plot for the Goedehoop North Operation.

b. Goedehoop South Operation

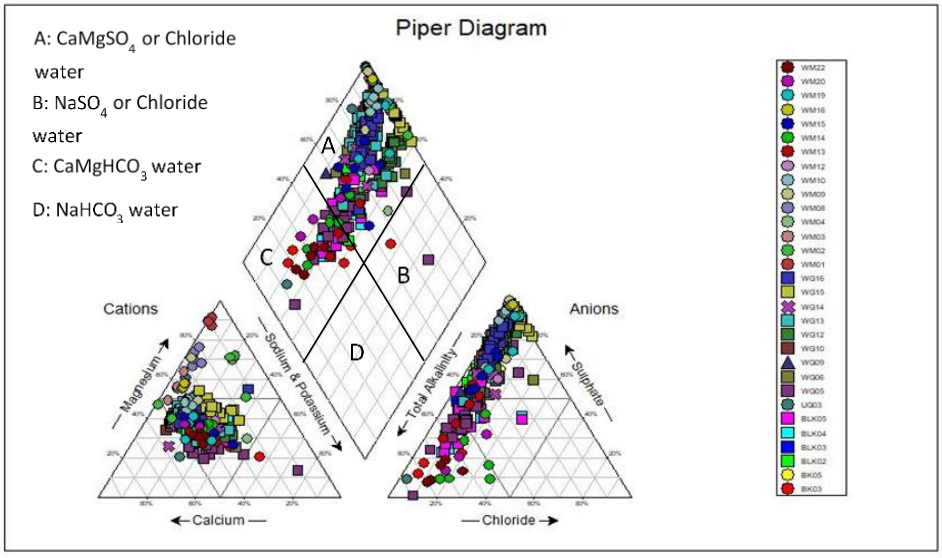

Figure 4.22: Piper diagram plot for the Goedehoop South Operation.

The cations show a high density plot approximately in the middle of the cation triangle; while anions show a high density along the SO_4-HCO_3+CO_3 (refer to Figure 4.22). Therefore, this

groundwater can be classified as $CaMgSO_4$ and $CaMgHCO_3$ water type with no dominant cation; and sulphate and bicarbonate as dominant anions.

The expanded Durov diagram (refer to Figure 4.23) shows high densities of samples that plotted in 2nd and 5th fields, with the highest density in the 5th field. The groundwater samples found in field 2 represent clean groundwater typically undergoing Mg ion exchange. Whereas the samples in field 5 can be classified as sulphate contaminated groundwater. The few samples in the 4th field can be classified as a mixture of water from fields 1 and 2 that has undergone sulphate contamination and NaCl mixing/contamination.

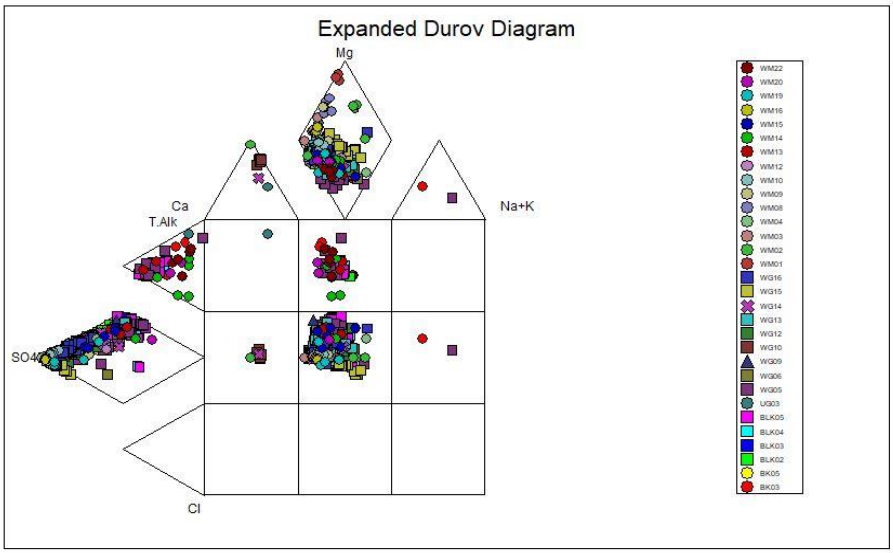

Figure 4.23: Expanded Durov diagram plot for the Goedehoop South Operation.

4.3.1.3 Mafube Colliery

The Piper diagram below (refer to Figure 4.24) shows that there are clusters of high density plots in the cation triangle approximately in the middle of the triangle, with major contributions from Na+K. The anions plot along the SO_4-HCO_3+CO_3 line with a high density cluster along the Ca-Cl line and at the SO_4 corner. The groundwater from this site can be classified as $CaMgSO_4$, $CaMgHCO_3$, $NaHCO_3$ and chloride water type with Ca and Na+K as the dominant cations, and sulphate and bicarbonate as the dominant anions.

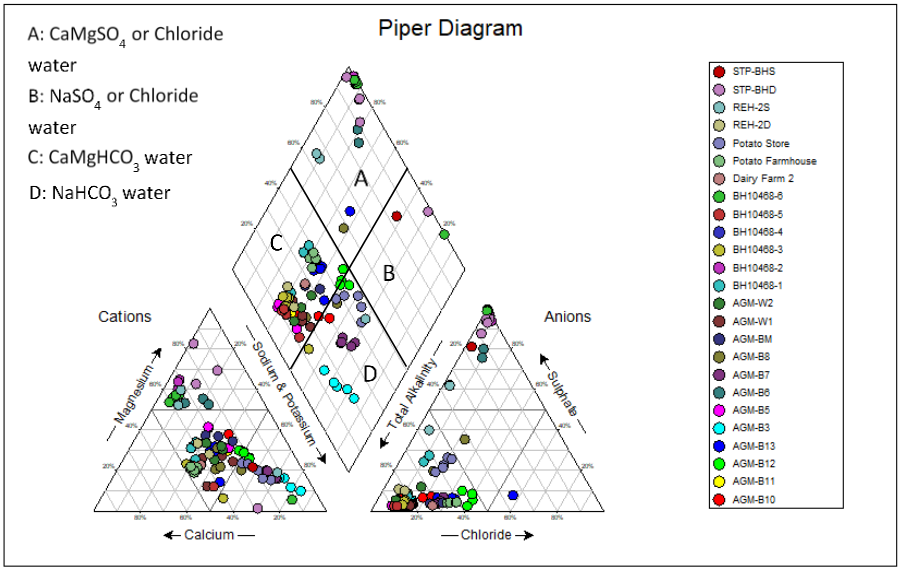

Figure 4.24: Piper diagram plot for the Mafube Colliery.

Figure 4.25 shows a high density of plots in the 2-3, and 5-6 fields. Samples found in fields 5 and 6 are indicative of sulphate contaminated groundwater that is undergoing NaCl or Cl mixing/contamination or that is in contact with a Na source. The samples found in fields 1 and 2 represent clean groundwater that is undergoing ion exchange.

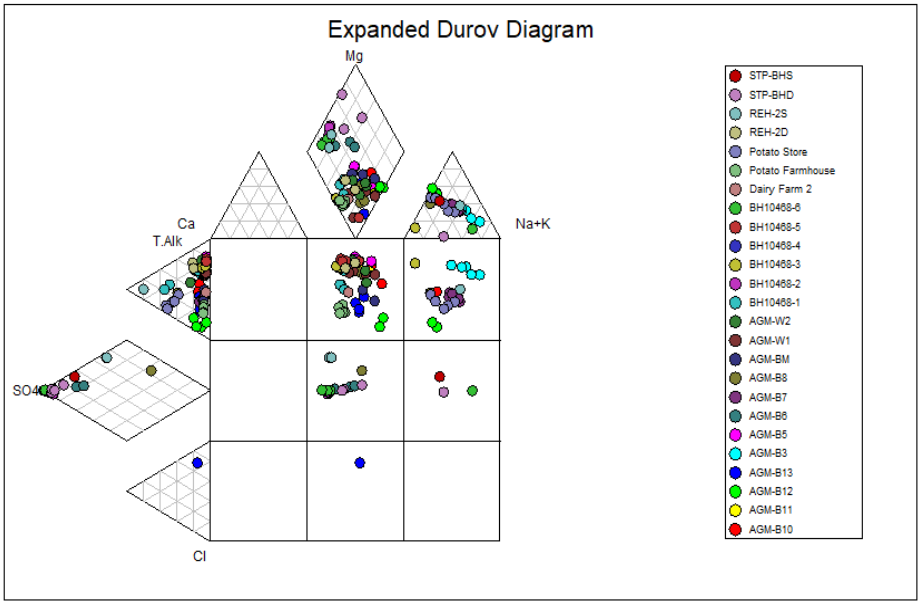

Figure 4.25: Expanded Durov diagram plot for the Mafube Colliery.

4.3.1.4 Zibulo Colliery

The cation triangle indicates a high density of plots in the middle of the triangle, with clear trends of dominance from Ca-Mg to Cl. Anions show a high density of plots on the HCO_3+CO_3 corner with small contributions from Cl and BSW04 plotting on the SO_4 corner (refer to Figure 4.26). Therefore, groundwater from this study site can be classified as $CaMgHCO_3$, $NaHCO_3$, chloride

water type and samples from borehole BSW04 classify as $CaMgSO_4$ water type. Bicarbonate is the dominant anion.

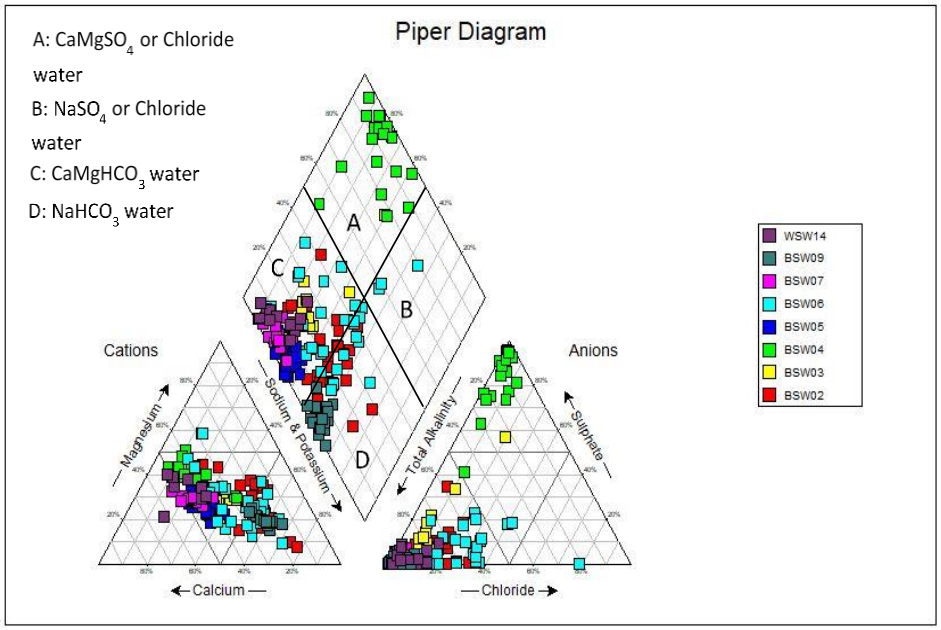

Figure 4.26: Piper diagram plot for the Zibulo Colliery.

The expanded Durov diagram (refer to Figure 4.27) shows a high density of boreholes in the 2nd, 3rd and 5th fields with borehole BSW04 only plotting in the 5th field. Therefore, samples found in fields 2 and 3 classify as clean groundwater that is undergoing Mg and Na ion exchange respectively. Groundwater in borehole BSW04 is classified as sulphate contaminated groundwater.

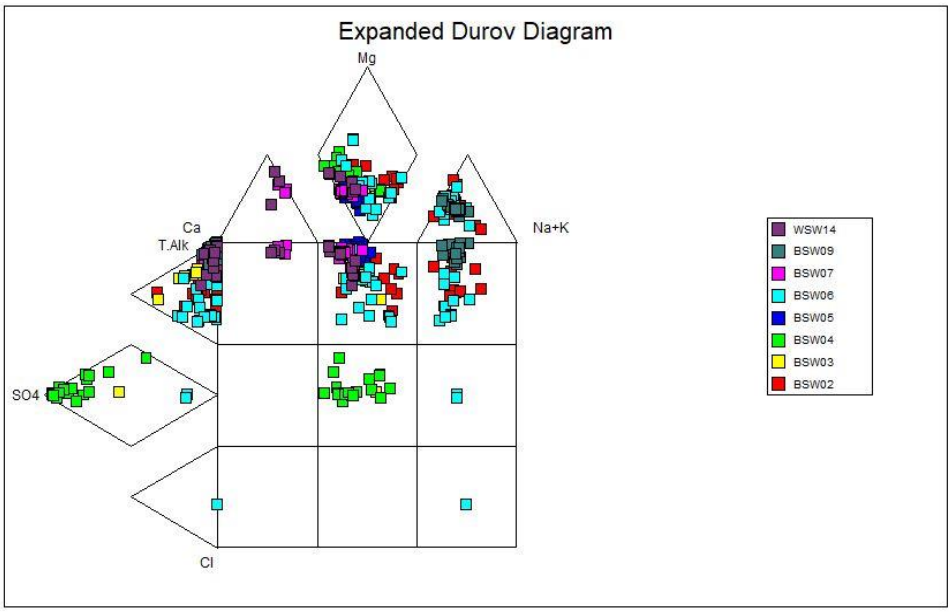

Figure 4.27: Expanded Durov diagram plot for the Zibulo Colliery.

4.3.1.5 SACE Complex

a. Landau Colliery

The Piper diagram (refer to Figure 4.28) shows that the samples plot mostly in the middle of the cation triangle. The majority of samples plot along the HCO_3-Cl line although there are few samples along the HCO_3+CO_3-SO_4 and a small cluster at the SO_4 corner. Groundwater from this study site classifies as $CaMgSO_4$, $CaMgHCO_3$ and chloride water type. Furthermore, Ca and Mg are the dominant cations with major contributions from Na+K; bicarbonate and chlorine are the dominant anions.

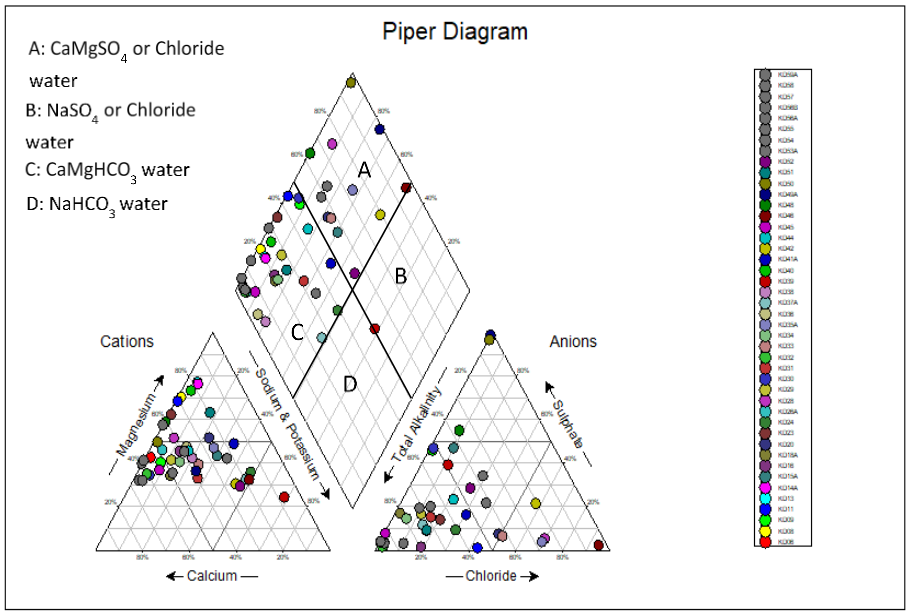

Figure 4.28: Piper diagram plot for the Landau Colliery.

The expanded Durov diagram (refer to Figure 4.29) shows a high density of samples in fields 1-2, 5 and 8. The groundwater samples found in field 5 are sulphate contaminated, and undergoing NaCl mixing/contamination. Fields 1 and 2 represent clean groundwater, which is undergoing ion exchange in field 2. Moreover, samples found in field 8 are typically indicative of a mixture of groundwater from fields 1 and 2 that has undergone sulphate contamination and Cl mixing.

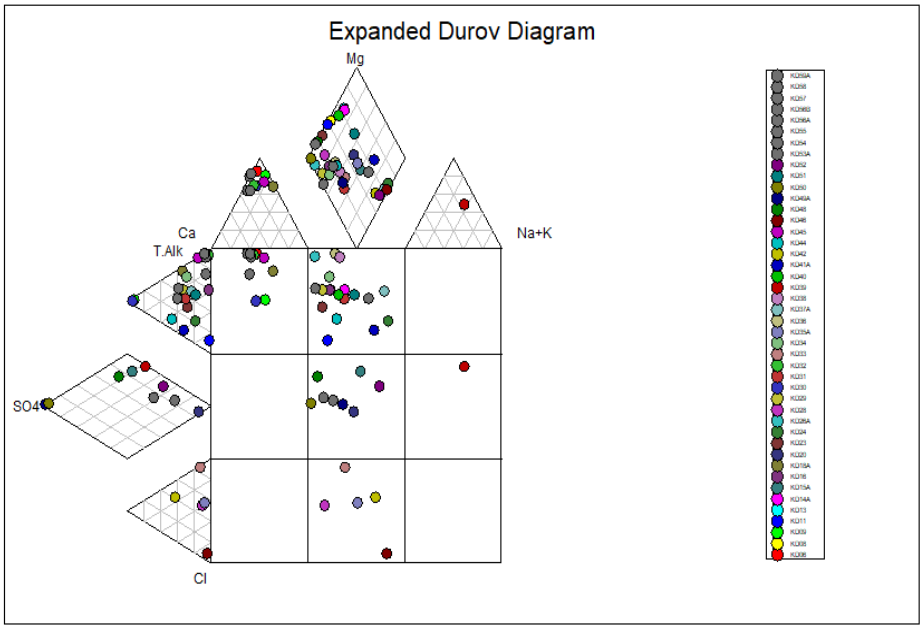

Figure 4.29: Expanded Durov diagram plot for the Landau Colliery.

b. Blaauwkrans Discard Facility

This Piper diagram shows that the majority of samples plotted along the SO_4-HCO_3+CO_3 line in the anion triangle; and clear trends of dominance from Ca-Mg to Na+K in the cation triangle can be observed (refer to Figure 4.30). The groundwater in this area can be classified as $CaMgSO_4$, $CaMgHCO_3$ and samples from borehole NAW005 classify as chloride type water. Sulphate and bicarbonate are the dominant anions and calcium as the dominant cation with major contributions from Mg and Na+K.

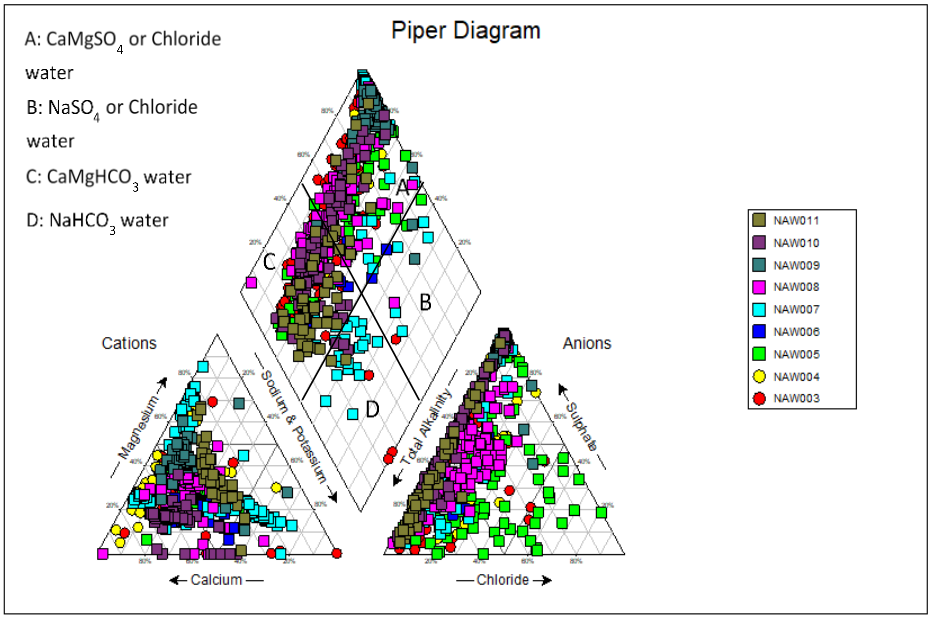

Figure 4.30: Piper diagram plot for the Blaauwkrans Discard Facility.

The expanded Durov diagram presented in Figure 4.31 indicates high densities of samples plotting in fields 1-5. The samples plotting in field 1 classify as recently recharged groundwater that is dominated by HCO_3 and CO_3 ions. The samples in fields 2-3 classify as clean groundwater that is undergoing Mg and Na ion exchange respectively. The samples in fields 4 and 5 classify as groundwater that is contaminated with sulphate. The samples plotting in the 6th field represents sulphate contaminated from field 5 that is in contact with a Na rich source. Borehole NAW005 samples plotting in fields 7 and 8 can also be classified and groundwater that is contaminated with sulphate.

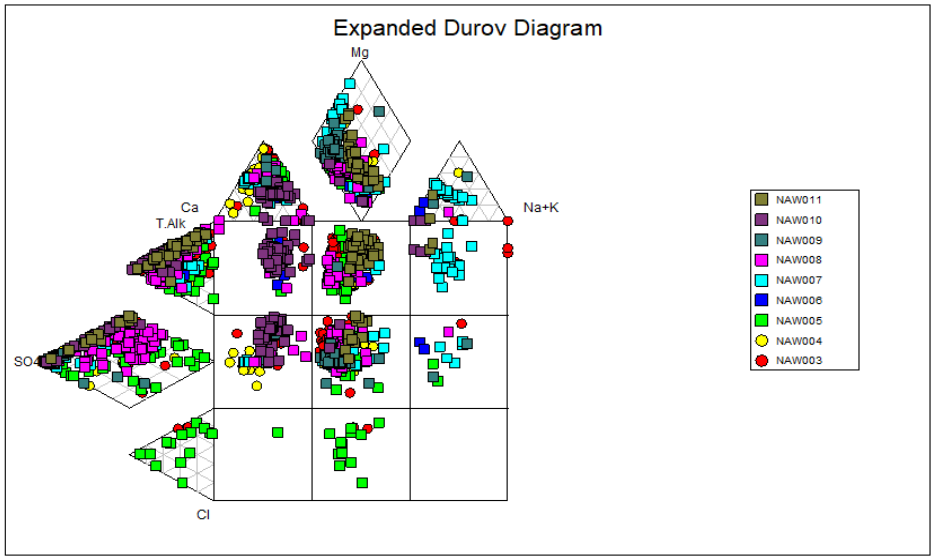

Figure 4.31: Expanded Durov diagram plot for the Blaauwkrans Discard Facility.

c. Greenside Colliery

The cation triangle shows two clusters of plots; high density cluster along the Mg-Ca line and the other cluster near the Na+K corner (refer to Figure 4.32). Furthermore, all samples plot along the SO_4-HCO_3+CO_3 line with small contributions from Cl. The water from this study site classifies as $CaMgSO_4$ and $CaMgHCO_3$ water type with Ca and Na+K as the dominant cations; with sulphate and bicarbonate being the dominant anions.

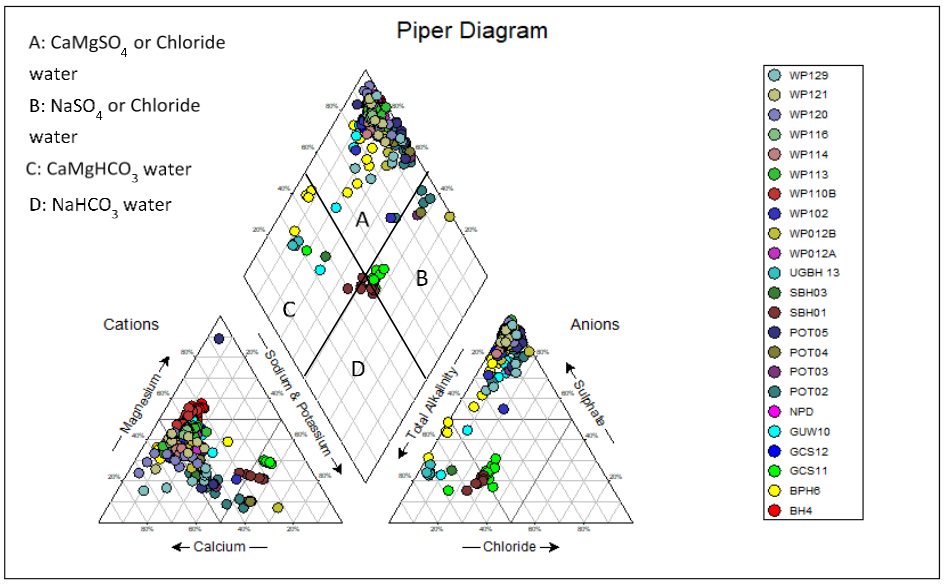

Figure 4.32: Piper diagram plot for the Greenside Colliery.

According to Figure 4.33, groundwater from this site can be classified as sulphate contaminated groundwater in fields 4 and 5. The samples found in the 6th field can be classified as SO_4 contaminated groundwater from field 5 that has been in contact with a Na rich source. Furthermore, samples plotting in fields 1-3 represent clean water that has been recently recharged, and/or is undergoing Mg and Na ion exchange.

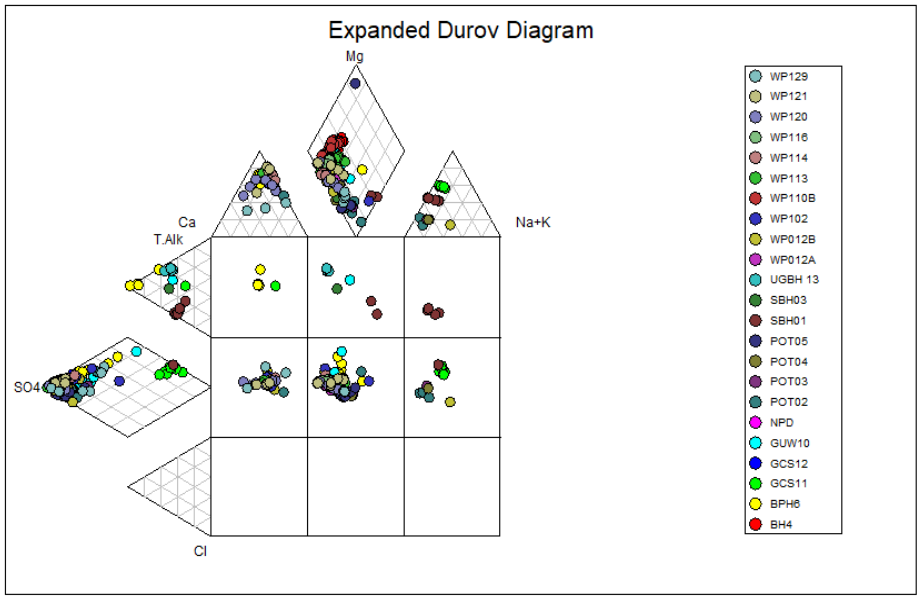

Figure 4.33: Expanded Durov diagram plot for the Greenside Colliery.

d. Greenside Discard Facility

The Piper diagram (refer to Figure 4.34) shows that there is a high density plot of cations along the Mg-Ca line; and all samples plot along SO_4-HCO_3+CO_3 in the anion triangle. Therefore,

groundwater from this study site can be classified as $CaMgSO_4$ and $CaMgHCO_3$ water type with calcium as the dominant cation, while bicarbonate and sulphate are the dominant anions.

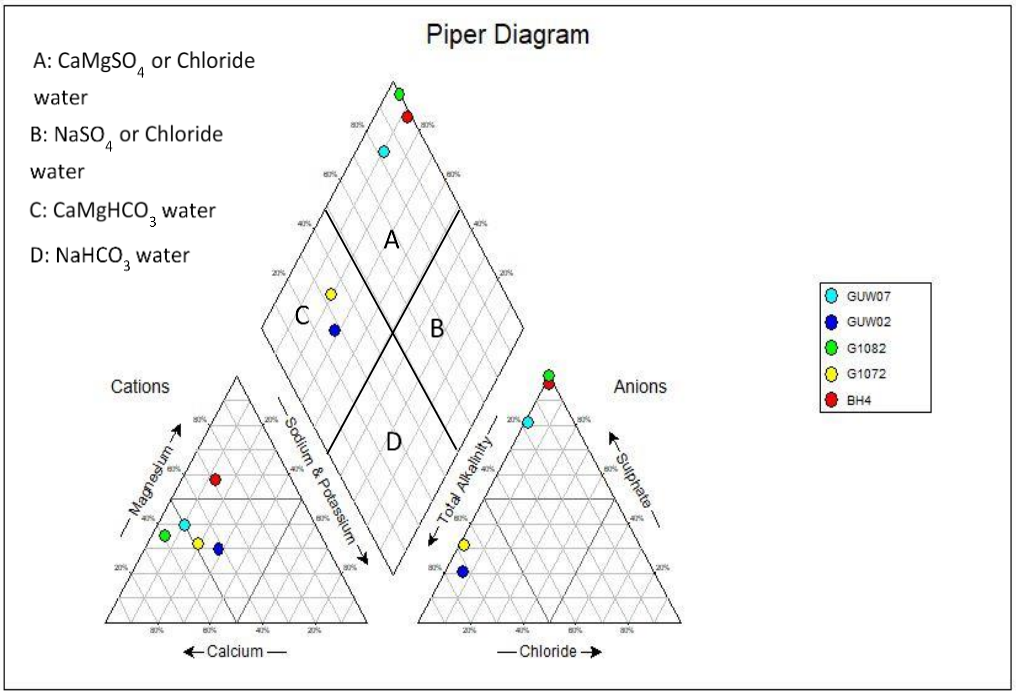

Figure 4.34: Piper diagram plot for the Greenside Discard Facility.

The Greenside discard dump groundwater samples plot in fields 2, 4 and 5; in which case the samples found in field 2 is clean groundwater that is undergoing Mg ion exchange. Furthermore, fields 4 and 5 are indicative of sulphate contaminated groundwater (refer to Figure 4.35).

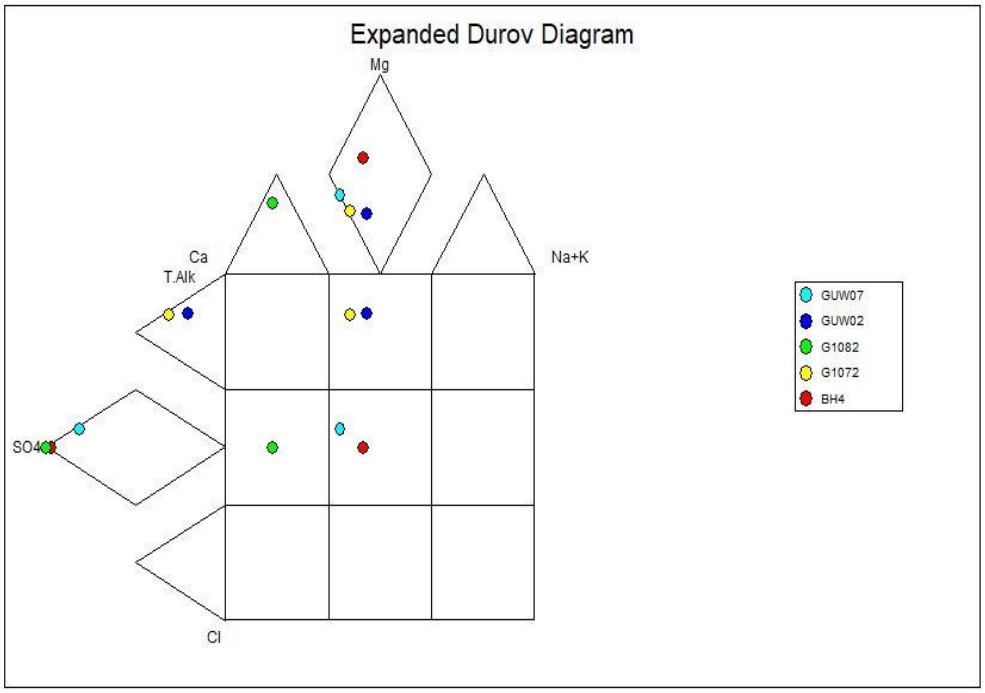

Figure 4.35: Expanded Durov diagram plot for the Greenside Discard Facility.

Summary of groundwater classification

The groundwater chemistry of the study sites was represented in Piper and expanded Durov diagrams to classify the groundwater samples. The summary of the two classification methods considering the majority of samples is as follows:

- Arnot Colliery: groundwater from this site can be classified as $CaMgSO_4$, $CaMgHCO_3$ and $NaHCO_3$ water type according to Piper diagram classification. The majority of samples were described as clean groundwater undergoing ion exchange and AMD impacted groundwater.
- Blaauwkrans Discard Facility: groundwater from this site classifies as $CaMgSO_4$ and $CaMgHO_3$. This groundwater is contaminated with sulphate and undergoing ion exchange
- Goedehoop North Operation: groundwater from this study site can be classified as $CaMgSO_4$, $NaSO_4$ and $NaHCO_3$ water. Groundwater from this site can be described as groundwater that is undergoing ion exchange and contaminated with sulphate.
- Goedehoop South Operation: groundwater from this site classifies as $CaMgSO_4$ and $CaMgHCO_3$ water type; and described as groundwater contaminated with sulphated and undergoing ion exchanging.
- Greenside Colliery: groundwater from this site classifies as $CaMgSO_4$ and $CaMgHCO_3$ water type; and described as groundwater that is sulphate contaminated and undergoing ion exchange.
- Greenside Discard Facility: groundwater from this site can be classified as $CaMgSO_4$ and $CaMgHCO_3$; and described as groundwater that is contaminated with sulphate and undergoing ion exchange.
- Landau Colliery: groundwater from this site classifies as $CaMgSO_4$ and $CaMgHCO_3$. The majority of samples can be described as groundwater that is undergoing ion exchange. However, there are few samples that can be classified as sulphate contaminated groundwater and old stagnant groundwater
- Mafube Colliery: groundwater classifies as $CaMgSO_4$, $CaMgHCO_3$ and $NaHCO_3$ water type; and the majority of samples can be described as groundwater undergoing ion exchange while few classify as sulphate contaminated groundwater.
- Zibulo Colliery: groundwater from this site classifies as $CaMgHCO_3$ and $NaHCO_3$ water type, and can be described as sulphate contaminated groundwater and water undergoing ion exchange.

- Sulphate dominance in the groundwater is due to sulphate contamination as a result of AMD.
- There are sites with no dominant cations due to cation exchange as confirmed by the expanded Durov diagram classification, which classifies some samples as clean groundwater undergoing Na and Mg ion exchange.
- Possible sources of sodium (Na) enrichment of the groundwater as seen in some samples include:
    - Dissolution of silicate minerals in the country rocks
    - Leachate infiltration from industrial and landfill sites
    - Irrigation and rainfall leaching through sodium rich soils
    - Salt water intrusion around coastal areas, which travels further inland due to groundwater flow gradient

4.3.2 Statistical analysis

4.3.2.1 Arnot Colliery

The position of the median lines for 2004, 2006 and 2018 lie outside the box plots for groups 2002 and 2011. This indicates that there were differences in sulphate concentrations among the groups (refer to Figure 4.36). Sulphate concentrations in years 2006, 2012 and 2018 were more dispersed; and less dispersed in years 2002, 2004 and 2011. Moreover, minimum and maximum concentrations varied widely in years 2002, 2006, 2011 and 2012. This means the sulphate concentrations of this study site were spread out and did not fluctuate around the same value. However, the degree to which the concentrations were spread out differed with each year. When these concentrations were compared to the SANS limit, they were all above the set limit of 500 mg/l.

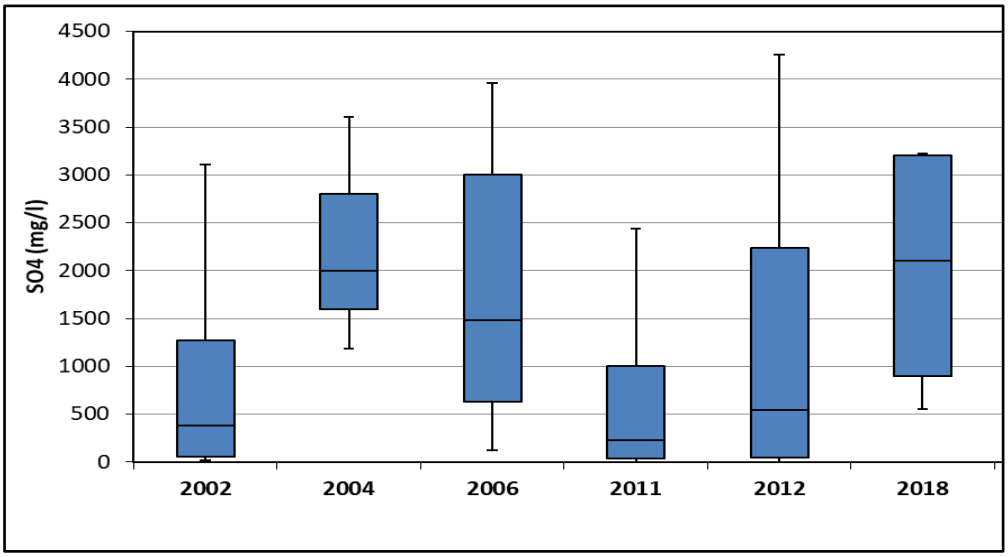

Figure 4.36: Box and whisker plots showing the change in the groundwater sulphate concentrations of the Arnot Colliery with time.

The sulphate concentration of the groundwater in this study site increased between 2002 and 2005. It then decreased to reach the lowest point in 2011 and increased again until 2018 (refer to Figure 4.37). The trend lines for both average and median values show that the sulphate concentrations of this site have steadily increased with time although there were fluctuations.

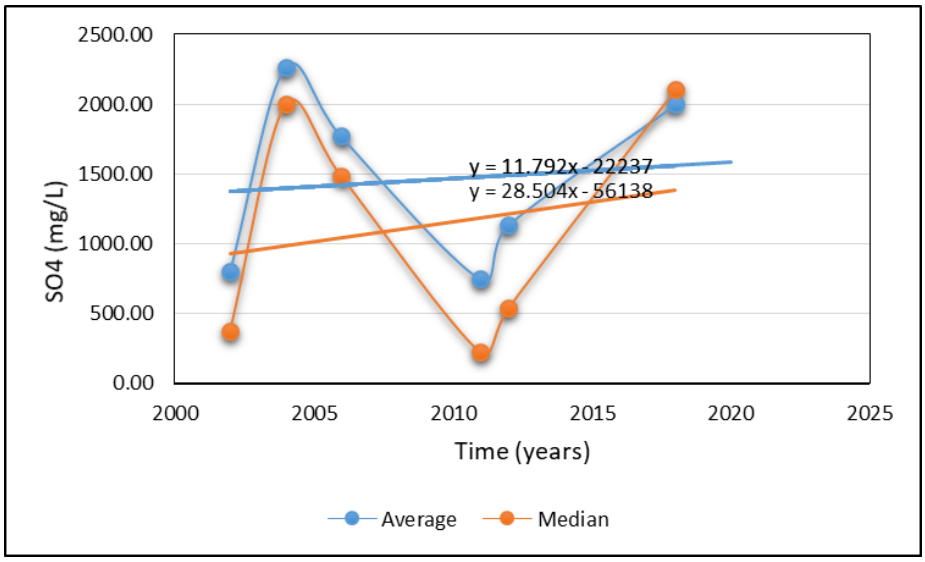

Figure 4.37: Time series plots showing the trend of sulphate concentrations with time for the Arnot Colliery.

4.3.2.2 Goedehoop colliery

a. Goedehoop North Operation

Figure 4.38 below shows that median lines for data groups 1994-1996, 1997-1998, 1999-2000, 2007-2008, 2011-2012, 2013-2014 and 2015 lie outside the 1990-1993 box plots; this means that the sulphate concentrations differed with each year. The figure also shows that 2001-2002, 2011-

2012 and 2013-2014 sulphate concentrations were more dispersed. The sulphate concentrations for years 1990-1993 and 2015 were widely distributed since the minimum and maximum values are not far apart in comparison with the other year groups. This means that the sulphate concentrations were spread out and did not fluctuate around a particular value and did not vary widely. The groundwater sulphate concentration for the 1990-1993 data group had a concentration that meets the SANS set limit, while the rest of the data groups are way above the set limit.

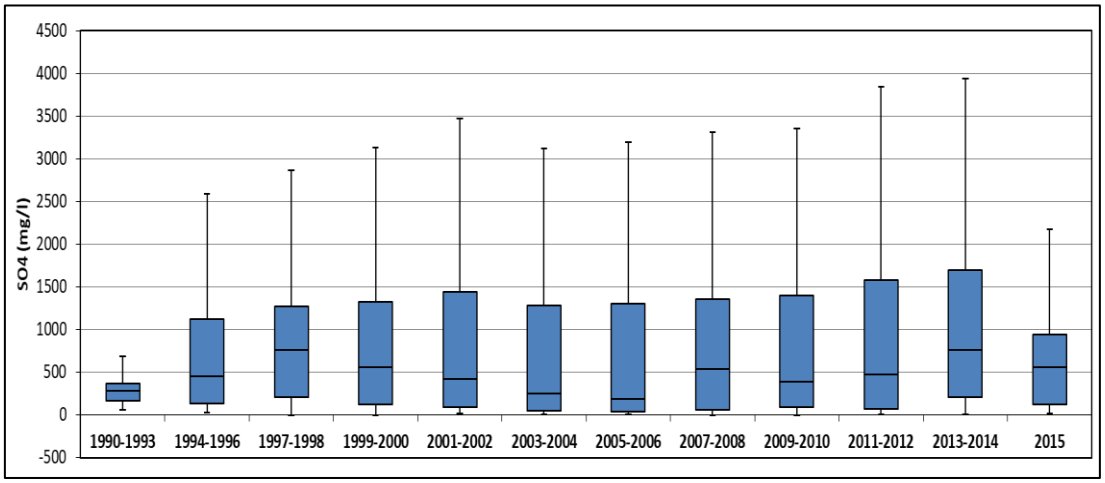

Figure 4.38: Box and whisker plots showing the change in the groundwater sulphate concentrations of the Goedehoop North Operation with time.

The groundwater sulphate concentration for this study site reached a lowest value between 1990 and 1993. It steadily increased until 2002 and fluctuated from 2002 until 2004 (refer to Figure 4.39). The concentration steadily increased until 2014. However, decreased rapidly in 2015. This can be regarded as an overall increasing trend.

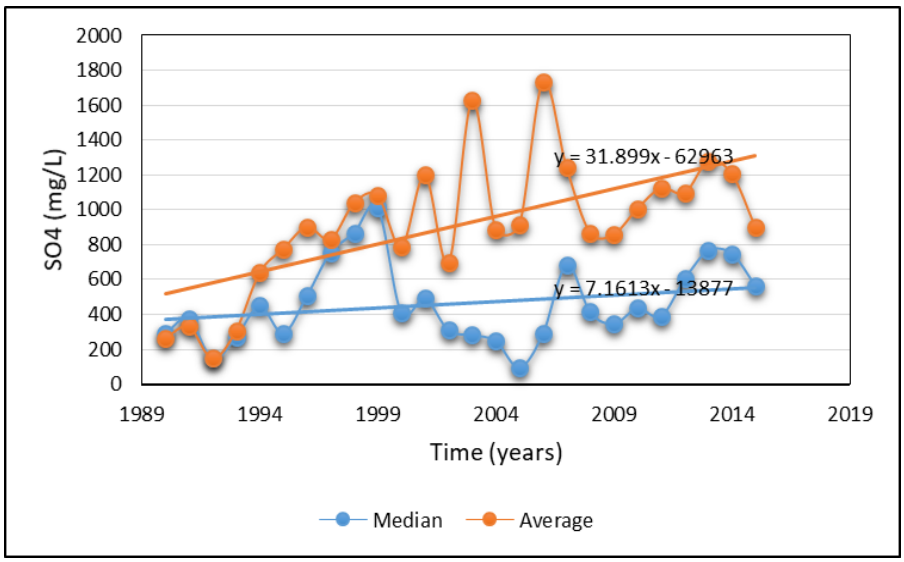

Figure 4.39: Time series plots showing the trend of sulphate concentrations with time for the Goedehoop North Operation.

b. Goedehoop South Operation

The box and whisker plots for the South operation (refer to Figure 4.40) show that no median lines lie outside other box plots. Therefore, there were no considerable differences among the sulphate concentrations of the presented years. This indicates that the sulphate concentrations did not differ much over the years.

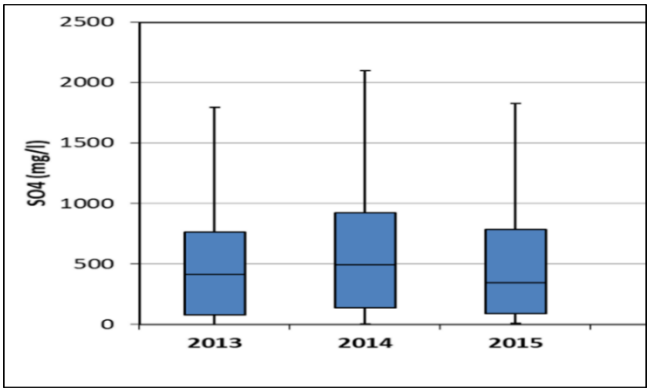

Figure 4.40: Box and whisker plots showing the change in the groundwater sulphate concentrations of the Goedehoop South Operation with time.

Sulphate concentrations for 2014 were more dispersed, and less dispersed in years 2013 and 2015; and concentrations across all years had large ranges. Therefore, it can be concluded that the sulphate concentrations were not spread out, and were fluctuating around a particular value. The groundwater sulphate concentration of this site between 2013 and 2015 were above the set SANS limit.

Figure 4.41 shows an increase in sulphate concentration from 2013 until 2014, and a slight decrease from 2014 to 2015. The trend line for average values indicates that the concentrations have steadily increased with time, whilst median values show a steady decrease with time. Therefore, the general trend for this site can be regarded as steadily increasing with time.

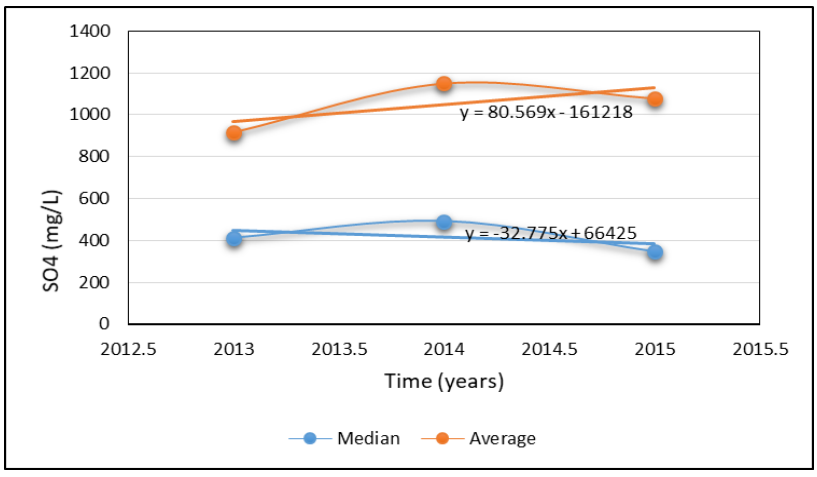

Figure 4.41: Time series plots showing the trend of sulphate concentrations with time for the Goedehoop South Operation.

4.3.2.3 Mafube Colliery

The box plots given in Figure 4.42 indicate that no median lines lie outside other box plots. Therefore, there were no differences among the data groups suggesting that the sulphate concentrations did not vary much from year to year or month to month. These box plots also indicate that sulphate concentrations for groups 15/01/2014, 07/04/2014 and 01/07/2014 were more dispersed. Minimum and maximum sulphate concentrations for data groups 15/01/2014 and 07/04/2014 were widely distributed. This means that the sulphate concentrations were spread out and did not fluctuate around a particular value. The box plots show that the sulphate concentrations for this site were below the set SANS limit between 2014 and 2015.

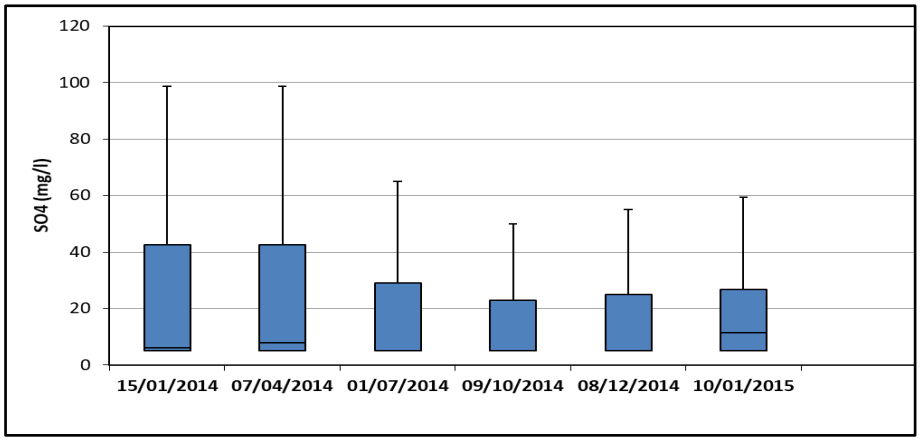

Figure 4.42: Box and whisker plots showing the change in the groundwater sulphate concentrations of the Mafube Colliery with time.

Figure 4.43 shows that the sulphate concentration decreased in a fluctuating manner until the lowest point was reached on 09/10/2014. Therefore, it slightly increased until 10/01/2015. The trend lines for both average and median values show that sulphate concentrations steadily increased with time.

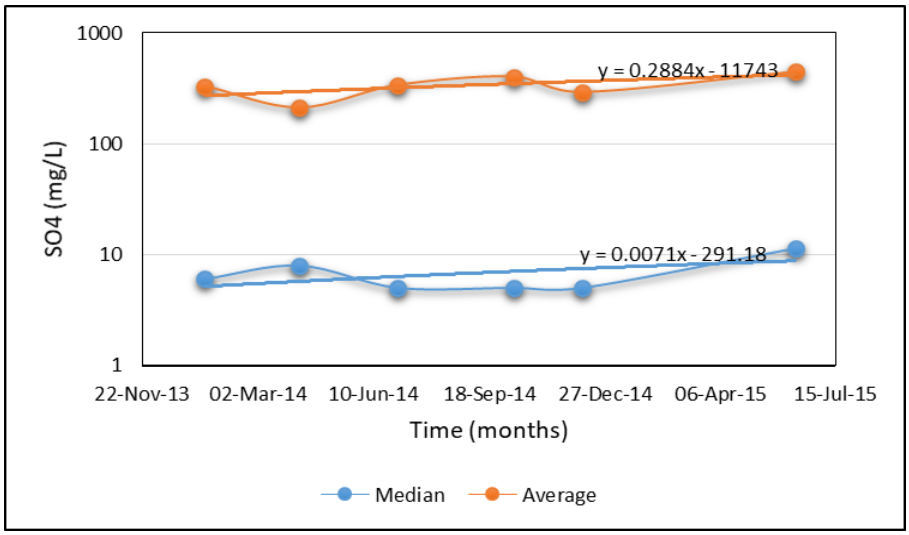

Figure 4.43: Time series plots showing the trend of sulphate concentrations with time for the Mafube Colliery.

4.3.2.4 Zibulo Colliery

Figure 4.44 indicates that the median lines for data groups 2013, 2014, 2015, 2016, 2017, 2018 and 2019 lie outside the box plot for the 2012 data groups. This indicates that the sulphate concentrations varied from year to year. In addition, 2016, 2017 and 2018 sulphate concentrations were more dispersed compared to the other years. Minimum and maximum sulphate concentrations in years 2016 to 2018 were widely distributed. This means that the sulphate concentrations were spread out and not fluctuating around a particular value. The box and whisker plots (refer to Figure 4.44) show that the sulphate concentrations for this site were below the set SANS limit.

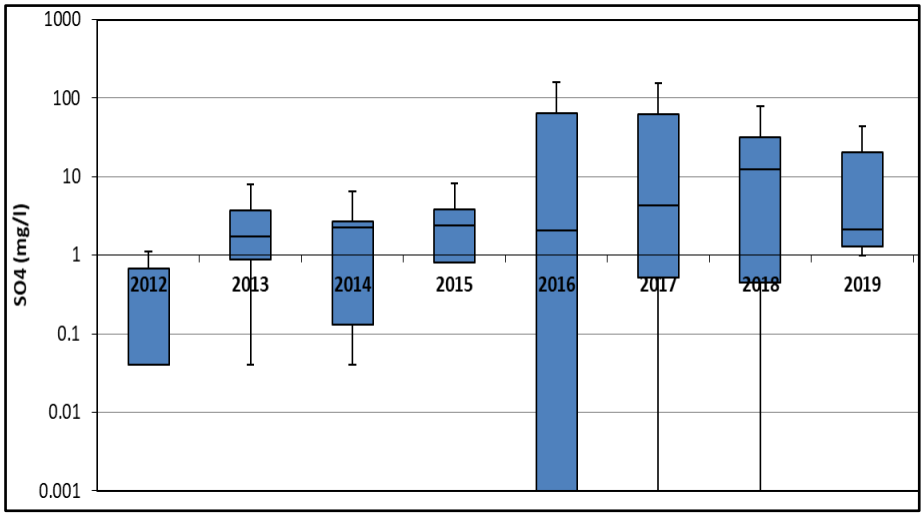

Figure 4.44: Box and whisker plots showing the change in the groundwater sulphate concentrations of the Zibulo Colliery with time.

Figure 4.45 shows that the sulphate concentrations in the groundwater were lowest in 2012, and then slowly increased while fluctuating between 2013 and 2016. Moreover, the concentration peaked between 2016 and 2018 according to both average and median values, and sharply decreased until 2019. The trend lines for both average and median values show an increasing trend.

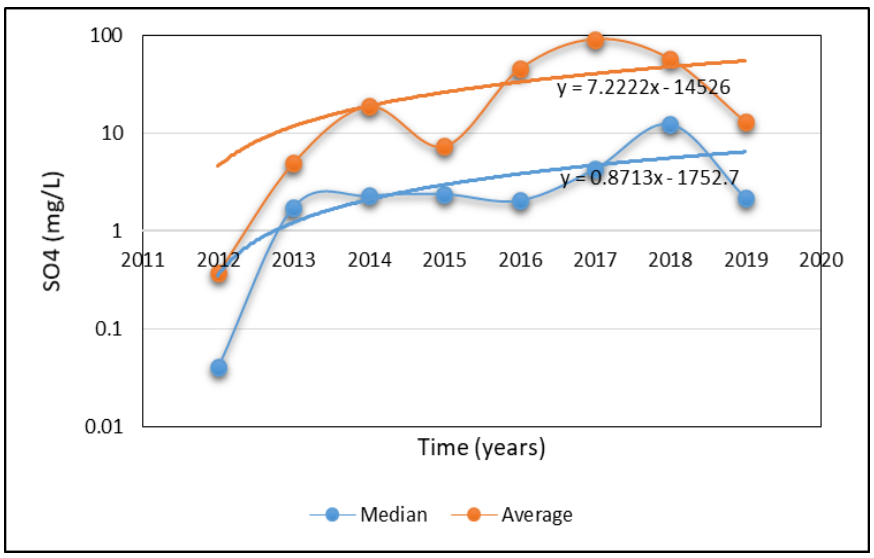

Figure 4.45: Time series plots showing the trend of sulphate concentrations with time for the Zibulo Colliery.

4.3.2.5 SACE Complex

a. Landau Colliery

Figure 4.46 shows that the median lines of data groups 2010, 2011 and 2014 lie outside the box plot of data group 2013. Therefore, there were differences among these groups and this means sulphate concentrations varied from year to year. This figure also shows that 2008-2009, 2010, 2011, 2013, 2014 and 2015 concentrations were more dispersed compared to the other years. Minimum and maximum sulphate concentrations were widely distributed in 2008-2009, 2010, 2011 and 2012. This indicates that the sulphate concentrations were spread out and not fluctuating around a particular value. The data group 2013 is the only group with a sulphate concentration that was below the set SANS limit.

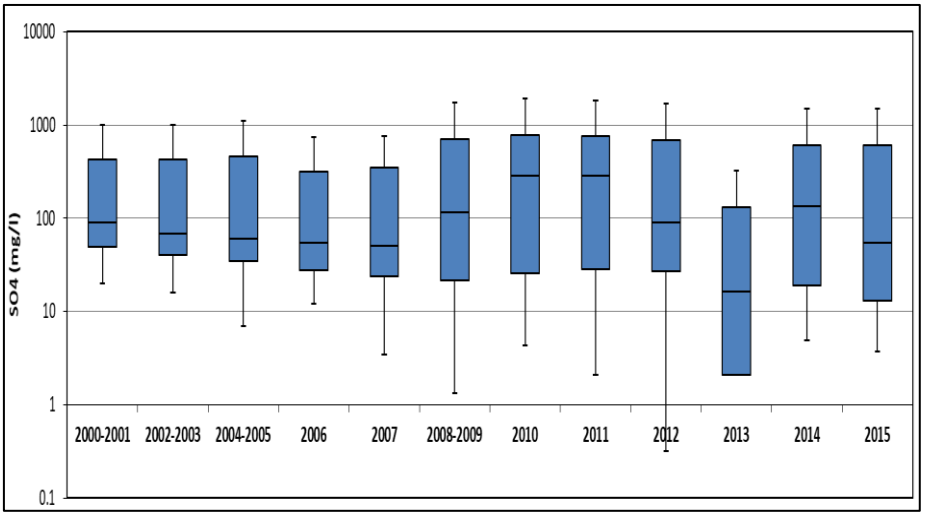

Figure 4.46: Box and whisker plots showing the change in the groundwater sulphate concentrations of the Landau Colliery with time.

Figure 4.47 indicates that the sulphate concentrations are fairly constant from 2002 until 2008 with small fluctuations. The concentrations increased from 2009 until 2012 and thereafter decreased in a fluctuating fashion. Trend lines for both average and median values show a steady increasing trend of sulphate concentrations with time.

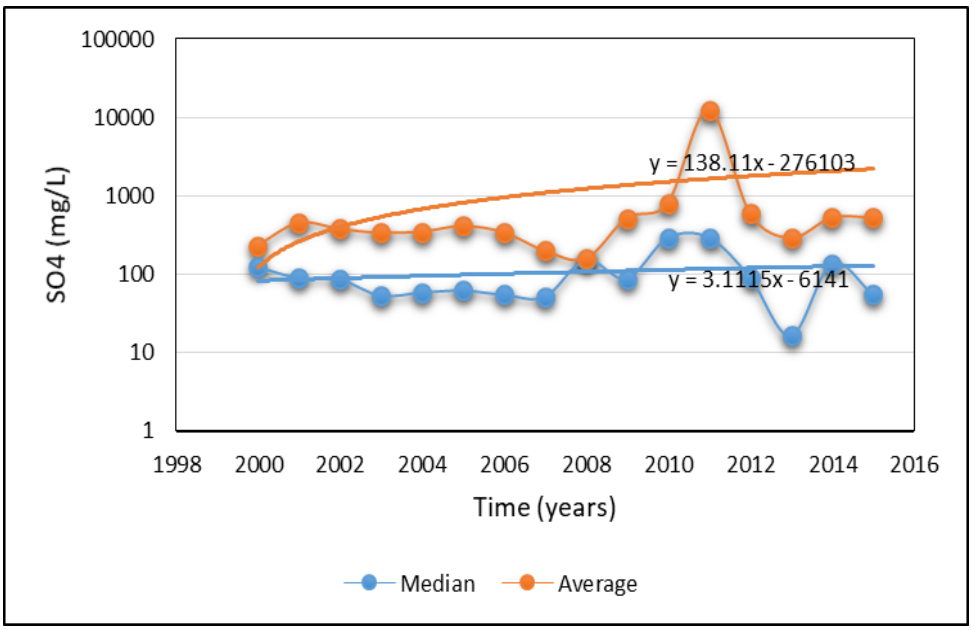

Figure 4.47: Time series plots showing the trend of sulphate concentrations with time for the Landau Colliery.

b. Blaauwkrans Discard Facility

The box and whisker plot presented in Figure 4.48 shows that no median lines lie outside other box plots. Therefore, there were no significant differences among the data groups and the sulphate concentrations did not vary much from year to year. Sulphate concentrations for groups 2002-2004, 2005-2006, 2007-2008, 2010, 2012 and 2015 were more dispersed, and less dispersed in years 2009, 2011, 2013, 2014, 2016 and 2017. In addition, minimum and maximum sulphate concentrations for groups 2005-2006, 2007-2008, 2009, 2010, 2011 and 2014 were widely distributed. Therefore, it can be concluded that the sulphate concentrations were spread out and did not fluctuate around a particular value. The groundwater samples collected in 2009, 2011-2017 had sulphate concentrations lower than the SANS limit.

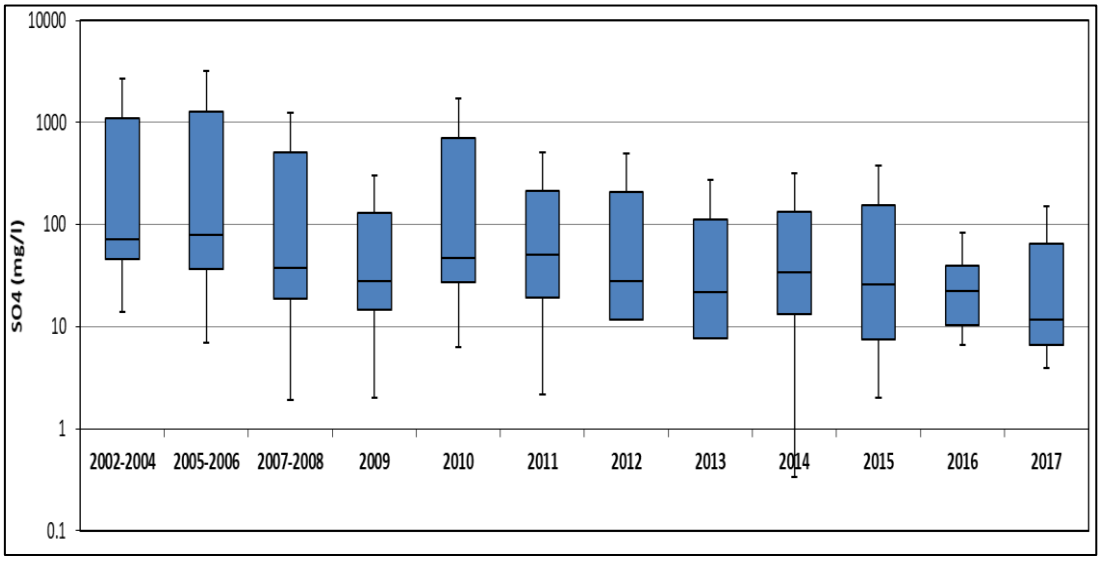

Figure 4.48: Box and whisker plots showing the change in the groundwater sulphate concentrations of the Blaauwkrans Discard Facility with time.

The time series graph shown in Figure 4.49 indicates that the sulphate concentration in the groundwater decreased in a fluctuating manner from 2002 until 2017. Both average and median concentrations show an increase between 2004 and 2005, followed by a decrease until 2008. Further increases and decreases are observed until 2017. Overall, sulphate concentrations in the groundwater decreased with time.

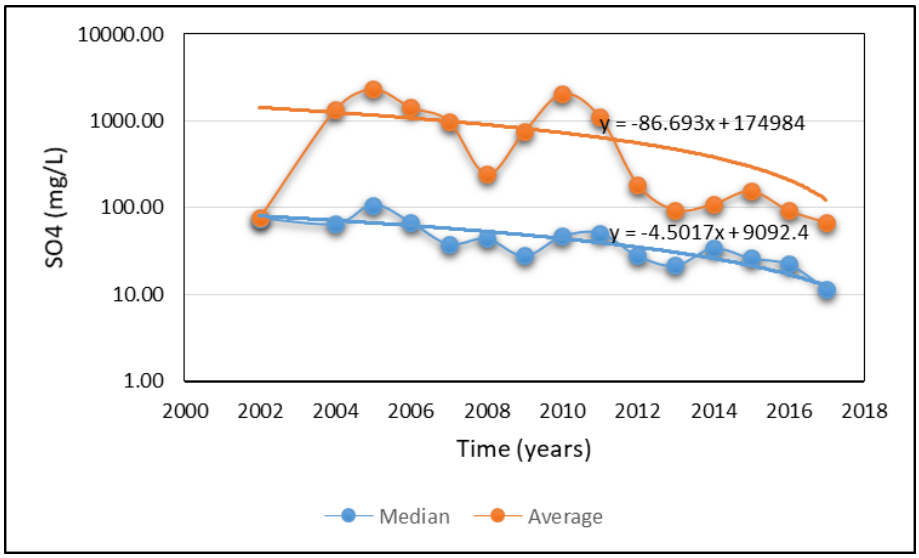

Figure 4.49: Time series plots showing the trend of sulphate concentrations with time for the Blaauwkrans Discard Facility.

c. Greenside Colliery

The box and whisker plots presented in Figure 4.50 indicates that no median lines lie outside other box plots. Therefore, there were no differences among the data groups. This means that sulphate concentrations did not vary much from year to year. Sulphate concentrations for groups 2016, 2017 and 2018 were more dispersed, and less dispersed in groups 2013, 2014 and 2015. In addition, minimum and maximum sulphate concentrations for groups 2016 and 2017 were widely distributed. It can be concluded that sulphate concentrations were spread out and did not fluctuate around a particular value. Moreover, the sulphate concentrations were above the set SANS limit.

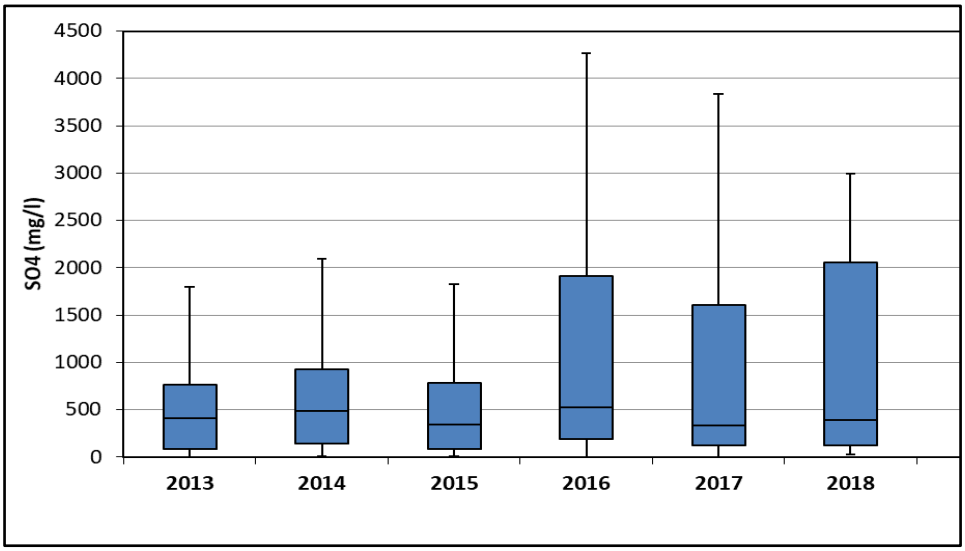

Figure 4.50: Box and whisker plots showing the change in the groundwater sulphate concentrations of the Greenside Colliery with time.

The sulphate concentrations of this study site show an increase from 2013 and 2014 (refer to Figure 4.51) and a fluctuating decreasing trend from 2014 until 2018. The trend lines for both average and median values suggest that the sulphate concentrations of the Greenside colliery decreased with time.

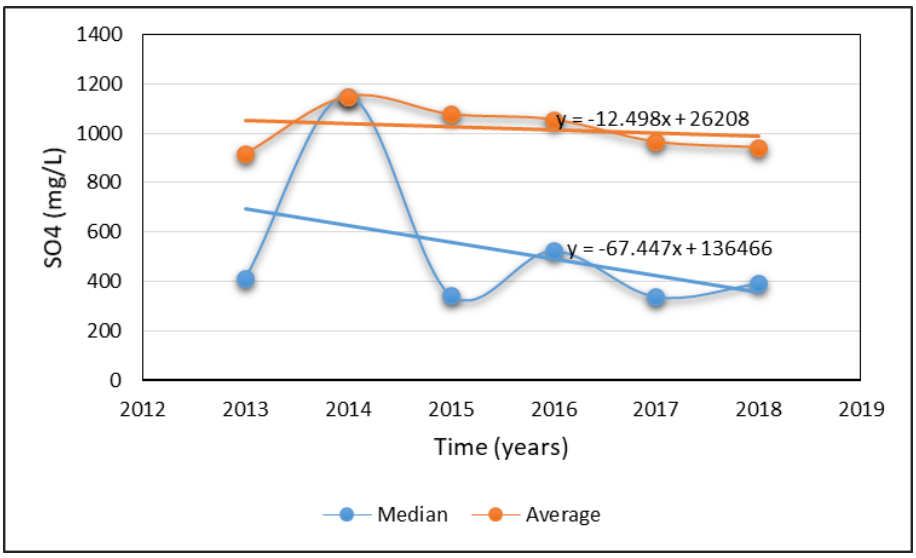

Figure 4.51: Time series plots showing the trend of sulphate concentrations with time for the Greenside Colliery.

d. Greenside Discard Facility

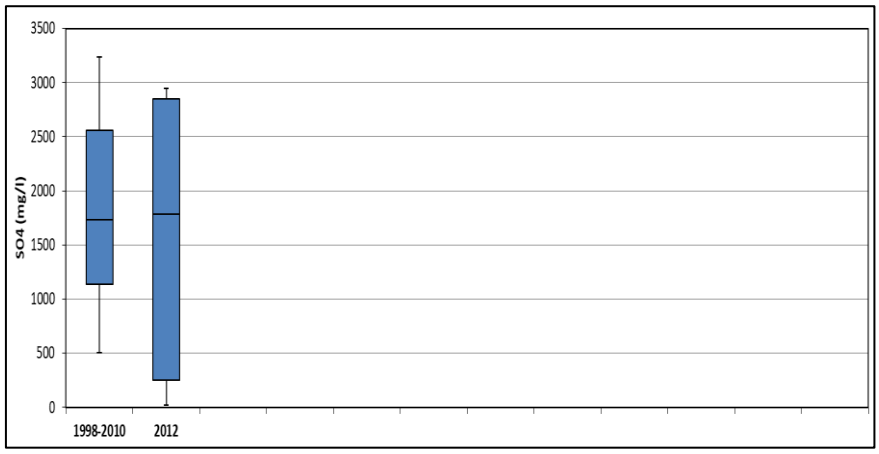

Figure 4.52: Box and whisker plots showing the change in the groundwater sulphate concentrations of the Greenside Discard Facility with time.

The box and whisker plots shown in Figure 4.52 indicates no median lines outside other box plots; therefore, there were no differences among the data groups. This indicates that sulphate concentrations did not vary much from year to year. The box plots also shows that the sulphate concentrations in year 2012 were more dispersed compared to the 1998-2010 data group. In addition, minimum and maximum sulphate concentrations varied widely from 1998 to 2010. This indicates that sulphate concentrations were spread out and did not fluctuate around a particular value. The sulphate concentrations reached a high of 2850 mg/l, which was above the set limit.

The average and median values trend lines in Figure 4.53 are contradicting each other, because the median values trend line shows an increasing trend while the average values trend line shows a decreasing trend. Therefore, an overall or resultant trend of sulphate concentrations could do not be deduced for this site.

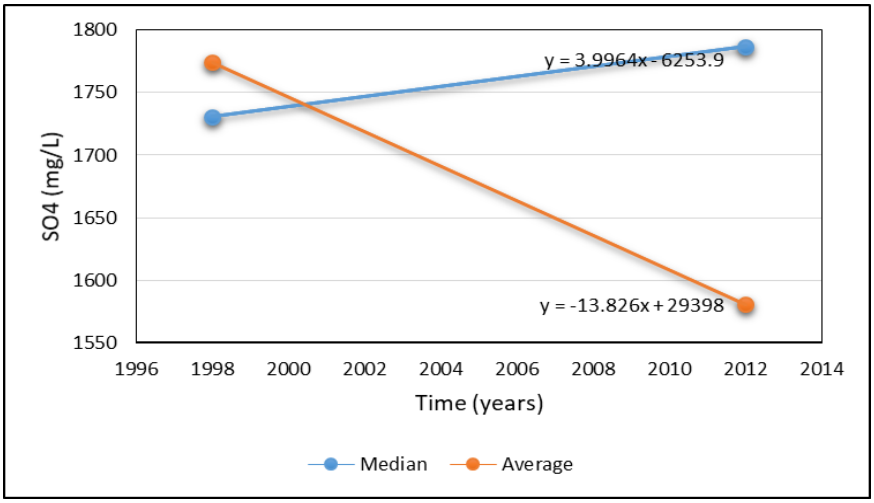

Figure 4.53: Time series plots showing the trend of sulphate concentrations with time for the Greenside Discard Facility.

4.3.2.6 Comparison of all study sites

Figure 4.54 summarises the distribution of sulphate concentrations of the various collieries and discard facilities analysed. Results indicated that the median lines for Arnot, Goedehoop North, Goedehoop South, Greenside colliery and Greenside discard dump lie outside box plots for Blaauwkrans, Landau, Mafube and Zibulo study sites. This suggests that there were sulphate concentration differences among these sites. Moreover, Arnot, Landau, Zibulo, Blaauwkrans and Goedehoop north study sites had more dispersed data; while Arnot, Goedehoop south, Greenside colliery and discard dump had a wide distribution of data.

When comparing the groundwater sulphate concentrations of all the study sites it can be seen that Arnot, Goedehoop north and south, Greenside colliery and discard dump had the highest concentrations compared to Blaauwkrans, Landau, Mafube and Zibulo. Mafube and Zibulo study sites, which had the lowest sulphate concentrations in the groundwater. According to the box and whisker plots, the SANS limit for sulphate concentration was met at the Blaauwkrans, Mafube and Zibulo study sites. However, the groundwater from the rest of the study sites did not meet the SANS sulphate limit.

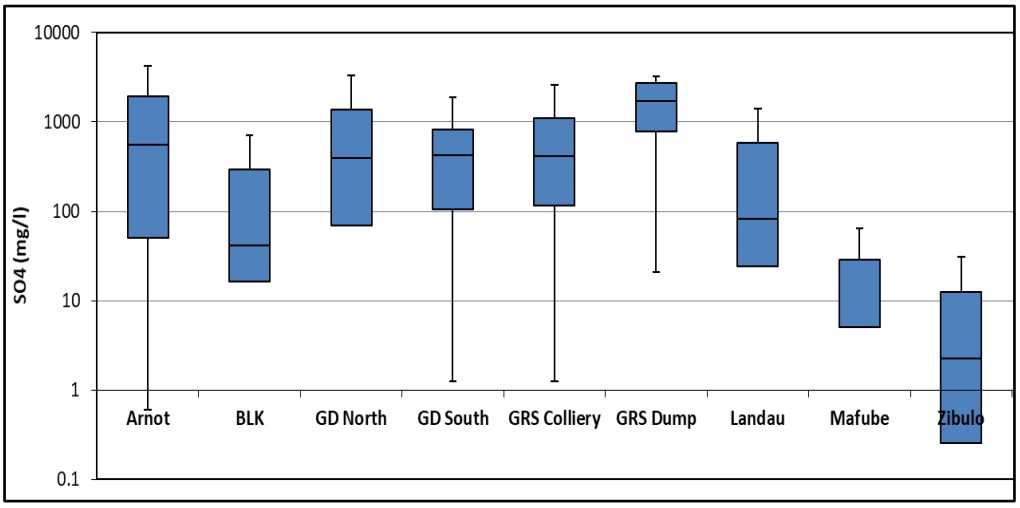

Figure 4.54: Box and whisker plots showing the change in the groundwater sulphate concentrations of each study site in comparison with one another.

Generally, high total sulphur means that there is a high possibility of acid generation. The average and median graphs both show that Landau, Arnot, Zibulo and Mafube had low total sulphur (refer to Figure 4.55 and Figure 4.56). In comparison, Landau and Arnot plotted on the high sulphate spectrum with low total sulphur on the Average graph. This could be due to the rock material being preferentially exposed over long periods to other important components related AMD formation, or due to different sampling methods used over the years. The graphs also show that Blaauwkrans, Goedehoop and Greenside had high total sulphur and high sulphate concentrations. The Median graph (Figure 4.56) linear regression shows an increase of sulphate production with an increase in

total sulphur; whilst the Average graph (Figure 4.55) shows a fairly constant relationship between the two variables. R-squared percentages for both Median and Average graphs show a lowest level of correlation between ABA (total sulphur) and total sulphate, which were 18.49 and 0.89% respectively.

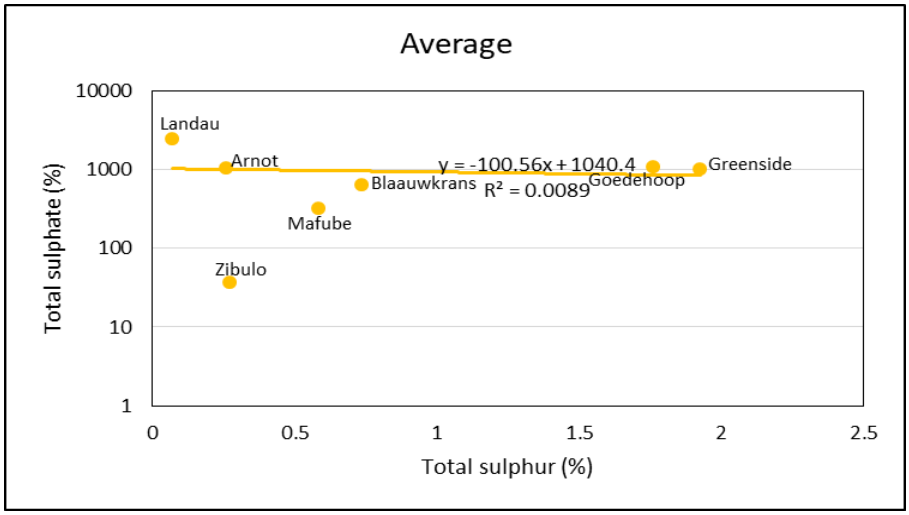

Figure 4.55: Total sulphur plotted against total sulphate using average values for all the study sites.

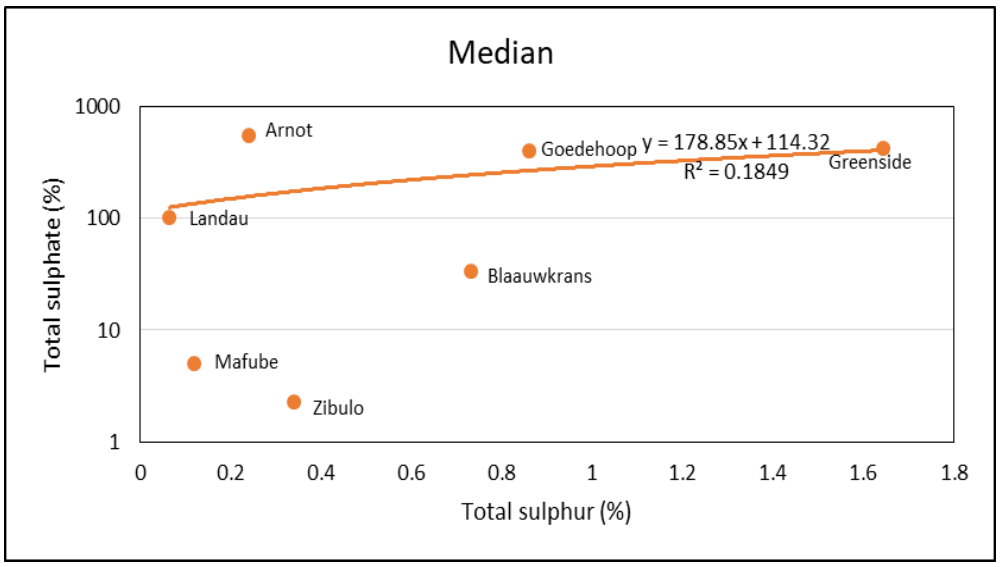

Figure 4.56: Total sulphur plotted against total sulphate using median values for all the study sites.

The NNP versus sulphate average and median graphs both show that Greenside, Goedehoop and Blaauwkrans have NNP values indicating acid generation and high sulphate concentrations (refer to Figure 4.57 and Figure 4.58). While Mafube, Zibulo, Arnot and Landau had low NNP values indicating low to medium probability of acid generation; however, the former two sites had low sulphate contents whilst the latter two sites had high sulphate concentrations.

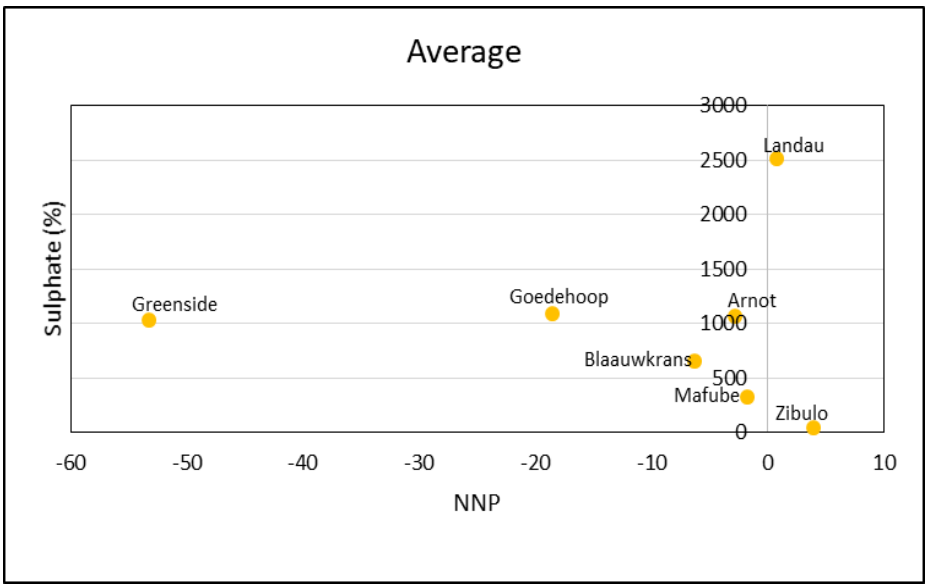

Figure 4.57: Net-Neutralising Potential plotted against total sulphate using average values for all the study sites.

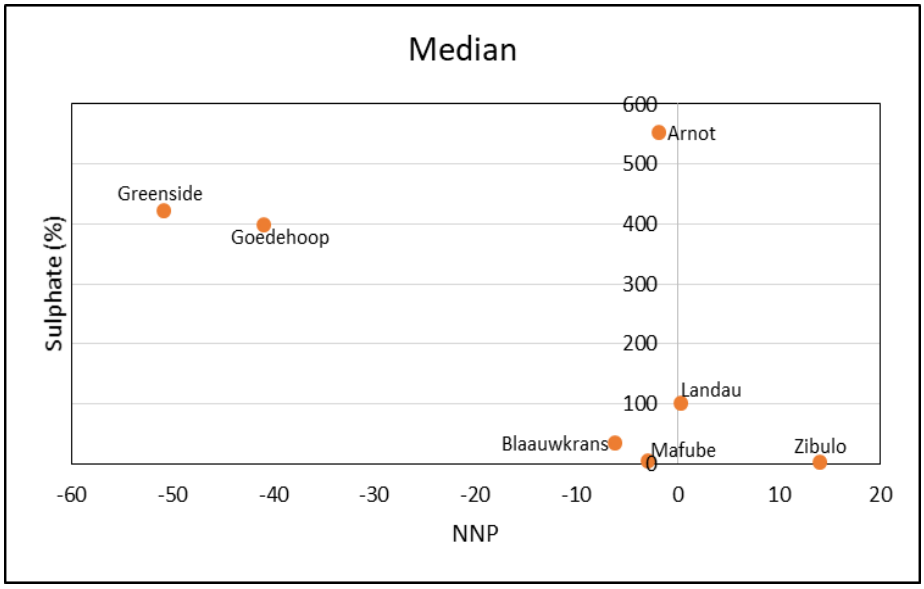

Figure 4.58: Net-Neutralising Potential plotted against total sulphate using median values for all the study sites.

The NPR versus groundwater pH graph (refer to Figure 4.59) below shows that Landau and Zibulo plotted in the NPR>2 zone, this indicates non-acid generating potential. Landau had an NPR closer to 2 with a pH of 5.5 on the acid end of the pH spectrum; whilst Zibulo had an NPR value closer 7 and pH of 7.38 on the neutral side of the pH spectrum. The graph shows that Arnot and Goedehoop had values in the 1<NPR<2 range (refer to Figure 4.60), which suggests possibility of acid generating if the sulphide bearing material is preferentially exposed; also considered inconclusive and therefore require more static and kinetic tests to be done to verify the results.

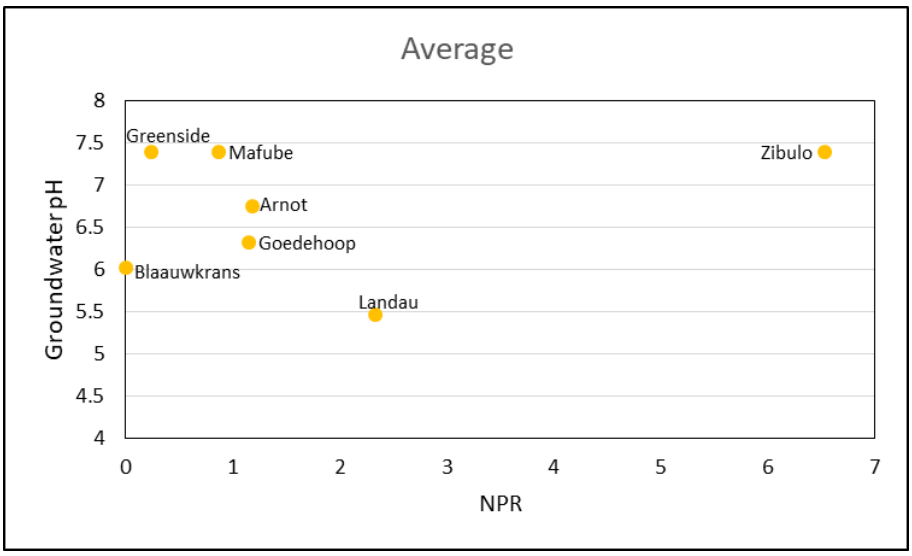

Figure 4.59: Neutralising Potential Ratio plotted against pH using average values for all the study sites.

Arnot and Goedehoop sites have pH values in the 6<pH<7 range, which are near-neutral to neutral. Greenside, Blaauwkrans and Mafube plot in the NPR<1 zone which indicates that the material from these sites was potentially acid generating. Furthermore, the pH values of these sites were in the near neutral range.

Zibulo plotted in the NPR>2 zone with a neutral pH; whilst Landau plotted in the 1<NPR<2 zone with a near neutral pH. The rest of the study sites plotted in the NPR<1 zone with near neutral pH values ranging between 6.4 to 7.5.

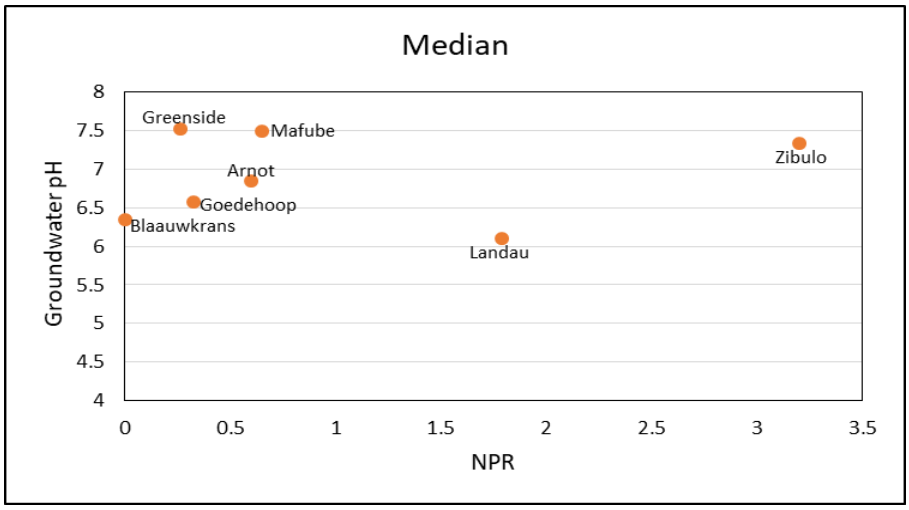

Figure 4.60: Neutralising Potential Ratio plotted against pH using median values for all the study sites.

The pH versus Sulphide-S graph below (refer to Figure 4.61) shows that Goedehoop had a high sulphide sulphur value, while Blaauwkrans and Mafube had sulphide sulphur values closer to

0.33%. Zibulo and Arnot had sulphide sulphur values less than 0.2%. Sites with high sulphide sulphur contents had low pH values except for Mafube, which had a pH of 7.39.

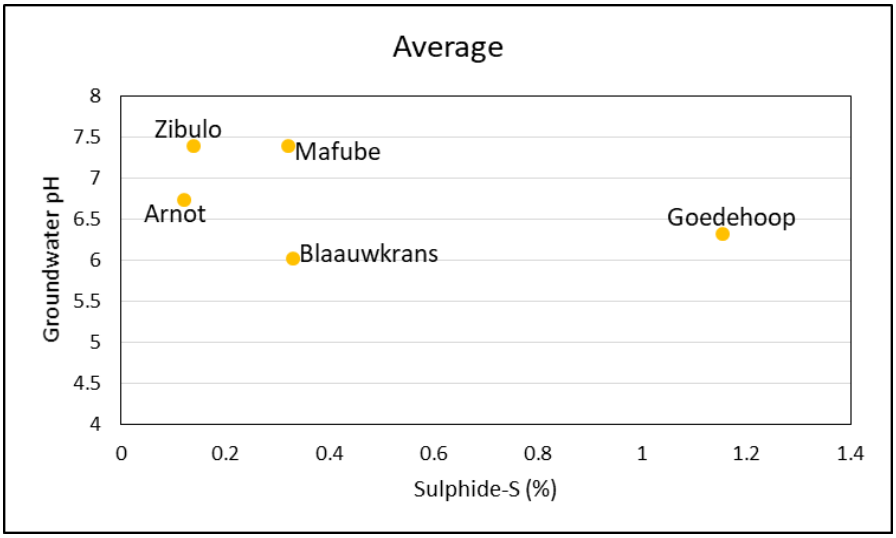

Figure 4.61: Groundwater pH plotted against sulphide sulphur using average values for selected study sites.

Sites with low sulphide sulphur values had near-neutral to neutral pH values. Landau and Greenside were not included in Figure 4.61 and Figure 4.62 because the available ABA data for these sites did not have sulphide sulphur results.

The median values graph (refer to Figure 4.62) show that Goedehoop and Blaauwkrans had high sulphide sulphur, while the rest of the sites had low sulphide sulphur values below 0.15%. Furthermore, sites with high sulphide sulphur values had low pH values in the acidic spectrum. Sites with low sulphide sulphur values had near-neutral to neutral pH values.

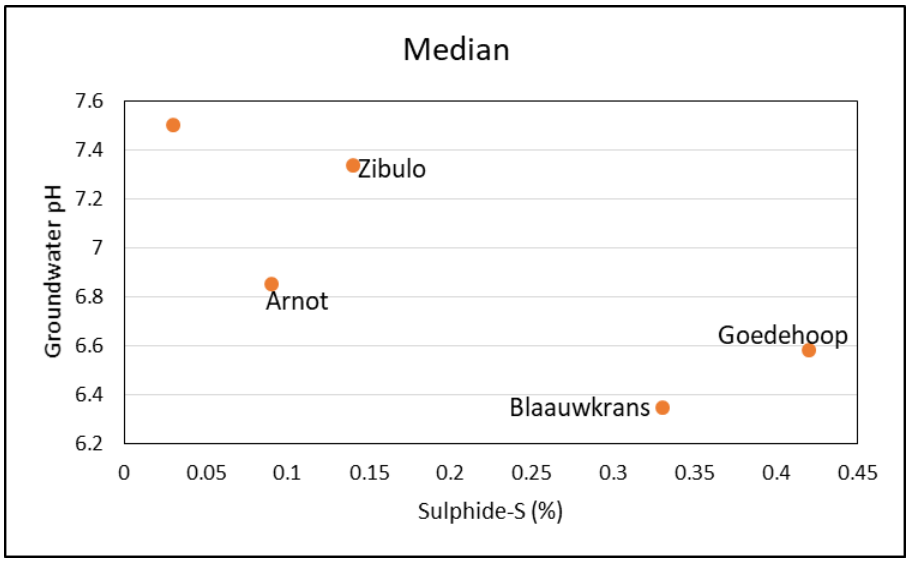

Figure 4.62: Groundwater pH plotted against sulphide sulphur using median values for selected study sites.

The groundwater pH versus total sulphur graph below shows that Goedehoop and Greenside had high total sulphur values (refer to Figure 4.63). The rest of the samples had low total sulphur values with Landau having the lowest value of 0.07%. All sites had pH values in the near-neutral to neutral range, except for Landau and Blaauwkrans; these two had low pH values in the acidic range.

Figure 4.64 below shows that Greenside, Goedehoop and Blaauwkrans had high total sulphur values with Greenside having the highest value of 1.645%. The rest of the sites had total sulphur values below 0.4% with Landau having the lowest value of 0.065%. Landau and Blaauwkrans had lower pH values than the rest of the sites.

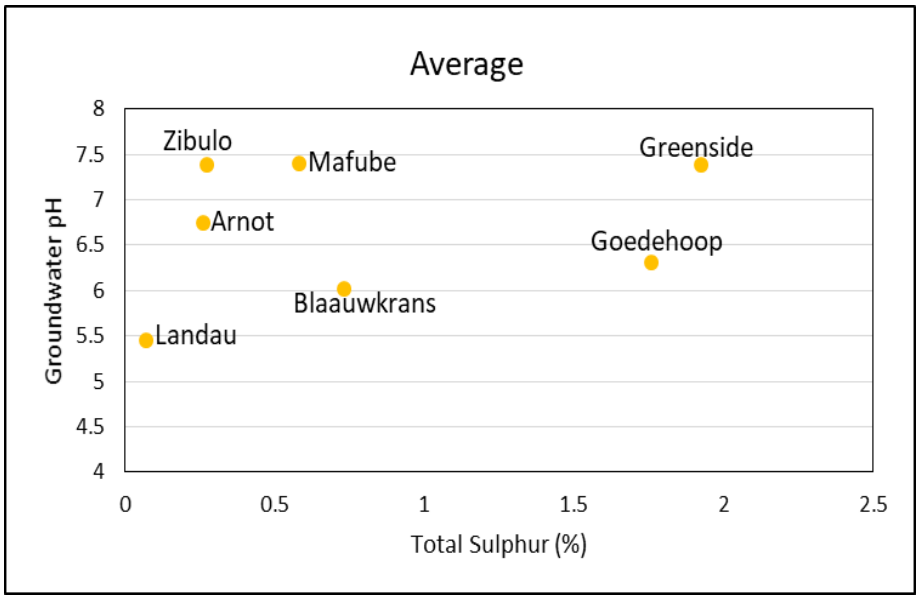

Figure 4.63: Groundwater pH plotted against total sulphur using average values for all study sites.

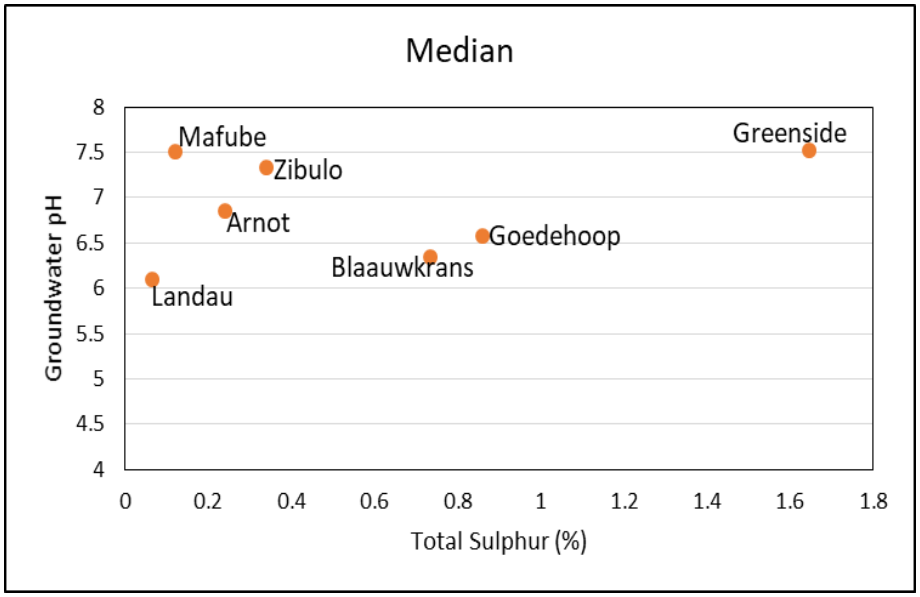

Figure 4.64: Groundwater pH plotted against total sulphur using average values for all study sites.

The above graphs show that material from all sites had the potential to generate acid and these sites tend to have near-neutral to neutral groundwater pH values. Sulphide sulphur would have to be used for further correlations between ABA and groundwater chemistry because a high potential of acid generation would require that a higher amount of sulphide sulphur is present. The pH and groundwater correlations could be due to enough time not having passed for the groundwater acidity to increase, or the presence of a neutralising agent that is not yet fully consumed and therefore balances the pH of the groundwater. Other factors that could contribute to the high pH values are influence of atmospheric carbon dioxide, lithological and aquifer composition. The ABA method conservatively over-predicts the acid generation when only considering total sulphur instead of the acid generating sulphide sulphur contents in the the samples. The ABA and groundwater chemistry correlations showed that sites with total sulphur subsequently had high total sulphate. The correlations also showed that sites with negative NNP values and NPR<1 had high sulphate concentrations and near-neutral to neutral pH values. Furthermore, study sites with high sulphide sulphur values had lower pH values compared to the other sites. From these correlations, it can be concluded that the ABA predictions worked.

Summary of Statistical analysis

- The 500 mg/l sulphate concentration limit from the SANS241:2015 domestic water standards was used in combination with the upper quartile of the boxes to examine whether or not the groundwater from the study sites meets the SANS set limit for sulphate concentration. However, it would have been ideal to use the Water Use Licences for each study site but these were not available to the student at the time of writing of this report.
- Arnot colliery: increasing trend of sulphate concentrations and these concentrations did not meet the SANS set limit.
- Goedehoop North operation: increasing trend of sulphate concentrations and these concentrations did not meet the SANS set limit.
- Goedehoop South operation: increasing trend of sulphate concentrations and these concentrations did not meet the SANS set limit.
- Mafube colliery: increasing trend of sulphate concentrations and these concentrations met the SANS set limit
- Zibulo colliery: increasing trend of sulphate concentrations and these concentrations met the SANS set limit.
- Landau colliery: increasing trend of sulphate concentrations and these concentrations met the SANS set limit.

- Blaauwkrans discard dump: decreasing trend of sulphate concentrations and these concentrations met the SANS set limit.
- Greenside colliery: decreasing trend of sulphate concentrations and these concentrations did not meet the SANS set limit.
- Greenside discard dump: trend is inconclusive and the sulphate concentrations did not meet the SANS limit.

4.3.3 Geochemical modelling

Mineral saturation indices (SI) of the mineral phases for the water quality data were calculated using PhreeqC and the Wateq4f.dat database. A positive saturation index indicates that the solution is oversaturated with respect to the particular mineral phase; while a negative saturation index indicates an under-saturation of the particular mineral phase in the solution. The geochemical speciation of the water quality data was used to understand which minerals are likely to precipitate from the different solutions of the different study sites.

The purpose of this section is to understand which minerals are likely to precipitate from the study sites because these minerals deplete certain elements and metals from the groundwater and therefore improve the water quality.

4.3.3.1 Arnot Colliery

Geochemical speciation of this colliery was done for four boreholes that show recent monitoring results. The results indicate that anorthite, chalcedony and cristabolite were only oversaturated in borehole BF2E1; whilst aragonite and magnesite were oversaturated in BF2P1. The results further show that barite, goethite, hematite and magnetite were oversaturated in borehole BF1P1 only. Moreover, calcite, dolomite, quartz and rhodochrosite were oversaturated in boreholes BF2P1, BF3E1 and BF3P1.

This study site is the only one with boreholes sampled for ABA testing being the same as the ones recently sampled for water quality. Therefore, equilibrium simulations could only be done for this study site. Furthermore, the database was changed from Wateq4f.dat to minteq.dat to accommodate microcline. Pure rainwater was equilibrated to the minerals (as determined by XRD) and compared against the observed pH and SO_4 concentrations. Mineral phases that were used in the input files are shown in Table 4.8, including the saturation indices and amount of moles that were used for each mineral. In addition, cristobalite, dolomite, calcite, magnesite and rhodochrosite were allowed to precipitate in the PhreeqC input files since these mineral phases have positive saturation indices from the initial simulations and are likely to precipitate in secondary mineral phases.

Table 4.8: The mineral phase data as added to the PhreeqC input files that was used for equilibrium simulations

	BF2E1		BF2P1		BF3P1	
Name	Sat. index	Amount (moles)	Sat.index	Amount (moles)	Sat.index	Amount (moles)
Albite	0	0	0	0	0	0
Calcite	0	0	0	0	0.12	0
Cristobalite	0.08	0	-	-	-	-
Dolomite	0	0.048	1.16	0.035	0.58	0.193
Kaolinite	0	9.083	0	14.351	0	14.276
Microcline	0	0.565	0	0.128	0	0.96
Muscovite	0	0.221	0	0.646	0	1.125
Pyrite	0	0	0	0	0	0
Quartz	0	91.118	0	66.259	0	55.812
Siderite	0	0.217	0	0.979	0	2.664
Sulfur	0	0.379	0	0.227	0	0.581
Magnesite	-	-	0.2	0	-	-
Rhodochrosite	-	-	0.34	0	0	0.581

The equilibrium simulation results are as follows:

- BF2E1: Cristobalite was the only mineral with a positive saturation index from the initial simulation, suggesting that it is likely to form as a secondary mineral phase. Therefore, it was equilibrated with the mineral phases (as determined via XRD analysis). The results showed that the number of moles and thus the amount that will precipitate could not be calculated; because another mineral precipitated first and depleted ions needed for cristobalite to precipitate. Dolomite, kaolinite, muscovite, pyrite, quartz and siderite were the only minerals for which final moles and amount that will precipitate could be calculated. However, not all of these minerals can form as secondary minerals. Dolomite and siderite are the only minerals that will likely precipitate from solution, 3.46 g for the former and 6.303 g for the latter (refer to Table 4.9). The pH of the initial solution was 2.7, whilst it increased to 5.67 for the final equilibrium solution and this still indicates that the solution remained slightly acidic. The distribution of species show that sulphate concentration of the initial solution was 6.46E+02 mg/L, and the final equilibrium solution had a sulphate concentration of 3.36E+03 mg/L, which means the output increased.

Table 4.9: The results of equilibrium simulation for borehole BF2E1

Mineral Phase	SI	Initial moles	Final moles	Molar Mass	Amount of Precipitate (g)
Albite	-6.12	0	0	262.219	0
Calcite	-0.04	0	0	100.086	0
Cristobalite	-0.42	0	0	60.083	0
Dolomite	0	4.80E-02	2.79E-02	124.391	3.46428935
Kaolinite	0	9.08E+00	8.63E+00	258.157	2228.927538
Microcline	-1.37	5.65E-01	0	278.327	0
Muscovite	0	2.21E-01	7.09E-01	398.303	282.2773361
Pyrite	0	0.00E+00	1.62E-01	119.965	19.482316
Quartz	0	9.11E+01	9.23E+01	60.083	5542.65675
Siderite	0	2.17E-01	5.44E-02	115.853	6.30356173
Sulphur	-5.88	3.79E-01	0.00E+00	32.06	0
	Distribution of species				
	Initial solution		Final equilibrated solution		
pH		2.7	5.687		
SO4-2		6.46E+02 mg/L	3.36E+03 mg/L		

- BF2P1: Initial simulation results showed that aragonite, dolomite, magnesite and rhodochrosite were the minerals with positive saturation indices and therefore were equilibrated with XRD mineral phases. Aragonite, magnesite and rhodochrosite indicated zero final moles and therefore, the amounts that will precipitate could not be calculated because other minerals precipitated first and depleted ions needed for these minerals to precipitate. Table 4.10 shows that dolomite (8.35 g) and siderite (102.101 g) are the only minerals that will precipitate from solution. Furthermore, the sulphate concentration of the initial solution was 1.83E+03 mg/L, and 2.83+03 mg/L for the final equilibrated solution. The pH of the initial solution was 7.2 and decreased to 5.6 in the final equilibrated solution. This shows that the sulphate output increased and pH decreased, indicating that the solution became slightly acidic.

Table 4.10: The results of equilibrium simulation for borehole BF2P1

Mineral Phase	SI	Initial moles	Final moles	Molar mass	Amount of Precipitate (g)
Albite	-6.16	0	0	262.219	0
Aragonite	-	0	0	100.086	0
Dolomite	-	3.50E-02	3.50E-02	124.391	4.353685
Kaolinite	0	1.44E+01	1.44E+01	258.157	3704.55295
Magnesite	-	0	0	84.313	0
Microcline	-1.37	1.28E-01	0	278.327	0
Muscovite	0	6.46E-01	6.91E-01	398.303	275.0680518
Pyrite	0	0.00E+00	9.73E-02	119.965	11.67139485
Quartz	0	6.63E+01	6.65E+01	60.083	3996.12033
Rhodochrosite	-	0.00E+00	0.00E+00	114.946	0
Siderite	0	9.79E-01	8.81E-01	115.853	102.1012489
Sulphur	-6	2.27E-01	0.00E+00	32.06	0

Distribution of species		
	Initial solution	Final equilibrated solution
pH	7.2	5.63E+00
SO4-2	1.83E+03 mg/L	2.83E+03 mg/L

- BF3P1: Initial simulation results showed that calcite, dolomite and rhodochrosite were the mineral phases with positive indices that are likely to precipitate in secondary environments. The amount of calcite that will precipitate could not be calculated because there were no sufficient ions for this mineral to precipitate from solution (refer to Table 4.11). Dolomite (24 g) and siderite (279.67 g) are the only minerals that will precipitate from solution. Moreover, the sulphate concentration of the initial solution was 1.84E+03 mg/L and increased to 6.18E+03 mg/L in the final equilibrated solution. In comparison, the pH of the initial solution was 6.9 and decreased to 5.3 in the final equilibrated solution. This indicates that the sulphate output increased resulting in a decrease in pH due to released acidity.

Table 4.11: The results of equilibrium simulation for borehole BF3P1

Mineral Phase	SI	Initial moles	Final moles	Molar mass (g/mol)	Amount of Precipitate (g)
Albite	-2.5	0	0	262.219	0
Calcite	-	0	0	100.086	0
Dolomite	-	1.93E-01	1.93E-01	124.391	24.007463
Kaolinite	0	1.43E+01	1.33E+01	258.157	3438.65124
Microcline	-1.36	9.60E-01	0	278.327	0
Muscovite	0	1.13E+00	2.09E+00	398.303	830.461755
Pyrite	0	0.00E+00	0.00E+00	119.965	0
Quartz	0	5.58E+01	5.77E+01	60.083	3468.59159
Rhodochrosite	-	0.00E+00	0.00E+00	114.946	0
Siderite	0	2.66E+00	2.41E+00	115.853	279.669142
Sulphur	-5.68	5.81E-01	0.00E+00	32.06	0
Distribution of species					
Initial solution		**Final equilibrated solution**			
pH	6.9	5.318			
S04-2	1.84E+03 mg/L	6.18E+03 mg/L			

4.3.3.2 Goedehoop Colliery

a. Goedehoop North Operation

The March 2015 monitoring water quality data for this site was used for geochemical speciation and the results indicated that alunite is oversaturated in all boreholes. Basaluminite was oversaturated in other boreholes except in boreholes S3, S4, S7 and S10, whilst boehmite and diaspore were oversaturated in all the boreholes except for S4. In addition, fluorapatite was undersaturated in boreholes S4, S5, S6, S7, S9, S10 and S22 and oversaturated in the rest of the boreholes. Gibbsite was oversaturated in all the boreholes except S4, whilst goethite, hematite and magnetite were oversaturated in the all the boreholes except in S2 and S4. The results further showed that maghemite was oversaturated in boreholes S3, S8, S9 and S22; whilst strengite was oversaturated in boreholes S8, S5, S9 and S22. Rhodochrosite was oversaturated only in borehole S8.

b. Goedehoop South Operation

The April 2015 monitoring groundwater data was used for geochemical speciation and the results showed that the solutions of many boreholes are oversaturated in most of the minerals. For instance, alunite was oversaturated in boreholes WG10, WG12, WG13 and WH02; whilst aragonite was oversaturated in BLK02, RDW7, RDW8, RWD20, WG14 and WG16. Basaluminite was oversaturated in WH02; diaspore and FCO_3Apatite were oversaturated in all boreholes except WH04; fluorapatite and gibbsite were oversaturated in all boreholes except in WH02 and WH04 for the former, and RWD20 and WHO4 for the latter. Mineral phases such as, alunite, calcite, dolomite, goethite, hematite, hydroxyapatite, maghemite, magnesite, magnetite and strengite were oversaturated in many of the boreholes, whilst rhodochrosite was oversaturated only in RWD Vlaklaagte.

4.3.3.3 Mafube Colliery

The recent (2015) groundwater quality data for this study site was used for geochemical speciation and the results have showed that aragonite, calcite, dolomite (including dolomite(d)) were oversaturated in BH10468-1 and Dairyfarm 1; whilst boehmite, diaspore, FCO_3Apatite, gibbsite, goethite and magnetite were oversaturated in all boreholes except in BH10468-2. Furthermore, siderite and vivianite were oversaturated in AGM-B8; whilst alunite was oversaturated in AGM-B8 and BH10468-2; basaluminite in AGM-B7, AGM-B8 and AGM-B13; fluorapatite in BH10468-1, Dairyfarm 1, potato farmhouse and potato store. The results also showed that hydroxyapatite was oversaturated in BH10468-1, Dairyfarm 1 and Potato farmhouse; jurbanite in BH10468-2; magnesite in Dairyfarm 1; and rhodochrosite in BH10468-1. Hematite was oversaturated in all boreholes; whilst strengite was oversaturated in AGM-B3, AGM-B7, AGM-B8 and Potato store.

4.3.3.4 Zibulo Colliery

The groundwater quality data for June 2019 for this study site was used for geochemical speciation and the results showed that aragonite, calcite, dolomite (including dolomite(d)) and FCO_3Apatite were oversaturated in all boreholes except in BSW06. In addition, diaspore, goethite, magnetite and maghemite were oversaturated in all boreholes; whilst jarosite-Na and magnesite were oversaturated in BSW03. The results also indicated that jurbanite and rhodochrosite were oversaturated in BSWO6 for the former and BSW07 for the latter.

4.3.3.5 SACE Complex

a. Landau Colliery

The groundwater quality data for November 2015 was used for geochemical speciation and the results indicated that boehmite, gibbsite and diaspore were oversaturated in all boreholes. Moreover, alunite was oversaturated in NAV2S9 and NAV5S7; FCO_3Apatite in NAV2S3 and NAV5S7; hydroxyapatite in NAV2S3. However, goethite, hematite, maghemite and magnetite were oversaturated in all boreholes except in NAV2S3.

b. Blaauwkrans Discard Facility

The March 2017 monitoring water quality data for this site was used for geochemical speciation using PhreeqC. The results showed that boehmite, diaspore and gibbsite were oversaturated in both the boreholes that were sampled during that time, whilst goethite, maghemite and magnetite were oversaturated only in borehole NAW007.

c. Greenside Colliery

The 2018 monitoring groundwater quality data for this study site was employed for geochemical speciation. Results indicated that alunite, diaspore and gibbsite were oversaturated only in WP012B. Other minerals, such as aragonite, calcite, dolomite, FCO_3Apatite, fluorapatite, magnesite and rhodochrosite were oversaturated in many of the boreholes. However, fluorite is oversaturated in POT05; goethite, maghemite and magnetite in POT05, WP102 and WP113; hematite in WP102 and WP113; huntite in WP129; hdroxapatite in WP116 and WP129; and rhodochrosite(d) in NDP, WP112 and WP116.

d. Greenside Discard Facility

Geochemical speciation of the groundwater quality data for the year 2012 indicated that goethite, magnetite and hematite are oversaturated in all boreholes. Additionally, maghemite and rhodochrosite were oversaturated in all boreholes except in BH3 and GUW07 for the former; and BH3, G1082, GUW02 and GUW07 for the latter.

Summary of Geochemical Modelling

Not all minerals with positive saturation indices will precipitate as secondary minerals due to various thermodynamic factors that make the environment to be conducive enough for secondary mineral precipitation. Therefore, based on the geochemical speciation results presented above, the following minerals are likely to precipitate as secondary mineral phases:

- Cristobalite
- Aragonite
- Dolomite
- Rhodochrosite
- Calcite
- Barite
- Goethite
- Hematite
- Maghemite
- Alunite
- Strengite
- Artinite
- Fluorite

- Huntite
- Jubarnite
- Siderite
- Vivianite
- Jarosite
- Chalcedony

The results showed that the solutions of the study sites are oversaturated in carbonate minerals and hydrated minerals of many metals. These hydrated metals and carbonates that precipitate out Ba, Mn, Fe, Mg, P and SO_4 from solution as well as other trace metals attached to their structures. The majority of these metals are iron-hydroxides, causing the yellow-reddish colouring of the soil in areas with AMD contaminated water. However, although these minerals are likely to precipitate as secondary minerals, goethite, jarosite, siderite, hematite and vivianite are the most common minerals that form in AMD systems (Jönsson *et al*., 2006; Dold, 2014). It is important to note that not all of these minerals will precipitate as precipitation of secondary minerals is dependent on pH-Eh conditions, presence of metal ions and other complexing ligands.

4.4 SULPHATE CONCENTRATION VERSUS SULPHUR CONTENT

The groundwater sulphate concentration of all study sites and the sulphur content of material samples from the SACE Complex were used to create concentrations maps to illustrate how these change spatially across the study area.

4.4.1 Sulphur Content

The sulphur contents of the coal seams and host rocks are expressed in percentage. The sulphur content map shows that Landau (north of the map) has a small patchy zone of high sulphur content with small areas of low sulphur content (refer to Figure 4.65).

Additionally, the map indicates that Blaauwkrans lies south-west of Landau in the area with many hot spots of elevated sulphur concentration surrounded by a large area of low sulphur concentrations. Greenside colliery and discard dump are in the south-east corner of the map showing a big zone of high sulphur content with small zones of low sulphur concentrations. These two study sites collectively have a relatively large hotspot of high sulphur content in comparison to the other study sites in the map. The sulphur content decreases away from the mining areas and locality of the discard dumps to lower concentrations on the outskirts.

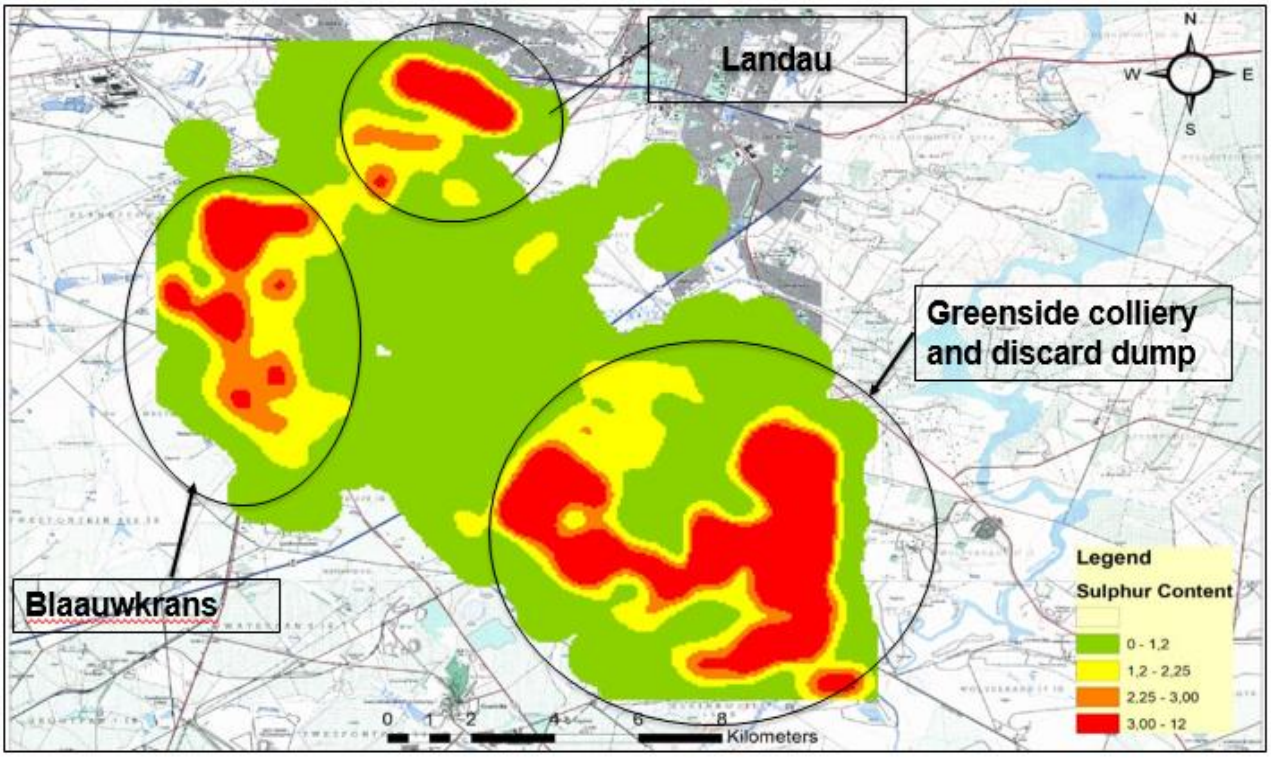

Figure 4.65: Map showing how the sulphur content of the SACE Complex changes spatially.

4.4.2 Sulphate Concentration

The sulphate concentrations of all the study sites are expressed in mg/L. The sulphate concentration map shows eight study sites, with the SACE Complex on the north-west corner (refer to Figure 4.66). The map shows Landau as an area with the lowest sulphate concentration; whilst Blaauwkrans, which is located sharp west side of the map, has a medium sized hotspot of high sulphate concentrations. In addition, Greenside colliery and discard dump together show a bigger zone of high sulphate concentrations compared to Blaauwkrans.

The sulphate concentration Figure 4.66 also shows that Zibulo, which appears on the south-west corner, a small zone of medium sulphate concentrations. Goedehoop colliery appears south of Middelburg and is subdivided into south and north operations. These operations both have big hotspot areas of high sulphate concentrations with the north operation having a bigger hotspot area.

The map shows that Arnot which is located near N11 has a small red zone of higher sulphate concentration, and big areas of low sulphate concentration. Additionally, Mafube, which is located near R104, has small area of medium sulphate concentrations.

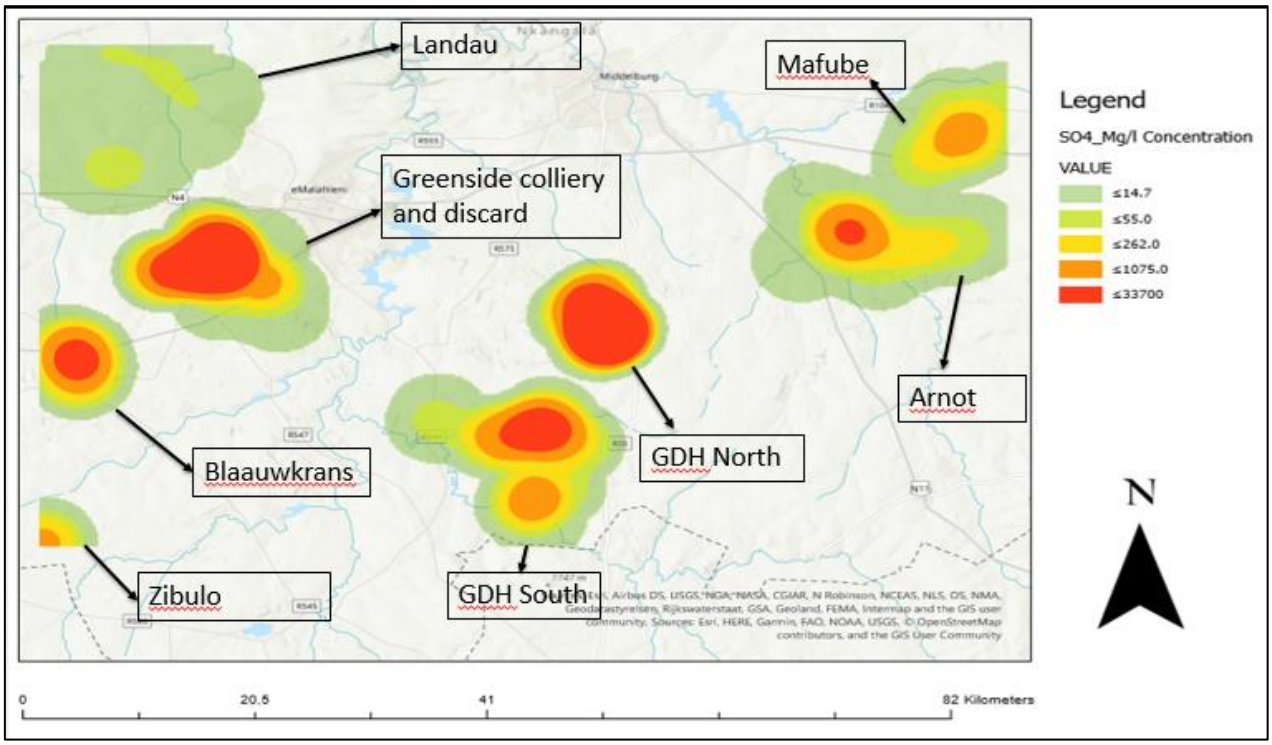

Figure 4.66: Map showing how the sulphate concentrations of all study sites change with location.

Comparison of SO_4 and S for the SACE Complex

The comparison between SO_4 and sulphur content maps shows that Landau has many small hotspots of high sulphur content with large area of low sulphur content but has low sulphate concentration. This could suggest the presence of neutralizing agent acting as a buffer to the generated acid or that the sulphide-bearing material is not exposed enough to oxidize and produce SO_4 and acidity. Additionally, Blaauwkrans has high sulphur content and sulphate concentration; whilst Greenside colliery and discard dump show big hotspots for both sulphur content and sulphate concentration indicating higher concentrations. Figure 4.67 shows the relationship between the groundwater sulphate concentrations and coal seam sulphur contents of the study sites from the SACE Complex. The graph shows a slightly increasing trend line with r^2 of 0.06%, which is a lowest correlation between the two variables. However, slightly increasing trend indicates that sites that have high sulphur contents in the coal seams are likely to have high sulphate concentrations in the groundwater once exposed to oxygen. It should be noted that the sulphide sulphur is the major contributor to AMD formation or the amount of sulphate that will be generated.

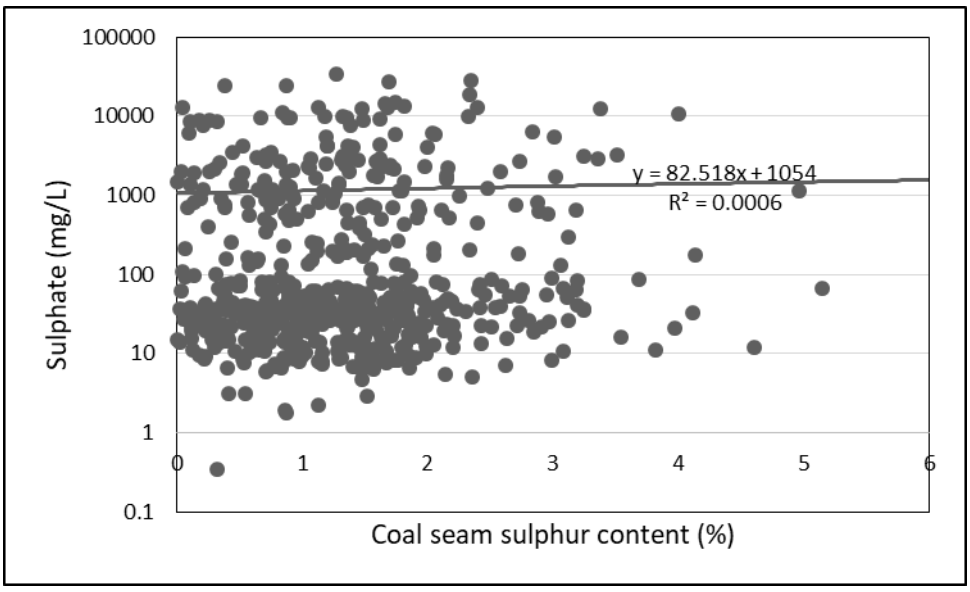

Figure 4.67: Graph showing the relationship between sulphate concentrations and coal seam sulphur contents of the sites from the SACE Complex.

4.5 DISCUSSION

This section links all the results as described above in order to have a better understanding of the groundwater quality and acid generating potential of the study sites. This section is also instrumental to show that the aims and objectives as stipulated in Chapter 1 have been achieved and answered.

The ABA results showed that most of the samples from the Goedehoop colliery are potentially acid generating or potentially acid generating if preferentially exposed. The groundwater quality data indicate that the groundwater has sulphate and bicarbonate as dominant anions. The presence of the bicarbonate means that although there might be a neutralising agent in the system, it is not enough to neutralise the acidity in the water completely. Additionally, the potentially acid generating nature of the majority of samples from the Goedehoop colliery is reflected in the sulphate concentration map (refer to Figure 4.66) wherein it can be seen that the groundwater from both of the Goedehoop North and South operations is sulphate contaminated (also see Piper and expanded Durov diagram explanations).

Moreover, the rock samples from the Arnot colliery showed that one of these samples is potentially acid generating whilst the others are non-acid generating as well as possibly acid generating if preferentially exposed. The groundwater quality data shows that groundwater from this study site has sulphate and bicarbonate as dominant anions. Few of the samples are potentially acid generating and this is reflected in the sulphate concentrations. Arnot has a small zone of high sulphate concentration with large zones of low to medium sulphate concentrations.

Few of the samples collected from Mafube are potentially acid generating, whilst the majority are possibly acid generating if preferentially exposed. The groundwater chemistry data shows that the water from this study site has sulphate and bicarbonate as dominant anions. The acid generating potential of the rocks from this study site is reflected in the groundwater quality data. It can be seen from the sulphate map that this study site has high-medium sulphate concentration in the groundwater with larger zones of low and low-medium concentrations.

Zibulo ABA results indicated that one sample is potentially acid generating whilst others are non-acid generating as well as possibly acid generating if preferentially exposed. The groundwater quality data for this study site has shown that all samples have bicarbonate as a dominant anion with exception of borehole BSW04, which has sulphate as a dominant anion. This could be due to the limestone observed in the borehole logs providing a neutralising agent (refer to Section 2.1.1.1.4). This study site is similar to Mafube, wherein the small percentage of potentially acid generating samples is responsible for the high-medium sulphate concentrations as seen in Figure 4.66.

The Blaauwkrans discard dump sample was classified as potentially acid generating and the groundwater quality data indicated that groundwater from this study site is sulphate contaminated, which supports the ABA predictions.

Moreover, the Greenside discard dump samples showed a high probability of acid generation; and the groundwater classification indicated that calcium is the dominant cation in the groundwater, with sulphate and bicarbonate as dominant anions. The material discarded at this facility is from the nearby Greenside colliery. Thus these two sites collectively show a large red zone of high sulphate output and sulphur contents as seen in Figure 4.65 and Figure 4.66.

Landau samples were analysed to be possibly acid generating if preferentially exposed, except for one sample that is non–acid generating. Groundwater chemistry data showed that sulphate and bicarbonate are dominant anions in the groundwater at this study site. Based on the sulphate concentration map (refer to Figure 4.66) Landau is the site with the lowest sulphate concentrations. Therefore, the groundwater quality data support the ABA predictions.

It is essential that the presented results provide answers to the objectives and meet the aims of the study, whether positive or negative. One of the objectives of this study (see Chapter 1) was to determine how “right or wrong” the ABA predictions were by comparing the ABA data to the groundwater chemistry data. The presented results showed that the groundwater quality data support the ABA data. Therefore, the ABA results were able to predict the range of sulphate concentrations. Study sites with the majority of samples being potentially acid generating have high sulphate outputs, and this indicates that the ABA predictions worked although there are discrepancies in the data, which may need more kinetic and static tests to verify the results.

Comparison of the sulphate output of the different study sites was one of the objectives of this paper. In section 4.3.2.6, it was pointed out that Arnot colliery, Goedehoop operations, Greenside colliery and discard dump are the study sites with the highest sulphate outputs compared to Blaauwkrans, Landau, Mafube and Zibulo (refer to Figure 4.54). Therefore, these study sites are problematic in terms of the quantities of sulphate that they generate in a year considering that this study also involved the investigation of sulphate output with time. The results of this time trend showed that Arnot, Goedehoop operations, Mafube, Zibulo, Landau have sulphate concentrations that increased with time; whilst Blaauwkrans and Greenside colliery sulphate concentrations decreased with time.

The coal seam sulphur content map of the SACE Complex shows that the Greenside colliery and discard dump collectively have a large zone of high sulphur content. Blaauwkrans has a patchy but relatively bigger zone of high sulphur content, which could be due to sample distribution in comparison to Landau. ABA results showed that Landau samples were non-acid generating; whilst the majority of Blaauwkrans and Greenside samples if not all were potentially acid generating. The sulphate concentration map showed that Greenside colliery and discard dump collectively still have a large zone of high sulphate concentration. The same accounts for the Blaauwkrans discard dump. However, Landau does not show a zone of high sulphate concentration. It can be pointed out that areas, which have high sulphur contents subsequently have high sulphate outputs in the groundwater. Therefore, the ABA, sulphur contents of the seams are supportive of the groundwater chemistry data.

NNP results from McCarthy & Pretorious (2009) showed that the coal seams and host rocks of the Witbank coalfield are highly acid generating and therefore need additional calcium carbonate for neutralisation. These results showed that seam 5 which is the source of bright coal rich in sulphur has the highest acid generating potential followed by seam 4, whilst Digby Wells & Associates (2011) showed that seam 2 and its host rock have a possible low acid generating potential. Seam 4 is exploited in all collieries except for Landau, whilst Goedehoop and Zibulo are the only two collieries wherein seam 5 is exploited.

The type of mining plays a large role in the sulphate output of a study site due to different recharge rates and residence time of the water. According to Vermuelen & Usher (2006b), the sulphate generation rate for underground mines is in the range of 0.4-2.7 kg/ha daily and 7 kg/ha daily for opencast mines. These rates depend on the availability of oxygen and residence time of the water. About three of the collieries, Zibulo, Arnot and Goedehoop employ both underground and opencast mining methods. These collieries have high sulphate concentration in exception of Zibulo. Moreover, the Mafube colliery employs the opencast method of mining and has a low sulphate

output; whilst the Greenside colliery uses the underground bord-and-pillar method and has a high sulphate concentration. Therefore, in this case the sulphate output in the groundwater is largely contributed by the recharge of the mining site, residence time of the water, presence of a neutralising agent and the sulphur content of the coal seams and host rocks. The discard dumps have high sulphate outputs and can be related to the material dumped at these facilities.

The observed sulphate concentrations are influenced by the presence of calcareous carbonates. This mineral group provides a neutralizing agent and results in a low sulphate output. However, many of the study sites have high sulphate concentrations, although the background geology of the coalfield has indicated that carbonates are present in this area in the form of limestone.

Statistical analysis of sulphate concentration showed that the majority of study sites have an increasing trend of sulphate output with time and the sulphate concentrations do not meet the SANS set limit. Moreover, a study by McCarthy & Pretorious (2009) showed that sulphate concentration of the Witbank and Middelburg dams increased with time and exceeded the recommended concentration for human consumption. Surface-groundwater interactions play a large role in movement of contamination between these two water resources (Sophocleous, 2002). This relationship is largely responsible for the presence of sulphate in the Witbank and Middelburg dams and thus a reflection of the groundwater.

4.6 SUMMARY

The groundwater data showed that most of the study sites have medium to high sulphate concentrations. The sulphur content of the rocks and coal seams is the major contributor to the high sulphate concentration of the groundwater. The results indicated that discard dumps have high sulphate outputs because of the type of the material dumped at these facilities. The results review and discussion section pointed out that the groundwater quality data supports the ABA data. Therefore, the estimation of acid formation using the latter was accurate. Although the results have also showed that more tests should be conducted; the objectives (see Chapter 1) of this study were achieved.

CHAPTER 5:
CONCLUSIONS AND RECOMMENDATIONS

Conclusions

The Witbank coalfield is one of the largest coal deposits hosted in the Ecca Group sediments in South Africa and has produced tons of coal over the decades since mining began. However, coal mining showed to have detrimental impacts on the environment, in which surface, groundwater resources and soil are contaminated. Therefore, it is important to understand the acid generating potential of the coalfield.

It can be inferred from this research that study sites containing samples that were mostly classified as potentially acid generating, ultimately also had high sulphate outputs. The results also showed that Arnot, Goedehoop North and South operations, as well as the Greenside colliery and discard dump are problematic areas among all the study sites investigated, due to their high sulphate outputs. Most of the investigated study sites depicted increasing sulphate concentrations over time. The geochemical speciation results showed that carbonates and hydrated metal minerals are likely to precipitate from these study sites, however this precipitation will not take place in AMD contaminated environments with limited carbonate sources.

Furthermore, the study indicated that the groundwater of the investigated areas is vulnerable to AMD contamination. More research still needs to be conducted in terms of remediation and mitigation measures.

Recommendations

To better understand the implications of the presented results, future studies should consider:

- Testing of the sulphur content of the coal seams and host rocks of the whole coalfield and not just for selected collieries.
- More kinetic and static tests should be conducted to improve the accuracy of the ABA data.
- Modelling of the contamination plumes of all mines within the coalfield to see how far the plumes extend beyond the coalfield, catchment and province as a whole to better understand the impact AMD from this area on downstream water resources.
- Remediation is mostly done on surface resources and discard dumps. Closed, abandoned mines should also be taken into consideration

REFERENCES

Akcil, A. & Koldas, S., 2006. Acid Mine Drainage (AMD): causes, treatment and case studies. *Journal of Cleaner Production,* Volume 14, pp. 1139-1145.

Anderson, G., 2005. Thermodynamics of Natural Systems. 2nd ed. Cambridge, Cambridge University Press.

Banks, V. J., Palumbo-Roe, B., Davies, J., van Tonder, D., Fleming, C. & Chevrel, S., 2011. Conceptual models of Witbank coalfield, South Africa. *Earth Observation for Monitoring and Observing Environmental and Societal Impacts of Mineral Resources Exploration and Exploitation,* CEC FP7 Project EO-MINERS, Deliverable D3. 1-2, p. 107.

Basson, M. S. & Rossouw, J. D., 2003. *Olifants Water Management Area Overview of Water Resources Availability and Utilisation,* Report No H141404, [September 2003].

Bell, F. G., Bullock, S. E. T., Hälbich, T. F. J. & Lindsay, P., 2001. Environmental impacts associated with an abandoned mine in the Witbank Coalfield, South Africa. *International Journal of Coal Geology*, Volume 45, pp. 195-216.

Bell, F. G., Hälbich, T. F. J. & Bullock, S. E. T., 2001. The effects of acid mine drainage from an old mine in the Witbank Coalfield, South Africa. *Quarterly Journal of Engineering Geology and Hydrogeology*, Volume 35, No. 3, pp. 265-278. doi:10.1144/1470-9236/00121

Berner, R. A., 1984. Sedimentary pyrite formation: An Update*. *Geochimica et Cosmochimica Acta,* Volume 48, pp. 605-615.

Boshoff, E. & Steenekamp, G., 2015. *Groundwater Monitoring Report for Greenside Colliery: March 2015 to December 2015,* [December 2015].

Bosman, C., 2019. '*Monitoring for Water Governance'*, lecture notes distributed in GEOH6865 at the University of the Free State, Bloemfontein on 07 October 2019.

Brough, C. P., Warrender, R., Bowell, R. J., Barnes, A. & Parbhakar-Fox, A., 2013. The process mineralogy of mine wastes. *Minerals Engineering*, Volume 52, pp. 125-135.

Buzzi, D. C., Viegas, L. S., Rodrigues, M. A. S., Bernardes, A. M. & Tenório, J. A. S., 2013. Water recovery from acid mine drainage by electrodialysis. *Minerals Engineering*, Volume 40, pp. 82-89.

Bullock, S. E. T. & Bell, F. G., 1997. Some problems associated with past mining at a mine in the Witbank coalfield, South Africa. *Environment Geology*, Volume 33, No. 1, pp. 61-71.

Cadle, A. B., Cairncross, B., Christie, A. D. M. & Roberts, D. L., 1993. The Karoo Basin of South Africa: type basin for the coal-bearing deposits of southern Africa. *International Journal of Coal Geology*, Volume 23, pp. 117-157.

Cairncross, B. & Cadle, A. B., 1987. A genetic stratigraphy for the Permian coal-bearing Vryheid Formation in the east Witbank Coalfield, South Africa. *South African Journal of Geology, Volume* 90, No. 3, pp. 219-230.

Cairncross, B. & Cadle, A. B., 1988a. Depositional paleoenvironments of the coal-bearing Vryheid Formation in the east Witbank Coalfield, South Africa. *South African Journal of Geology*, Volume 91, No. 1, pp. 1-17.

Cairncross, B & Cadle, A. B., 1988. Paleoenvironmental control on coal formation, distribution and quality in the Permian Vryheid Formation, East Witbank Coalfield, South Africa. *International Journal of Coal Geology*, Volume 9, No. 4, pp. 343-370.

Cairncross, B., Hart, R. J. & Willins, J. P., 1990. Geochemistry and sedimentology of coal seams from the Permian Witbank Coalfield, South Africa; a means of identification. *International Journal of Coal Geology*, Volume 16, pp. 309-325.

Cairncross, B., 2001. An overview of the Permian (Karoo) coal deposits of southern Africa. *African Earth Sciences*, Volume 33, pp.529-562.

Datamine Africa Pty Ltd, 2017. *Klippan and Blaauwkranz Coal Discard Facilities- Geological Modelling Methodology and Current Resources*, Report No. PJ1705_03, [19 June 2017].

Delta-H Water Systems Modelling Pty Ltd, 2016a. *Mafube Colliery- Post-closure Groundwater and Geochemical Model*, Report No. Delh. 2014.011-5, [January 2016].

Delta-H Water Systems Modelling Pty Ltd, 2016b. *SACE COMPLEX- Post-closure Groundwater and Geochemical Model*, Report No. Delh. 2014.011-8, [October 2016].

Delta-H Water Systems Modelling Pty Ltd, 2017. *Technical Memo: Mafube Colliery- Update of Geochemical Model,* Report No. Delh.2016.011-5_c1, [May 2017].

Delta-H Water System Modelling Pty Ltd, 2018a. *Goedehoop Colliery-Static Geochemical Test Results,* Report No. Delh.2017.011-3/01G, [July 2018].

Delta-H Water Systems Modelling Pty Ltd, 2018b. *Zibulo Colliery Geochemical Investigation- 38 000 Ton Coal Stockpile Area,* Report No. Delh.2018.011-9C, [April 2018].

Delta-H Water System Modelling Pty Ltd, 2019. *Arnot Colliery: Preliminary Geochemical Assessment,* Report No. Delh.2018.090-02, [February 2019].

Digby Wells & Associates, 2011. *Geohydrology Report for the Weltevreden Project,* Environmental Solutions Provider, Randburg.

Dold, B., 2014. Evolution of Acid Mine Drainage Formation in Sulphidic Mine Tailings. *Minerals,* Volume 4, pp. 621-641.

Erasmus, C. A., 2018. *Groundwater Impact Assessment in a Coal Mine Area of Witbank, Mpumalanga.* Unpublished MSc Thesis, University of the Witwatersrand.

Falcon, R. M. 1986. Spontaneous combustion of the organic matter in discards from the Witbank coalfield. *Journal of the South African Institute of Mining and Metallurgy,* Volume 86, no. 7, pp. 243-250.

Favas, P. J. C., Sarkar, S. K., Rakshit, D., Ventakachalam, P. & Prasad, M. N. V., 2016. Acid mine drainages from abandoned mines: Hydrochemistry, Environmental impact, Resource recovery, and Prevention of pollution. In: M. N. V. Prasad & K. Shih (eds). Environmental Materials and Waste: Resource Recovery and Pollution. Academic Press, pp. 413-462. doi:10.1016/C2014-0-05144-1

Foli, G. & Gawu, S. K. Y., 2017. Modified acid-base accounting model validation and pH buffer trend characterisation n mine drainage at the AngloGold Ashanti Obuasi mine in Ghana, West Africa. *Environ Earth Sci, Volume* 76, No. 663, pp. 1-10.

Fourie, P. J., 2007. *The description of physico-chemical processes in coal mine spoils and associated production of acid mine drainage,* Unpublished MSc Thesis, University of the Free State.

Golder Associates Africa Pty Ltd, 2010. *Groundwater Assessment at Greenside Colliery,* Report No. 12666-9568-1, [July 2010].

Golder Associates Africa Pty Ltd, 2018. *Greenside Water Balance Basis of Designs (rev 5)- Final,* Report No. 1788279-317023-5, [June 2018].

Gomo, M. & Vermeulen, D. 2014. Hydrogeochemical characteristics of a flooded underground coal mine groundwater system. *Journal of African Earth Sciences,* Volume 92, pp. 68-75.

Gray, N. F., 1997. Environmental impact and remediation of acid mine drainage: a management problem. *Environmental Geology,* Volume 30, No. 1/2, pp. 62-71.

Grobbelaar, R., 2001. *The Long-Term Impact of Intermine Flow from Collieries in the Mpumalanga Coalfields.* Unpublished MSc Thesis, University of the Free State.

Hammarstrom, J. M., Seal II, R. R., Meier, A.L. & Kornfield, J. M., 2005. Secondary sulfate minerals associated with acid mine drainage in the eastern US: recycling of metals and acidity in surficial environments. *Chemical Geology*, Volume 215, pp. 407-431.

Hancox, P. J. & Gotz, A. E., 2014. *South Africa's coalfields- a 2014 perspective.* Available at: https://repository.up.ac.za/bitsream/handle/2263/58453/Hancox_South_2014.pdf?sequence=1&Allowed=y
[Accessed 30 May 2019].

Havenga, A., 2011. *Quantification and management of intermine flow in the Western Witbank coalfield: Implication for mine water volumes and quality,* Unpublished MSc Thesis, University of the Free State.

Hobbs, P., Oelofse, H. H. & Rascher, J., 2008. Management of Environmental Impacts from Coal Mining in the Upper Olifants River Catchment as a function of Age and Scale. *Water Resources Development*, Volume 24, No. 3, pp. 417-431. doi:10.1080/07900620802127366

Hodgson, F. D. I. & Krantz, R. M., 1995. *Investigation into groundwater quality deterioration in the Olifants river catchment above the Loskop dam with specialised investigation in the Witbank dam sub-catchment,* WRC Report NO. 291/1/95.

Hodgson, F. D. I., 2011. *Mine-water balance for Goedehoop Colliery*, Report No. 2011/0/FDIH, [18 May 2011].

Hodgson, F. D. I., 2013. *Mine-water balance for SACE,* Report No. 2013/18/FDIH, [28 December 2013].

Hodgson, F. D. I., 2014. *Mine-water balance for SACE,* Report No. 2014/01/FDIH, [26 March 2014].

Holland, M. J., Cadle, A. B., Pinheiro, R. & Falcon, R. M. S., 1989. Depositional environment and coal petrography of the Permian Karoo Sequence: Witbank Coalfield, South Africa. *International Journal of Coal Geology,* Volume 11, pp. 143-169.

Hounslow, A.W. (1995) Water Quality Data: Analysis and Interpretation. CRC Press LLC, Lewis Publishers, Boca Raton.

Jeffrey, L. S., 2005. Characterization of the coal resources of South Africa. *The South African Institute of Mining and Metallurgy,* pp. 95-102.

Jeen, S. W. & Mattson, B., 2016. Evaluation of layered and mixed passive treatment systems for acid mine drainage. *Environmental Technology*. doi:10.1080/09593330.2016.117249

JMA Consulting (Pty) Ltd, 2012a. *Goedehoop- Northern Site Groundwater Specialist Study Report*, Report No. JMA/10419/2012, [November 2012].

JMA Consulting (Pty) Ltd, 2012b. *Goedehoop-Southern Site Groundwater Specialist Study Report*, Report NO. JMA/10339/2012, [November 2012].

Jones & Wagener Engineering & Environmental Consultants, 2015. *Goedehoop and Koornfontein Colliery, South Africa*, Report No. JW238/14/E582-Rev 0, [June 2015].

Johnson, D. B., & Hallberg, K. B., 2005. Acid mine drainage remediation options: a review. Science of the Total Environment, Volume 338, pp. 1-14.

Johnson, M. R., Van Vuuren, C. J., Hegenberger, W. F., Key, R. & Shoko, U., 1996. Stratigraphy of the Karoo Supergroup in Southern Africa: an overview. Journal of African Earth Sciences, Volume 23, No. 1, pp. 3-15.

Jönsson, J., Jönsson, J. & Lövgren, L., 2006. Precipitation of secondary Fe(III) minerals from acid mine drainage. *Applied Geochemistry,* Volume 21, pp. 437-445.

Longwell, J. P., Rubin, E. S. & Wilson, J. 1995. Coal: Energy for the future. *Prog. Energy Combust. Sci,* Volume 21, pp. 269-360.

Lukas, E., n.d *Windows Interpretation System for Geohydrologists,* Bloemfontein: Water Research Commision.

Marais, H., 2014. Greenside colliery, 3A North Discard Dump: Seepage flux and chemical quality prediction, Report No. 53814v1, [28 March 2014].

Maree, J. P. & du Plessis, P., 1994. Neutralization of acid mine water with calcium carbonate. *Water Science & Technology,* Volume 29, no. 9, pp. 285-296.

McCarthy, T. & Rubidge, B., 2005. *The Story of Earth and Life: A South African Perspective on a 4.6-Billion-Year Journey.* Struik Publishers: Cape Town.

McCarthy, T. S. & Pretorious, K., 2009. 'Coal mining on the Highveld and its implications for future water quality in the Vaal river system'. Paper presented at the *International Mine Water Conference,* IMWA, Pretoria, 19-23 October 2009.

McCarthy, T. S., 2011. The impact of acid mine drainage in South Africa. *S. Afri. J. Sci.,* Volume 107, No. 5/6, pp. 1-7. doi: 10.4102/sajs.v107i5/6.712

McCarthy, T. S. & Humphries, M. S., 2013. Contamination of the water supply to the town of Carolina, Mpumalanga, January 2012. *South African Journal of Science*, Volume 109, No. 9/10, pp. 1-10. doi:10.1590/sajs.2013/20120112

Mokoena, M. P., 2012. *Evaluation of Acid-Base Accounting Methods and the Prediction of Acid-Mine Drainage in the Middelburg Area,* Unpublished MSc Thesis, University of the Free State.

Munawer, M. E., 2018. Human health and environmental impacts of coal combustion and post-combustion wastes. *Journal of Sustainable Mining,* Volume 17, pp. 87-96.

Ochieng, G. M., Seanego, S. & Nkwonta, O. I., 2010. Impacts of mining on the water resources in South Africa: A review. *Scientific Research and Essays, Volume* 5, No. 22, pp. 3351-3357.

Oyewo, O. A., Agboola, O., Onyango, M. S., Popoola, P. & Bobape, M. F., 2018. Current Methods for the remediation of acid mine drainage including continous removal of metal from watsewater and mine dump. In: M. M. V. Prasad, P. J. C. Favas & S. K. Maiti (eds). *Bio-Geotechnologies for Mine Site Remediation*: Elsevier, pp. 103-114.

Parkhurst, D. L. & Appelo, C. A. J., 1999. *User's guide to PhreeqC (version 2)- A computer program for speciation, batch-reaction, one-dimensional transport, and inverse geochemical calculations,* Denver.

Parkhurst, D. L. & Charlton, S. R., 2011. Modules based on the geochemical model PHREEQC for use in scripting and programming languages. *Computers & Geosciences,* Volume 37, pp. 1653-1663.

Peppas, A., Komnitsas, K. & Halikia, I., 2000. Use of organic covers for acid mine drainage control. *Minerals Engineering,* Volume 13, No. 5, pp. 563-574.

Pinetown, K. L. 2003. *Quantitative evaluation of minerals in coal deposits in the Witbank and Highveld coalfields and the potential impact on Acid Mine Drainage,* Unpublished MSc Thesis, University of the Free State.

Pope, J., Weber, P., Mackenzie, A., Newman, N. & Rait, R., 2010. Correlation of acid base accounting characteristics with the Geology of commonly mined coal measures, West Coast and Southland, New Zealand. *New Zealand Journal of Geology and Geophysics*, Volume 53, No. 2-3, pp. 153-166. doi:10.1080/00288306.2010.498404

Pozo-Antonio, S., Puente-Luna, I., Laguela-Lopez, S. & Veiga-Rios, M., 2014. Techniques to correct and prevent acid mine drainage: A review. *DYNA,* Volume 81, No. 186, pp. 73-80. doi:10.15446/dyna.v81n186.38436

Roberts, D. L., 1988. The relationship between macerals and sulphur content of some South African Permian Coals. *International Journal of Coal Geology*, Volume 10, pp. 399-410.

Sakala, E., Fourie, F., Gomo, M., Coetzee, H. & Magadaza, L. 2016. '*Specific groundwater vulnerability mapping: Case study of Acid Mine Drainage in the Witbank Coalfield, South Africa*', Proceedings of the sixth IASTED International Conference on Environment and Water Resource Management, pp. 93-100, 5-7 September, Gaborone, Botswana.

Sakala, E., Fourie, F., Gomo, M. & Coetzee, H., 2017. 'Hydrogeological investigation of the Witbank, Ermelo and Highveld Coalfields: Implications for the subsurface transport and attenuation of acid mine drainage', In *Mine Water and Cicular Economony: proceedings of the IMWA 2017 conference* (eds). C. Wolkersdorfer, L. Sartz, M. Sillanpää, A. Häkkinen, Finland, pp. 564-571.

Sakala, E., Fourie, F., Gomo, M & Coetzee, H., 2019. Groundwater vulnerability mapping of Witbank coalfield in South Africa using deep learning artificial neural networks. *South African Journal of Geomatics*, Volume 8, No. 2, pp. 282-293. doi:10.4314/sajg.v8i2.12

Scholtz, O., 2017. *Draft: Landau Colliery: Old Blaauwkrans Dump Waste Assessment and Characterisation*, Report No. AS-ANG-LAN-17-05-10, Witbank, [June 2017].

Sherlock, E. J., Lawrence, R. W. & Poulin, R., 1995. On the neutralization of acid rock drainage by carbonate and silicate minerals. *Environmental Geology*, Volume 25, pp. 43-5.

Skousen, J., Simmons, J. & Ziemkiewicz, P., 2001. The Use of Acid-Base Accounting to Predict Post-mining Drainage Quality on West Virginia Surface Mines. January, pp. 1-16.

Skousen, J., Simmons, J. & Ziemkiewicz, P., 2014. *The Use of Acid-Base Accounting to Predict Post-mining Drainage Quality on West Virginia Surface Mines.* Available at: https://www.researchgate.net/profile/Jeffrey_Skousen/publication/242761672_The_Use_of_Acid-Base_Accounting_to_Predict_Post-mining_Drainage_Quality_On_West_Virginia_Surface_Mines/links/00b7d5295aced8d93a000000/The-Use-of-Acid-Base-Accounting-to-Predict-Pos
[Accessed 26 February 2019].

Skousen, J. G., Ziemkiewicz, P. F. & McDonald, L. M., 2019. Acid mine drainage formation, control and treatment: Approaches and strategies. *The Extractive Industries and Society*, Volume 6, pp. 241-249.

Smith, G. L., 1980. Genetic stratigraphy of the Witbank coalfield. *Trans. geol. Soc. S. Afri*, Volume 83, pp. 313-326.

Sophocleous, M., 2002. Interactions between groundwater and surface water: the state of science. *Hydrogeology Journal*, Volume 10, pp. 52-67.

Steenekamp, G., 2011. *Geohydrological impact assessment as part of the EMPR for the proposed coal mining operations*, [February 2011].

Teichmüller, M., 1989. The genesis of coal from the viewpoint of coal petrology. *International Journal of Coal Geology*, Volume 12, pp. 1-87.

Telfer, C. A., de Klerk, E. S., Hancox, P. J., Dippenaar, K., Raath, L. & de Vries, C. W., 2017. *Independent compentent persons's report on the coal assets of Keaton Energy Holdings Limited*, Report No. VMD2127R, [31 January 2017].

Udayabhanu, S. G. & Prasad, B., 2010. Studies on Environmental Impact of Acid Mine Drainage Generation and its Treatment: An Appraisal. *Indian Journal of Environmental Protection*, Volume 30, No. 11, pp. 953-967.

Usher, B.H., 2000. *Acid Base Accounting Cumulative Screening tool (ABACUS)*, Pretoria: Water Research Commission.

Usher, B. H., Cruywagen, L.-M., de Necker, E. & Hodgson, F. D. I., 2003. *On-site and laboratory Investigations of Spoil in Opencast Collieries and the Development of Acid-Base Accounting Procedures*, WRC Report No. 1055/03, [September 2003].

van Niekerk, A. M., 1997. *Generic Simulation Model for Opencast Mine Water Systems*, WRC Report No. 528/1/97.

van Vuuren, M. C. 1989. *The chemical properties and derived sedimentary patterns of the coals seams in the Witbank-Highveld area*, Unpublished MSc Thesis, University of Pretoria.

van Zyl, H. C., Maree, J. P., van Niekerk, A. M., van Tonder, G. J. & Naidoo, C., 2001. Collection, treatment and re-use of mine water in the Olifants River Catchment. *The Journal of the South African Institute of Mining and Metallurgy*, pp. 41-46.

Vermeulen, P. D. & Usher, B. H., 2006a. An investigation into recharge in South African underground collieries. *The Journal of the Southern African Institute of Mining and Metallurgy*, Volume 106, pp. 771-788.

Vermeulen, P. D. & Usher, B. H., 2006b. Sulphate generation in South African underground and opencast collieries. *Environmental Geology*, Volume 49, pp. 552-569. doi: 10.1007/s00254-005-0091-2.

Water Research Commission, n.d *The South Africa Mine Water Atlas*, WRC Report No. K5/2234//3, Gezina.

Weather Spark, 2019. *Average Weather in Witbank, South Africa, Year Round.* [Online] Available at: https://weatherspark.com/y/95842/Average-Weather-in-Witbank-South-Africa-Year-Round
[Accessed 28 June 2019].

World Coal Association, 2009. *The Coal Resource: A comprehensive Overview of Coal.* [Online] Available at: https://www.worldcoal.org/file_validate.php?file=uses_of_coal(01_06_2009).pdf
[Accessed 22 March 2019].

XMP Consulting CC, n.d *South African Coal: Desktop Study,* South Africa. [Online]
Available at: http://www.xmpconsulting.com/documents/SA%20Desktop%20Study.pdf
[Accessed 22 March 2019].